CONTENTS

Animal Model Study of Reproductive Toxicity of the Chronic Exposure of Dicofol

Afaf A. El-Kashoury[1] , Afrah F. Salama[2*] , Adel I. Selim[3] and Rania A. Mohamed[1]

[1]Dept. of Mammalian and Aquatic toxicology, Central Agricultural Pesticides Laboratory (CAPL), Agricultural Research Center (ARC), Dokki, Giza, Egypt; [2]Chemistry Department, Biochemistry Section, Faculty of Science, Tanta University, Egypt; [3]Chemistry Department, Organic Chemistry Section, Faculty of Science, Tanta University, Egypt

Received April 15, 2009

Abstract

Dicofol is an organochlorine acaricide widely used in local market. The present study was conducted to evaluate the dicofol chronic toxicity of male fertility indices and reproductive toxicity resulted from acaricide through sexual and reproductive hormones as well as investigate the effect on testicular function and epididymal oxidative parameters I a animal model. In this investigation, two equal groups of male albino rats were orally administered dicofol, at 4.19 and 16.75 mg/kg body weight/day through drinking water for consecutive 90 weeks. Dosages represent $^1/80$ and $^1/20$ of LD_{50} of dicofol respectively. The third group was kept as control group. At the end of each experimental period (16, 28 and 90 weeks), blood samples were taken to exam sexual, reproductive and thyroid hormones. Also, animals were dissected and the reproductive organs (epididymus and testes) were taken to measure fertility indices, oxidative parameters and testicular biomarkers. The results indicated dicofol decreased testes and epididymus weights for both low and high doses. This effect was dose-related and should be associated with decline in epididymus sperm count, percent of sperm motility, viability and maturity and increased abnormal sperm morphology. Decline in serum testosterone, follicle stimulating hormone and luteinizing hormone levels concomitant with an elevation in estradiol and progesterone levels were observed. Dicofol-treated group demonstrated de-generation and atrophy of some seminiferous tubules associated with depression in luminal spermatozoal concentration. Meanwhile, dicofol increased oxidative stress by elevation of lipid peroxidation index associated with depletion in glutathione level. Concerning the testicular biomarkers, dicofol increased total protein level and decreased the activities of the enzymes responsible of spermatogenesis, *i.e.* lactate dehydrogenase, acid and alkaline phosphatase activities. [Life Science Journal. 2009; 6(3): 1 – 18] (ISSN: 1097 – 8135).

Keywords: Rats, pesticide, dicofol, chronic toxicity, fertility, testes, epididymus, lipid peroxidation, glutathione, testicular markers, hormones**.**

1 INTRODUCTION

Pesticides are agricultural chemicals used for controlling pests on the plant or animals. Problems associated with pesticide hazards to man and environment are not confined to the developing countries, but extended to developed nations and still facing some problems in certain locations[1]. The severity of pesticide hazards is much pronounced in third world countries. A number of long persistent organochlorines (O`Ch), which have been banned or severely restricted are still marketed and used in many developing countries[2].The ideal pesticide is a pesticide which be effective only against the pests and be harmless to people, animals and environment. However, they have some side / non-target effects that may show undesired actions appears latter[3]. A large number of chemicals occurring in our environment may have potential to interfere with the endocrine system of animals[4]. Many of these chemicals can disrupt development of the endocrine system and of the organs that respond to endocrine signals in organisms indirectly exposed during prenatal and/or early postnatal life; effects of exposure during development are permanent and irreversible[5]. Several pesticides have been reported to produce gonadal toxicity, among these are persistent and bioaccumulative organochlorine pesticides (O`Ch). Increasing interest has been observed among environmental and health institutions regarding the potential reproductive effects due to exposure to occupational and environmental chemicals[4]. Over the past decade, there has been an increasing focus on the effects of synthetic chemicals on human endocrine system-specially on effects related to androgen and estrogen homeostasis[6]. An understanding of the developmental consequences of endocrine disruption in wildlife can lead

to new indicators of exposure to endocrine disrupting contaminants. Thus, wildlife serve as important sentinels of ecosystem health, including human public health[7]. There is much concern that exposure to such environmental contaminants causes decreased sperm counts, impairment of sperm motility, reduced fertilization ability, producing abnormal sperm in men and wildlife[8]. It has been reported that, pesticides with such properties have been shown to cause overproduction of reactive oxygen species (ROS) in both intra- and extracellular spaces, resulting in a decline of sperm count and infertility in wildlife and human[9]. The antioxidant system plays an effective role in protecting testes and other biological tissues below a critical threshold of ROS thus preventing testicular dysfunction[10]. ROS has been shown to damage macromolecules, including membrane bound polyunsaturated fatty acid (PUFA), causing impairment of cellular function[11]. Spermatozoa are rich in PUFA, and, therefore, could be highly susceptible to oxidative stress. Dicofol, an organochlorine acaricide, is used widely on agriculture crops and ornamentals and in or around agricultural and domestic buildings for mite control[12]. It tends to accumulate in steroid producing organs such as adrenal gland, testes and ovary[13] and has antispermatogenic and antiandrogenic properties[14]. Previous studies have suggested that O`Ch, pesticides impaired the testicular functions through altering the activities of revelant enzymes[15,16]. Studies have been conducted on reproductive toxicity of dicofol in male rats following short-term exposure[13,14]. However, few and olden literature in this respect following long-term exposure specifically in mammals are available[17,18]. For the above mentioned, the objective of the current study was to characterize the endocrine-disrupting effects and reproductive toxicity of chronic daily exposure to dicofol in male albino rats via evaluation of male fertility indices and reproductive and sexual hormone levels. As well as oxidative parameters in cauda epididymus and testicular functions were studied

2. Materials and Methods

2.1 Experimental Animals

In the present study, a total of seventy two male Wistar albino rats, Rattus norvegicus were obtained from the Farm of General Organization of Serum and Vaccine, Egypt. Male rats initially weighing 150±10 g were used. Animals were acclimated to holding facilities for two weeks prior to the experiment. The rats were housed in groups and kept in room under controlled temperature (24°C), humidity (30-70 %) and light (12: 12 hr / light: dark). All animals were provided balanced diet throughout the experimental period, these diet were obtained from Agricultural-Industrial Integration Company, Giza. Which formed of proteins, lipids, fibers, wheat, clover, maize, beans, crushed bones, molasses, choline, lysine, methionine, NaCl, Mn, Zn, Co, Mg, Cu, Fe, Se, I2 and many vitamins like A, E, D3, K, B1, B2, Biotin, B6, B12, Niacin and Folic acid. Animals were given food and water *ad libitum.*

2.2 Experimental Materials

Dicofol (an O'ch pesticide), formulation 18.5 % Emulsifiable Concentrate (EC), was received from El-Nassr Company, was used through this investigation. Commercial name (Kelthane). The oral median lethal dose (LD50) of dicofol (administered to rats *per* OS.) was 348.86 mg/kg b.w, according to Weil's method (Weil, 1952). In this investigation, the used dosages were chosen according to the maximum tolerated dose (MTD), which suppressed body weight gain slightly i.e.; 10 %, generally ¼ MTD and 1/16 MTD, are then selected for testing (Hayes, 1989). Accordingly, dicofol was administered to rats at 4.19 and 16.75 mg/kg body weight (representing 1/80 and 1/20 LD_{50}) in drinking water.

2.3 Experimental Design

Seventy-two adult albino rats were allocated into three groups- 24 each - and treated with dicofol through drinking water for 90 successive weeks as the following:
Group (1): Rats received tap water only as an emulsifier of the pesticide dicofol (Emulsifiable concentrate).
Group (2): Rats received 4.19 mg/kg b.w. /day (30 ppm dicofol, which represents the lower dose).
Group (3): Rats received 16.75 mg/kg b.w. /day (120 ppm dicofol, which represents the higher dose).
dicofol emulsified daily in drinking water in glass bottle, and the bottles were cleaned daily.

All animals were observed at least once daily for behavior; signs of intoxications, mortality, morbidity, and food and water consumption were monitored daily. Animals weighed weekly and the dose was adjusted accordingly.

2.4 Sampling

2.4.1 Blood samples

At the end of each experimental period, (16, 28 & 90 weeks), blood samples were collected, from fasted rats (control and treatanimals), from the orbital sinus vein using anesthetic ether by heparinized capillary tubes in plain tubes, according to Schalm[19], and allowed to be clotted at room temperature to obtain serum for hormonal assay

2.4.2 Sacrifice and tissues preservation

Five animals/group were sacrificed by design 16, 28 and 90 weeks on study. Testes and epididymus from sacrificed rats were removed immediately, clean of adhering tissues and weighed. Then, epididymus prepared for fertility evaluation and determination of oxidative biomarkers. Testes samples were taken for histopathological examination through the light microscope[20], and estimation of testicular functions.

2.5 Data Collection Techniques

2.5.1 Evaluation of Fertility

Spermatozoa were obtained by mincing the cauda epididymus in a known volume of physiological saline (w/v) at 37°C for evaluation of semen parameters under microscope (40X) as the following:

2.5.1.1 Sperm concentration (count)

The spermatozoa concentration was carried out by diluting the sperm suspension with water (1: 20), then mixed together, after that a drop of them delivered into the Neubaure haemocytometer in each side of the counting chamber. The haemocytometer is allowed to stand for 5 min. for sedimentation, then sperms were counted in the large five squares and expressed as sperm concentration in million, according to Feustan et al[21].

2.5.1.2 Sperm motility

The motility of sperm was evaluated directly after mincing in drop of sperm suspension, microscopically. Non-motile sperm numbers were first determined, followed by counting of total sperm. Sperm motility was expressed as percent of motile sperm of the total sperm counted, according to Linder et al[22].

2.5.1.3 Sperm viability by Eosin stain

This technique is used to differentiate between live and dead sperms. A drop of the Eosin stain added into sperm suspension on the slide and stand for 5 min. at 37°C, then examined under microscope. The head of dead spermatozoa stained with red color. While, the live spermatozoa unstained with Eosin stain. Sperm viability was expressed as percentage of live sperm of the total sperm counted, according to Krzanowska et al[23].

2.5.1.4 Sperm maturation by aniline-blue

Nuclear maturation was evaluated by aniline-blue stain, according to Morel et al[24]. Sperm nuclei that stained with blue color were considered to be immature. But nuclear mature sperm was not stained with aniline-blue. The percentage of immature sperm was calculated from the observation of one hundred sperm preparation from each group.

2.5.1.5 Sperm morphology

A drop of Eosin stain was added to the sperm suspension and kept for 5 min. at 37°C. After that a drop of sperm suspension was placed on a clean slide and spread gently to make a thin film. The film was air dried and then observed under a microscope for changes in sperm morphology, according to the method of Feustan et al[21]. The criteria chosen for head abnormality were; no hook, excessive hook, amorphous, pin and short head. For tail, the abnormalities recorded were; coiled flagellum, bent flagellum, bent flagellum tip. The result are the percentage overall abnormal form.

2.5.2 Hormonal assay

2.5.2.1 Determination of serum testosterone

Testosterone determination was performed according to the method adopted by Jaffe and Behrman[25], by using the coat-A-count technique,(radioimmunoassay)

2.5.2.2 Determination of serum estradiol

Estradiol determination was performed according to the method of Xing et al[26] by the coat-A-count technique,(radioimmunoassay**)**

2.5.2.3 Determination of serum progesterone

Progesterone determination was performed according to Yalow and Berson[27], by the coat-A-count technique, (radioimmunoassay)

2.5.2.4 Determination of serum follicle-stimulating hormone (FSH) and luteinizing hormone (LH)

Follicle stimulating hormone and Luteinizing hormone determination Were performed according to Santner et al[28], by the coat-A-count technique , (immunoradiometric assay).

2.5.2.5 Determination of serum total thyroxine (T_4) and total tri-iodothyronine (T_3)

Thyroxine and tri-iodothyronine determination were performed in serum according to the method adopted by Britton et al[29], by the coat-A-count technique, (radioimmunoassay)

2.5.3- Oxidative biomarkers in epididymus

After evaluation of fertility related parameters, the remaining sperm suspension was collected and centrifuged by using cooling centrifuge. Then, the supernatant separated and kept at (-40°C) until determination of oxidative biomarkers.

2.5.3.1 Lipid peroxidation assay

Lipid peroxidation (LPO)was measured in epididymus homogenates accordingly to the method of Ohkawa et al[30]. Based on the formation of thiobarbituric acid reactive substances (TBARs) and expressed as the extent of malondialdehyde (MDA) production.

2.5.3.2 Determination of total glutathione (GSH & GSSG) :Principle

Total glutathione (GSH) was measured according to the method of Bergmeyer and Graβl[31] is based on the catalytic action of glutathione is a system, in which GSH undergoes periodical oxidation by DTNB and reduction by NADPH. The measure of the concentration of glutathione in samples is the velocity increase of absorbance (but not the end value).

2.5.4 Testicular functions

A 10 % homogenate (W/V) of testes was prepared in ice cold normal saline using a chilled glass-teflon porter-Elvehjem tissue grinder tube, then centrifuged at 10,000 xg for 20 min. at 4°C. The supernatant used for determination of protein contents[32], alkaline phosphatase activity[33], and acid phosphatase activity[34]. Also, a 10 % homogenate of testes was prepared in ice-cold 0.1 M phosphate buffer, the homogenate was centrifuged at 12,000 xg for 30 min. at 4°C. The supernatant was used for determination of lactate dehydrogenase (LDH) activity[35].

2.6 Statistical analysis

Data obtained were statistically analyzed using student's t-test at $p<0.05$ or less was considered significant[118].

3. RESULTS & DISCUSSION

3.1 Clinical observation and Mortality

In the present chronic toxicity study, dicofol was administered into male rats at 4.19 amd 16.75 (ml/kg b.w), equal to 30 and 120 ppm respectively, in drinking water, for long-term exposure (90 weeks).

No visible signs of toxicity were noted during the experiment period, except emaciation (alopecia) and rough hair. The mortality were 30, 25, 13 % in the groups of rats dosed with higher and lower-dose and the control group, respectively.

3.2 Effect of dicofol as Endocrine Disruptor

3.2.1 Effect on male fertility indices

3.2.1.1Testes and epididymus weight

The testes of humans and other animals are highly susceptible to damage produced by genetic disorders, environmental or occupational exposure to chemicals or other means. Specific causes of testicular damage have been catalogued[36-38].

Results demonstrated that dicofol at lower and higher-doses significantly decreased the weight of testes in all treated groups at week 16, 28 and 90 (Table 1). These changes were more marked at higher-dose and prolonged dicofol exposure. Meanwhile, decline in epididymus weight was observed only at the higher-dose level after 28 and 90 weeks (Table 1). In the present study, decline in testes weight was confirmed by the histopathological observations, since most of the somniferous tubules were degenerated and atrophied, as shown in Figures 1, 2, 3.

Table 1. Influence of Dicofol on testes, epididymus weight and semen parameters after chronic exposure in drinking water, for 90 weeks.

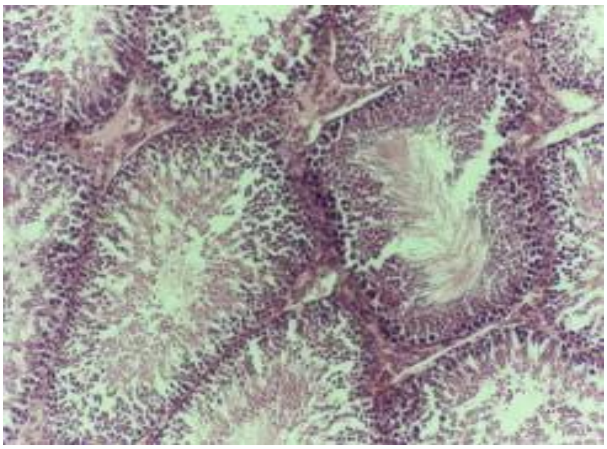

Figure 1. Light photomicrograph of a section of the Testes of rats in control group, showing the normal mature seminiferous tubules with complete series of spermatogenesis and high spermatozoal concentration in the lumen. (H & E X40)

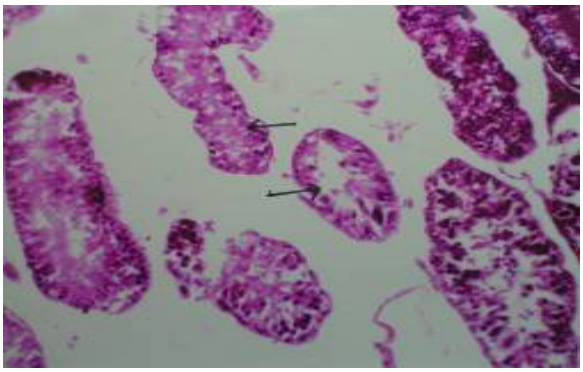

Figure 2. Light photomicrograph of a section of the Testes of rats administrated 30 ppm of dicofol (lowere dose) for 28 weeks, showing degeneration and atrophy of some seminiferous tubules (arrow). (H & E X40)

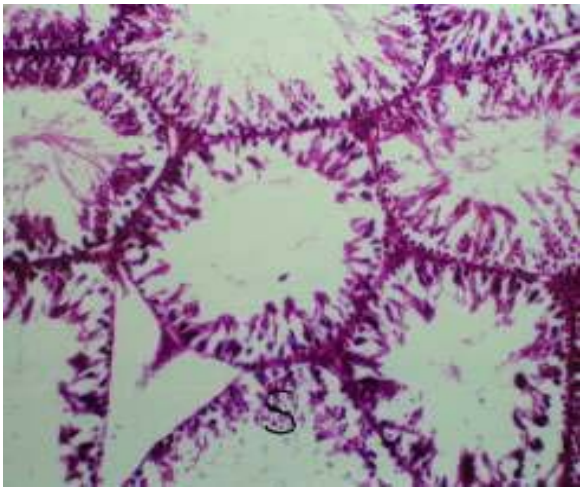

Figure 3. Light photomicrograph of a section of the Testes of rats administrated 120 ppm of dicofol (higher dose) for 16 weeks, showing degeneration of the seminiferous tubules (S) with depression in lumenal spermatozoal concentration. (H & E X40)

Similar results were recorded with O`Ch pesticides at different experimental period: i.e. DDT[39], lindane[40,41] and endosulfan[42] Much data have been reported on the reproductive toxicity of chlorinated hydrocarbons and confirm our results. Brown and Casida[43] and Jadaramkunti and Kaliwal[14] showed that reduction of testes and epididymus weights in rats treated with the highest dose of dicofol for long-term are the result of reduction diameter of somniferous tubules, spermatogenic, Leydig and Sertoli cells. On discussing the results with previous reports, it is proposed that, dicofol probably imped the activity of testes and epididymus by inhibition of androgen production, its antiandrogenic nature or its direct action on these organs[44]. Moreover, the deleterious effects of dicofol on reproductive organ weights might be due to a decrease in testosterone T level after 16, 28 and 90 weeks from the onset of the treatment[45].

Several studies have shown that the epididymis and accessory sex organs require acontinuous androgenic stimulation for preservation of their normal structural and functional integrity[46]. Thus, the slight reduction in the weight of theepididymis and accessory sex organs in the treated rats may be due to lower bioavailability of androgens[47].

Also, Sujatha et al[41] reported that, the decrease in testicular weight of lindane-treated rats (O`Ch) may be due to reduced tubule size, spermatogenic arrest and inhibition of steroid biosynthesis of Leydig cells. Furthermore, there is much concerns that exposure to estrogen –or estrogen-like chemicals induce major pathological effects in epididymus in men and experimental animals[40]. It could be concluded that dicofol may be acting on testes and accessory reproductive organs by blocking androgen biosynthesis and/or by antagonizing the action of androgens[48]. Also, the same authors mentioned that dicofol may be acting directly on the normal function of the hypothalamo-pituitary-gonadal axis.

3.2.1.2 Epididymal sperm count

Sperm count is one of the most sensitive tests for spermatogenesis and it is highly correlated with fertility. Our results showed that, treatment of rats with dicofol at the lower and higher-dose levels for three durations; 16, 28 and 90 weeks, significantly, reduced the total sperm count in all treated groups (Table 1), the effect was dose and time dependent. Histological structure of the testes confirmed this; where it revealed degeneration and atrophy in some of somniferous tubules associated with low luminal spermatozoal concentration. These findings go hand in hand with those of Jandaramkunti and Kaliwal[14] who found that the number of spermatogenic, spermatocytes, spermatides and Leydig cells were significantly decreased with higher-dose of dicofol and thus reduced sperm count. Also, the authors reported that quantity and quality of sperm production has been adversely affected following exposure of certain drugs and chemicals, particularly mutagens and teratogens. Furthermore, there is a clear correlation between the degree and duration of exposure to pesticides and the extent of spermatogenic arrest and hormonal imbalance.

3.2.1.3 Motility and viability of sperm

The assessment of sperm vitality is one of the basic elements of semen analysis, and is especially important in samples where many sperm are immotile, to distinguish between immotile dead sperm and immotile live sperm[49].

Our results revealed that, at week 16, after the administration of dicofol, a dose-dependent reduction in percentage of motile and live were observed. Also, at week 28 and 90, significant decrease was observed, the changes noted did not follow the expected dose-relationship. As regards the effect of time, dicofol has time dependent effect, however, not in uniform fashion (Table 1) and Figures (4, 5). Choudhary and Joshi[42], also stated that, oral administration of rats with endosulfan (O`Ch) at doses of 5, 10 and 15 mg/kg b.w./day for 30 days, significantly, decreased the spermatozoal motility and density in cauda epididymus and testes in dose-dependent manner. Decline in sperm motility and density after oral administration of endosulfan is may be due to androgen insufficiency[16,50], which caused impairment in testicular functions by altering the activities of the enzymes responsible for spermatogenesis, this clearly suggests an antiandrogenic effect of endosulfan[15,51].

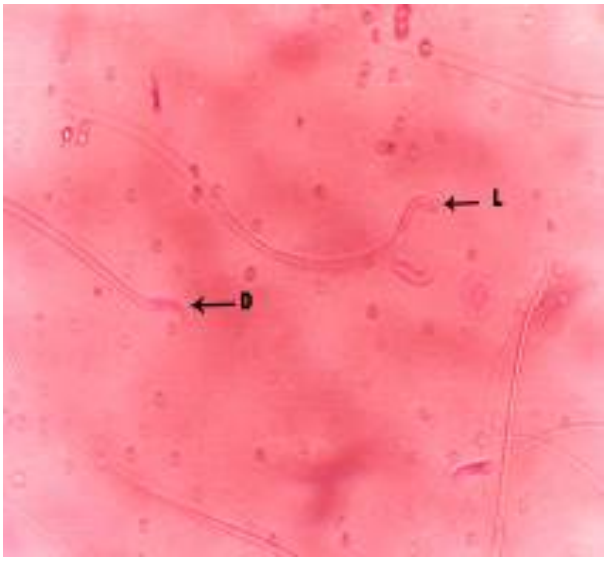

Figure 4. Showed live unstained sperm (L) and dead sperm (D) stained with eosin stain in rats treated with dicofol in drinking water. (40X)

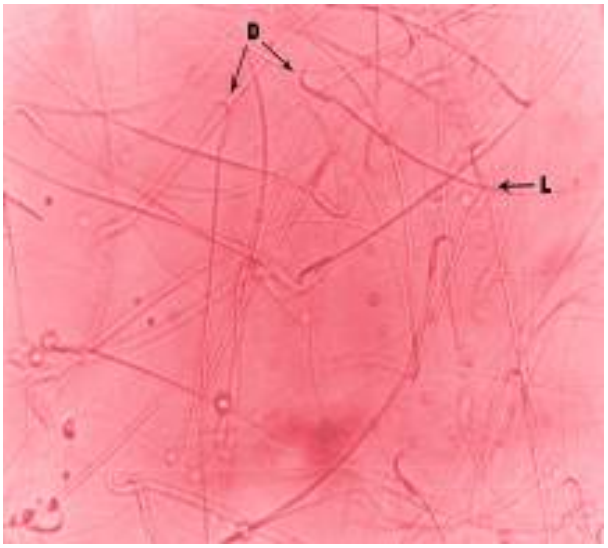

Figure 5. Showed live unstained sperm (L) and dead sperm (D) stained with eosin stain in rats treated with dicofol in drinking water. (40X)

3.2.1.4 Maturation of sperm

From the aforementioned presentation, there were meaningful changes in the number of mature sperms in epididymus. Where, at week 16 and 28 results revealed marked decline in number of mature sperms, the differences seen were dose dependent. Furthermore, a time-related decreased in number of mature sperms was observed in dicofol-treated rats at the lower-dose; whereas, a trend (not significant) for this effect in dicofol-treated rats at the higher dose (Table 1) and Figures (6,7). Morel et al[24], found a positive correlation between chromosomal abnormalities at the time of meiosis that cause disturbance during the transition of nucleoprotein and percentage of sperm nuclei that stained with aniline blue. The acidic aniline blue stains lysine-rich nucleoprotein of immature sperm. During spermatogenesis lysine rich histones are replaced by intermediate nucleoproteins which then are replaced by arginine and cysteine-rich protamines. Then, abnormal chromosome segregation at the time of meiosis allows the persistence of lysine-rich nucleoproteins in spermatozoa. It has been concluded that immature sperms were usually increased in infertile men[52].

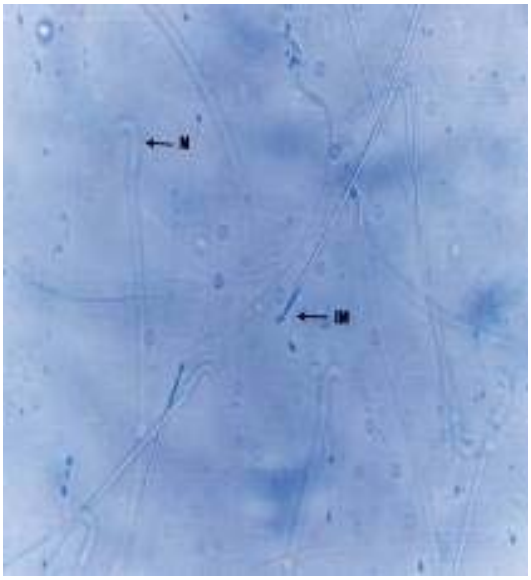

Figure 6. Showed nuclear mature sperm (M) was not stained and immature sperm (IM) with abnormal chromosomes stained with aniline blue in rats treated with dicofol in drinking water. (40X)

Figure (7) Showed immature sperm (IM) stained with aniline blue color in rats treated with dicofol in drinking water. (40X)

3.2.1.5 Sperm morphology

Abnormal form percent was significantly increased in dose and time-dependent manner in all treated groups at the three durations (Table 1) and Figures (8, 9, 10 and 11). This occurred as a result of toxic injury of dicofol to somniferous tubules as postulated from the histological examinations of testes in the treated animals.

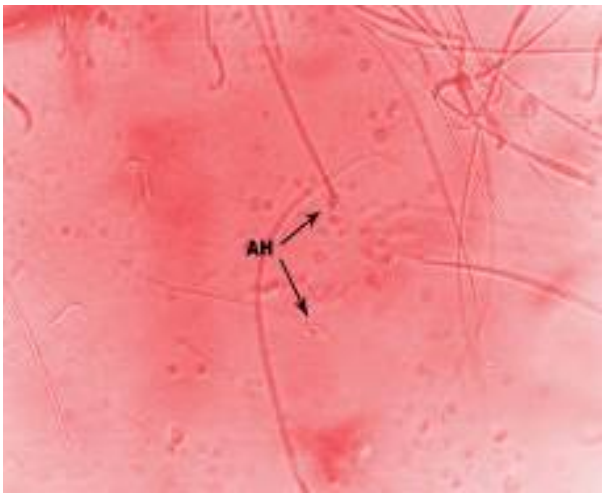

Figure 8. Showed abnormal head sperm miss-shape (AH) stained with eosin stain in rats treated with dicofol in drinking water. (40X)

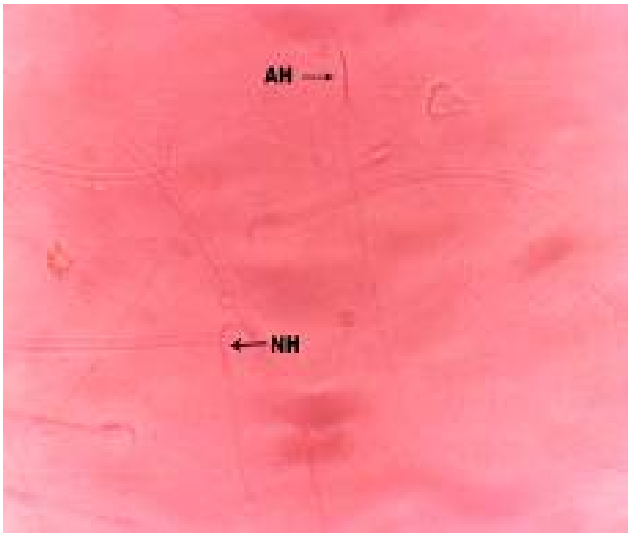

Figure 9. Showed normal sperm with normal head hook shape (NH) and abnormal head sperm no hook (AH) in rats treated with dicofol in drinking water. (40X)

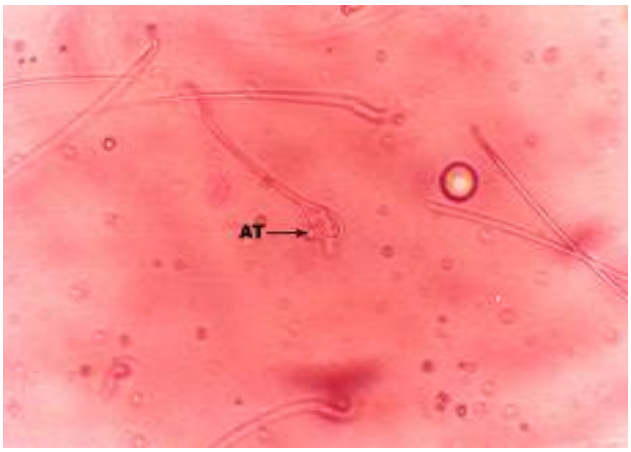

Figure 10. Showed bent tail tip sperm (AT) stained with eosin stain in rats treated with dicofol in drinking water. (40X)

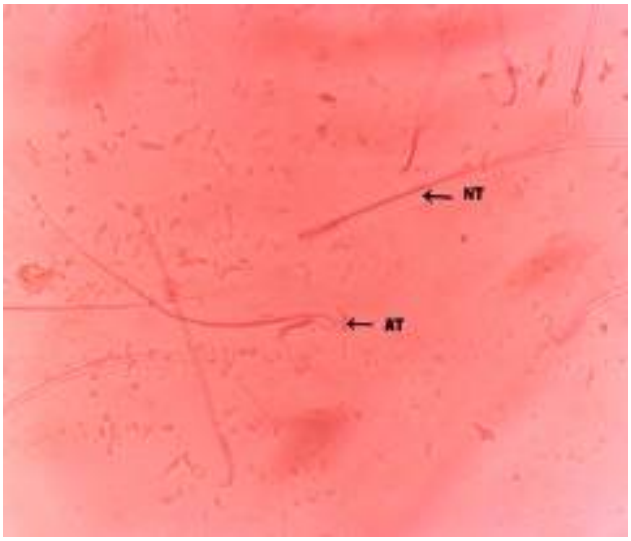

Figure 11. Showed normal tail sperm (NT) and bent tail sperm (AT) in rats treated with dicofol in drinking water. (40X)

Similar results were reported with certain organochlorine pesticides (O`C) at different experimental periods such as (i.e.), DDT[39], lindane[40,41], dicofol[14], and endosulfan[42].

Our results are in accordance with those of Tag El-Din et al[53], who reported that treatment with dicofol in higher dose (16.75 mg/ kg b.w./day, 5 days/week), for 6 months dosing period, significantly, reduced testes and epididymus weight, the total sperm count and percentage of motile and live sperms than lower dose (4.19 mg/kg b.w.). As well as, a significant increase in the percentage of abnormal forms was seen in higher-dose group, and this effect was dose-dependent. The authors noticed a marked depletion in number of mature sperm in the higher-dose group.

From the obtained results, it is interesting to notice that, dicofol seems to be more hazardous at higher dose and prolonged exposure period than lower dose and short exposure period, as revealed from its powerful effects on the weight of testes and epididymus or other semen parameters measured including; sperm motility, total sperm count, cauda epididymus sperm count, percentage of mature and live sperm, as well as abnormal forms.

Generally, the differences in fertility index data including statistical significant differences believed to dicofol effect. Notably, dicofol as well as, the administration periods played an important role in this respect, *i.e.* the effect was treatment and time dependent. The present study reveals that an exposure to dicofol may affect the histology of testes and sperm morphology. Accordingly, this testicular and spermatotoxic changes may be responsible for observed male mediated developmental toxic effects.

3.2.2 Effect on sex hormones

Persistence of chlorinated insecticides and their congeners in the tissues of man and animals and in the environment post health problems of toxicological importance. One of these problems is the endocrinal dysfunction[54,55].
Recent evidence had suggested that organochlorine pesticides, even at low concentrations, may disrupt the endocrine system, which was responsible for proper hormone balance[56,57].

3.2.2.1 Testosterone

Testosterone T is the main steroid sex-hormone in male albino rats, it secreted by leydig cells of the testes under the control of complex neuroendocrine interactions[58,59].

In the present study, T level, significantly, decreased in all treated groups at lower and higher-doses at 16, 28 and 90 weeks of administration, except, in lower-dose group at 16 weeks, where T level unchanged after dicofol treatment (Table 2). Notably, there were no dose-related changes in T level, while a time-dependent reduction in higher-dose group was observed.

The significantly decrease of testosterone level, may be as a result of direct damage of dicofol on leydig cells, which are the main site of testicular androgen biosynthesis.

Results of the present work agree with those found by Krause[60], Desaulniers[61], Lafuente[62], Ben Rhouma[39], and Choudhary and Joshi[42], who noted that T level was significantly decreased in male rats treated with organochlorine pesticides at different doses, *i.e.* DDT, PCB-126 and 153, methoxychlor, DDT, endosulfan, respectively.

Contrary to the results of the present investigation are those reported by Foster[63] and Desaulniers[64], who mentioned that, rats administered with tris (4-chlorophenyl (TCPM), that is structurally related to DDT and dicofol, and PCB-28 (2, 4, 4`-trichlorobiphenyl) or PCB-77 (3. 3`, 4, 4`-tetrachlorobiphenyl) did not exhibit meaningful changes in T level.

3.2.2.2Estradiol and progesterone:

Organochlorine pesticides have some estrogenic properties, and may modify the feed-back mechanism of steroids on the hypothalamus and pituitary[62]. Exogenous estrogens (natural or synthetic) elicit all the pharmacologic responses usually produced by endogenous estrogens.

Estradiol (E_2) determinations have proved of value in a variety of contexts, including the investigation of precocious puberty in girls and gynecomastia in men[65]. The present study also revealed that, significant, increase in E_2 level was observed in all dicofol-treated groups at the three durations (16, 28 and 90 weeks) of administration. In addition, dicofol significantly increased progesterone (P_4) level in treated groups; the effect was restricted only in duration of 16 and 28 weeks, and also there were no positive trend in this respect. (Table 2)

The present investigation in comparable to other (O`Ch) pesticides on account of exhibiting estrogenic activity of dicofol when used in higher-dose for long-term[66-69]. The significant elevation of steroids for example, P_4 and E_2 in male rats which received lower and higher-doses of dicofol for long-term exposure could be attributed to increase the incidence of hypertrophy and/or vacuolation (empty cavities) of the adrenal cortex that enhanced the steroidogenic activity[70,71]. Moreover, Jadaramkunti and Kaliwal[14] and Tag El-Din[53] suggested that dicofol mimic estrogenic activity when compared to other chlorinated pesticides (O`Ch) which may have a direct effect on the testes or indirectly through the hypothalmo-hypophyseal testicular axis or by desensitizing the testes to gonadotropins. Furthermore, it has been reported that, the estrogenic like effects may be produced as a result that dicofol binds to estrogen receptors and exhibits estrogenic activity[72] or by direct effect on sertoli cells resulting decreased FSH receptor binding and decreased 3-hydroxy-steroid-dehydrogenase activity that change estradiol to androgen, thus raising estradiol levels[5, 73].

These findings are in close agreement with those reported by Tag El-Din[53], who stated that dicofol at two doses 4.19 and 16.75 mg/kg b.w./day, in drinking water, for 6 months increased E_2 and P_4 levels in male rats in a dose-dependent manner.

Many pesticides are able to block or activate the steroid hormone receptors and/or to affect the levels of sex hormones, thereby potentially affecting the development or expression of the male and female reproductive system or both. This emphasizes the relevance of screening pesticides for a wide range of hormone-mimicking effects[74].

3.2.3 Effect on reproductive hormones:

3.2.2.1 Luteinizing hormone and follicle-stimulating hormone

Luteinizing hormone (LH) is glycoprotein released from the anterior pituitary; it stimulates T production by leydig cells of the testes in males. Hypothalamic control of LH appears to be by a common releasing hormone termed gonadoliberin (GnRH, LHRH), with negative feedback control at the hypothalamic level by E_2 in the female and T in the male[58].

Our results revealed that, short-term dicofol exposure (16 weeks) did not exert appreciable changes in LH and FSH levels in both lower and higher-dose groups. On the contrary, prolonged dicofol-exposure (28 and 90 weeks) significantly decreased LH and FSH levels in dose and time-dependent manner (Table 2). These results go hand in hand with those of Tag El-Din[53] who reported that dicofol at 4.19 and 16.75 mg/kg b.w./day, for 6 months, induced significant decrease in LH level in male rats.

According to the suggestion reported by Singh and Pandey[67], the changes in the pattern of the steroidogenic enzymes 3 ß-hydroxysteroid dehydrogenase and 17 ß-hydroxysteroid dehydrogenase lead to inhibition of testicular androgen biosynthesis in adult rats, which is required for spermatogenesis in seminiferous tubules and sperm maturation in the epididymus. A complementary proposed mechanism, could explain dicofol induced toxicity, is blocking gonadotropin production and/or release by the pituitary, thereby testosterone production by leydig cells is not stimulated, causing spermatogenesis arrest[75]. This mechanism is supported by the data previously reported by Mably[76] who recorded that, the alteration of LH had led to destruction of seminiferous epithelium and loss of germinal elements results in the reduction of the number of spermatids, sperm production in the testes as well as increase abnormality of sperms.

Marked decline in LH and FSH levels in the present study confirm the findings of Desaulniers[61] and Lafuente[62], who investigated the toxicological influences of PCB (126 and 153) and methoxychlor, O`Ch, at different concentrations on male rats. On the other hand, the results of the present study disagree with the findings of Tag El-Din[53], who mentioned that FSH level increased significantly after treatment with dicofol at lower and higher-doses (4.19 and 16.75 mg/kg b.w./day), in drinking water, for 6 months. It was proved that certain O`Ch pesticides did not alter LH and FSH levels when administered into rats at different doses for short-term intervals, such as : TCPM[63], DDT[60] and PCB[28] and 77[64].

An elevation in circulating levels of inhibin, a glycoprotein of primarily sertoli cell origin which inhibits FSH synthesis and secretion by the pituitary[77], could account for the observed decrease in serum FSH level in the current study which was confirmed histopathologically by degeneration and atrophy of seminiferous including leydig and sertoli cells. FSH stimulates the sertoli cells of the seminiferous tubules to produce androgen binding protein, probably moves via the sertoli cells to other germ cells and to the epididymus where the testosterone is released to exert its physiological effects in sperm maturation[76].

3.2.4 Effect on thyroid hormones

3.2.4.1 Tri-iodothyronine and thyroxine

The disruption of thyroid hormone homeostasis by a variety of xenobiotics has been associated with thyroid follicular cell hypertrophy, hyperplasia, and the development of thyroid tumors in rats[78,79]. Thyroid toxicants affect circulating levels of thyroid hormone by either direct action on the thyroid gland or by increasing peripheral elimination of thyroid hormone[79].

Concerning the thyroid hormones; dicofol, at lower and higher-doses, induced significant decrease in thyroxine (T_4) and tri-iodothyronine (T_3) levels throughout the experimental periods (16, 28 and 90 weeks), except at 16 weeks T_4 level did not alter significantly in lower-dose group (Table 2). These changes were more marked at higher dose of dicofol as well as, prolonged dicofol exposure. It is worth to say, results revealed evident affection of thyroid gland, such affection was dose and time-dependent.

Hypothyrodism significantly reduced seminiferous tubule and lumen diameter, where in hypothyroid rats, the proliferation and differentiation of germ cells were arrested and their number was decreased[80], the present study clearly indicates that hypothyrodism adversely affects spermatogenesis; it also indicates that thyroid hormones are essential for normal spermatogenesis.

In accordance with the findings of the present study, El-Kashoury[81] described similar changes in T_4 and T_3 levels after dicofol exposure at lower and higher-doses. They also mentioned that the decrease in T_4 levels may be a result of iodine deficiency, the gland fails to synthesize T4 and hypothyrodism occurs. Another suggestion reported by Hotz[82] who reported that, pesticide increased deiodination and biliary excretion of thyroid hormone T_4 which led to increased rate of T_4 elimination from the blood.

A complementary proposed mechanism, could explain organochlorine (O`Ch) induced toxicity, is attributed to their ability to deplete stores of vitamin A and thyroid hormones from the body by 30-50 %, through interaction with a common plasma protein carrier called transthyretin (TTRs) and alteration of their metabolism in the liver and other organs. T_4 and Vit. A are known to be important regulators of normal epithelial differentiation and

proliferation[83]. Another support to the interaction of O`Ch with TTRs was established by Van den Bery[84] who mentioned that hydroxylated PCBs and number of halogenated industrial chemicals, mainly pesticides (O`Ch) may decrease thyroid hormone levels in rats through interference with hormone transport carriers (TTRs).

An alteration in thyroid hormone T_4 and/or T_3 level in the present study confirm the findings of Desaulniers[64]. Desaulniers[61] and Fisher[85], who investigated the toxicological influences of certain organochlorine pesticides "O`Ch" at different concentrations,*i.e.*, PCB-28 (2, 4, 4`-trichlorobiphenyl) and PcB-126 (3, 3`, 4, 4`, 5-pentachlorobiphenyl).

Another mechanism was postulated by Villa[86] who stated that "O`Ch" might alter the expression of a membrane of genes by a direct receptor mechanism. This receptor is made of a basic protein and known as aryl hydrocarbon receptor (AHR) which is maintained in a ligand binding state in association with cytosolic protein[87]. Exposure to "O`Ch" and related compounds leads to dissociation of AHR from the binding protein[88], which is transferred to the nucleus and then it binds to specific DNA leading to severe harmful effects such as induction of cytochrome P_{450} (CYP_{450}) 1A1 gene[89]. Lastly, bioactivation of these compounds can make them more toxic which may modulate the expression of the related genes in the tissues[90].

3.3 Effect on Oxidative Parameters

Pesticides and environmental chemicals may induce oxidative stress leading to generation of free radicals and alteration in antioxidants or oxygen free radical (OFR) scavenging enzyme system [91].

3.3.1 Lipid peroxidation

Generation of oxidative stress and consequent lipid peroxidation (LPO) by pesticides is reported in many species. It has been reported that increase in ROS can cause the destruction of all cellular structures including membrane lipid[92]. Hence in the present study, lipid peroxidation is used as an index of oxidative stress. Several drugs, xenobiotics and environmental pollutants are known to cause imbalance between formation and removal of free radicals[93].

ROS such as superoxide anions ($O^{\cdot}_2$), hydroxyl radical ($O^{\cdot}H$) and H_2O_2 enhance oxidative process and produce lipid peroxidative damage to cell membranes. The ($O^{\cdot}H$) radical has been proposed as an initiator of LPO through an iron-catalysed Fenton reaction[94]. LPO is the process of oxidative degeneration of polyunsaturated fatty acid (PUFA) and its occurrence in biological membranes causes impaired membrane function, structural integrity[7], decrease in membrane fluidity and inactivation of a several membrane bound enzymes.

Results in (table 3) showed that, an administration of rats with dicofol, at lower and higher doses for two durations 28 and 90 weeks, increased oxidative stress in cauda epididymus of rats, as evidenced by enhanced levels of malondialdehyde (MDA) level.

An elevation of LPO in cauda epididymus, as evidenced by increased production of MDA in the present study, suggests participation of free radical-induced oxidative cell injury in mediating the toxicity of dicofol. These intentionally introduced environmental xenobiotics are known to have a strong affinity for interaction with membrane phospholipids[95]. An elevation in LPO caused by other O`Ch in different experiments has also been reported; methoxychlor[96], methoxychlor[97], endosulfan[98] and 2, 3, 7, 8-tetrachlorobenzo-P-dioxin (TCDD) [99].

3.3.2 Glutathione level

Glutathione (GSH) one of the most abundant antioxidant in cells has been found to decrease during apoptosis. GSH has been hypothesized to play a role in the rescue of cells from apoptosis, by buffering an endogenously induced oxidative stress[100]. In our study, a decrease in GSH levels in dicofol-intoxicated animals may be responsible for enhanced LPO[101, 102]. Our results confirm the findings of Tithof[103], Selzak[104], Luna Samanta[105], Latchoumycandane[96], and Saradha and Mathur[106], who reported that repeated administration of several organochlorine at different concentrations (dicofol, 2, 3, 7, 8-tetrachlorodibenzo-P-dioxin (TCDD), hexachlorocyclohexane (HCH), methoxychlor and lindane, respectively) induced disturbances in the activities of the enzymes regulating GSH metabolism.

As regards GSH level and lipid peroxidation in normal rats (control group), it is worth to mention that, there were significant differences between the control groups (28 and 90 weeks). A noticeable decrease in GSH level accompanied by concomitant increase in LPO in 90 weeks compared with their levels in 28 weeks was observed. It is well documented that advancing age an organism is under greater oxidative stress as the result of impairment of the function of mitochondrial respiratory chain[107]. This leads to an accumulation of DNA, RNA and protein free radical damage[108] and causes alterations in antioxidant enzyme levels[109].

3.4 Effect on Testicular Functions

Organochlorine pesticides (O`Ch), having estrogenic property, impaired the testicular functions through altering the testicular biochemistry[15, 16, 42].

3.4.1 Total protein

The testicular fluid contains both stimulatory factors as well as inhibitory factors that selectivity alters the protein secretions[110]. Thus, the changes in protein suggested that there is a reduction in the synthetic activity in testes.

From Table 4, it is clear that, an administration of dicofol into rats leads to elevation of protein concentration in testes at two doses (lower and higher). Except, at higher-dose for 28 weeks, no appreciable changes in protein content were observed.

Similar elevation in protein content caused by other "O`Ch" has also been reported[111, 112].

The accumulation of protein occurred in testes and epididymus due to androgen deprivation to target organs. This deprivation effect also led to a reduction in testicular and cauda epididymal sperm population, loss of motility in the latter and an increase in number of abnormal spermatozoa, thereby manifesting 100 % failure in fertility in treated animals[113].

Concerning the protein content, our findings, are in accordance with those reported by El-Kashoury and Mansour[81] who studied the effect of dicofol at two doses, for long term, on testicular biochemistry.

3.4.2 Acid and alkaline phosphatase (ACP & ALP)

Acid phosphatases are enzymes capable of hydrolyzing orthophosphoric acid esters in an acid medium. The testicular acid phosphatase gene is up-regulated by androgens and is down-regulated by estrogens[114]. Activities of free lysosomal enzymes have been shown to rise when testicular steroidogenesis is increased[47].

Based on the data obtained in this study, dicofol when administered into rats, at lower and higher doses for different duration (28 and 90 weeks) induced significant decrease in ALP activity (Table 4). It is clear that, the changes noted did not follow the expected dose and/or time relationship. A decrease in ALP activity indicated that dicofol treatment produced a state of decreased steroidogenesis where the inter- and intracellular transport was reduced as the metabolic reactions to channalize the necessary inputs for steroidogenesis slowed down[115].

As regards ACP enzyme, results of the present study showed significant decrease in its activity during two durations (28 and 90 weeks). While, there were no treatment-related changes, but a time-dependent effect in higher-dose groups was detected.

As regards ALP and ACP activities, results of the present investigation were similar to those reported by Chitra[16]. A decrease in the ACP in Free State would thus reflect decreased testicular steroidogenesis in rats and this may be correlated with the reduced secretion of gonadotrophins[115].

3.4.3 Lactate dehydrogenase (LDH)

Testicular LDH is an essential component of the metabolic machinary of spermatozoa and involved in the energy generation processes. An administration of rats with dicofol at both doses (lower and higher) decreased significantly LDH activity in testicular tissues. All changes in LDH activity mean that no dose relationship. On the other hand, the higher-dose exhibited time-dependent effect (Table 4). The decreased in LDH activity in dicofol-treated rats points toward the interference of dicofol with the energy metabolism in testicular tissues[116].

The correlation between LDH and motility and living sperm could be a sign that extracellular LDH ensures metabolism of spermatozoa, perhaps even in anaerobic conditions. This hypothesis is underlined by the significant negative correlation between LDH and pathomorphology of sperm[117].

In the present study, male fertility indices were measured confirm the above-mentioned suggestion where, marked declined in count, motility and viability of sperm were observed as well as an elevation in abnormalities of sperm. It means that LDH enzyme has an important role in the normal energy supply in spermatogenesis.

Notably, decline in serum T level was observed with a reduced reproductive organ weights, which means that male reproductive toxicity induced by dicofol would be augmented by decreased serum T level as well as a decreased function of sertoli and leydig cells, in addition to the direct cytotoxic effect on germ cells[45].

In view of this data, it can be concluded that dicofol induced disorders of reproductive system result from a disturbance of the androgen-estrogen balance, as well as oxidative stress and impairment in testicular functions. Although, it is not possible link all these events together, it is assumed that their collective impact to ultimately leads to a perceptible change in sex hormone balance and arrest of spermatogenesis. Further studies are need for better understanding of the cause of reproductive toxicity induction of dicofol, and possibly of o'ch as a whole.

Table 1. Influence of Dicofol on testes, epididymus weight and semen parameters after chronic exposure in drinking water, for 90 weeks

Periods Parameters	16 Weeks			28 Weeks			90 Weeks		
	Control (0 ppm)	Lower-dose (30 ppm)	Higher-dose (120 ppm)	Control (0 ppm)	Lower-dose (30 ppm)	Higher-dose (120 ppm)	Control (0 ppm)	Lower-dose (30 ppm)	Higher-dose (120 ppm)
Testes weight (g)	1.55±0.035	1.35±0.016*** a	1.30±0.071*a	1.58±0.034	1.50±0.041	1.38±0.051* a	1.95±0.011	1.48±0.137**a	1.19±0.092***a
Epididymus weight (g)	0.20±0.007	0.19±0.011	0.18±0.010	0.35±0.020	0.30±0.019	0.25±0.014** a	0.47±0.005	0.39±0.037**b	0.24±0.025***a
Sperm count	100.0±3.536	90.0±2.236*a ***b	60.0±3.162***a	90.0±2.915	35.0±3.536***a	30.0±2.550***a	110.0±3.742	20.0±3.536***a	15.0±3.536***a
Motility (%)	90.0±1.581	65.0±3.536** a **b	40.0±3.536***a	85.0±3.317	20.0±2.915***a	15.0±2.550***a	85.0±2.449	35.0±8.367***a	25.0±8.660***a
Viability (%)	90±2.236	70±2.550***a **b	50±3.536***a	90±2.550	40±3.536***a	30±3.317***a	90±1.225	40±3.742***a	35±6.708***a
Mature sperm (%)	90±2.550	80±3.53 **b	60±3.536***a	80±3.536	65±2.550**a * b	50±5.100** a	90±1.225	55±5.099***a	50±6.403***a
Abnormal forms (%)	15±2.236	25±3.536*a **b	40±1.871***a	20±1.871	35±3.536**a ***b	65±3.536***a	20±1.225	65±2.236***a **b	50±3.742***a

Values represent means ± SE, n = 5; * P <0.05; * * P <0.01; * * * P <0.001 (Student's t-test).
a: treated group versus control group; b: lower dose group versus higher dose group

Table 2. Influence of dicofol on sex steroid, reproductive and thyroid hormones

after chronic exposure in drinking water for 90 weeks

Periods Parameters	16 Weeks			28 Weeks			90 Weeks		
	Control (0 ppm)	Lower-dose (30 ppm)	Higher-dose (120 ppm)	Control (0 ppm)	Lower-dose (30 ppm)	Higher-dose (120 ppm)	Control (0 ppm)	Lower-dose (30 ppm)	Higher-dose (120 ppm)
Testosterone (ng/ml)	1.30±0.230	1.10±0.311	0.60±0.141 * a	3.60±0.311	1.40±0.270*** a	1.30±0.230*** a	2.10±0.241	1.30±0.230*a	1.20±0.270*a
Estradiol (Pg/ml)	9.40±0.540	23.0±0.707*** a ** b	17.00±1.414 ** a	14.80±0.354	21.70±0.212*** a * b	23.80±0.707*** a	8.70±0.283	13.20±0.270*** a *** b	9.90±0.396* a
Progesterone (ng/ml)	11.63±0.396	18.42±0.544*** a	18.89±0.652*** a	7.23±0.326	9.00±0.707* b	11.44±0.439*** a	4.84±0.334	4.97±0.369	6.00±0.500
FSH (ng/ml)	2.00±0.354	1.40±0.070	1.20±0.141	2.50±0.354	1.90±0.192 *** b	0.30±0.071*** a	3.20±0.184	0.80±0.071*** a *** b	0.25±0.050*** a
LH (ng/ml)	3.53±0.212	3.10±0.283	2.90±0.241	3.20±0.184	1.34±0.114*** a	1.18±0.141*** a	2.90±0.200	0.97±0.130*** a	1.40±0.184*** a
Thyroxine (ng/ml)	26.88±3.942	18.8±2.628	14.45±0.987* a	29.37±1.170	21.00±1.043*** a *** b	14.41±0.544*** a	43.83±0.472	37.82±2.381* a *** b	20.02±2.038*** a
Tri-iodothyrine (ng/ml)	0.46±0.046	0.32±0.029* a	0.27±0.012** a	0.41±0.012	0.36±0.016 * a * b	0.29±0.019*** a	0.33±0.014	0.28±0.016* a *** b	0.16±0.003*** a

Values represent means ± SE, n = 5; * P <0.05; * * P <0.01; * * * P <0.001(Student's t-test).
a: treated group versus control group; b: lower dose group versus higher dose group.

Table 3. Influence of Dicofol on oxidative parameters in cauda epididymus and testicular functions

Periods	28 Weeks			90 Weeks		
Parameters	Control (0 ppm)	Lower-dose (30 ppm)	Higher-dose (120 ppm)	Control (0 ppm)	Lower-dose (30 ppm)	Higher-dose (120 ppm)
Malondialdehyde (µmol /g tissue)	93.07±1.516	146.84±11.048** a	166.76±14.210** a	181.44±9.610	219.75±8.740* a	199.69±7.814
Total glutathione (µmol /g tissue)	374.26±1.692	280.36±3.382*** a *** b	321.91±4.368*** a	291.41±5.074	154.69±4.227 *** a *** b	220.98±2.537*** a
Total protein (mg/g tissue)	17.90±0.511	22.09±0.371** a ** b	18.19±0.686	16.57±0.399	20.41±1.220* a	20.14±0.621** a
Alkaline phosphates (U/mg protein)	0.085±0.007	0.054±0.001** a	0.057±0.003* a	0.094±0.003	0.070±0.004** a	0.074±0.005* a
Acid phosphates (U/mg protein)	0.112±0.002	0.084±0.003*** a * b	0.099±0.004* a	0.125±0.003	0.089±0.004*** a	0.084±0.004*** a
Lactate dehydrogenase (U/mg protein)	1.55±0.043	1.11±0.046*** a *** b	1.53±0.036	1.60±0.034	1.28±0.090* a	1.33±0.045** a

Values represent means ± SE, n = 5; * P <0.05; * * P <0.01; * * * P <0.001 (Student's t-test)
a: treated group versus control group; b: lower dose group versus higher dose group.

ABBREVIATIONS USED

O`Ch, Organochlorine insecticides; ROS, Reactive oxygen species; PUFA, Polyunsaturated fatty acid; EC, Emulsifiable concentrate; T_4,Thyroxine; T_3,Triiodothyronine;T,Testosterone;P_4,Progesterone; E_2,Estradiol;FSH,Follicl-Stimulating hormone;LH,Luteinizinghormone;ALP,AlkalinePhosphatase;ACP,Acid Phosphatase;LDH, Lactate Dehydrogenase;LPO, Lipid Peroxidation;GSH,Glutathione.

ACKNOWLEDGEMENTS

The authors thank the Central Agricultural Pesticide Laboratory (CAPL) Agricultural Research Center, Dokki, Giza, Egypt for its support and facilities.

References

1. Nuckols JR, Gunier RB, Riggs P, *et al*. Linkage of California pesticide use reporting data-base spatial land use for exposure assessment. Environ. Health Perspect 2007; 115 (5) : 684-689.
2. Hajjo RM, Afifi FU, Bathah AH. Multiresidue pesticide analysis of the medical plant *Organum suriacum*. Food Addit Contam 2007;24 (3) : 274-279.
3. El-Kashoury AA, Mohamed OM, Said NA. Effect of abamectin from different sources on some hormonal, biochemical, immunological and haematological indices in adult male albino rat. Egypt. J. of Appl. Sci. 2005;20 (12) : 32-46.
4. Dalsenter PR, Faqi AS, Chahoud I. Serum testosterone and sexual behavior in rats after prenatal exposure to lindane. Bull. Environ Contam Toxicol 1997; 59: 360-366.
5. Colborn T, Vom Saal FS, Soto AM. Developmental effects of endocrine-disrupting chemicals in wildlife and humans. Environ. Health Perspect 1993;101(5): 378-384.
6. Boas M, Feldt-Rasmussen U, Skakkebaek NE, *et al*,.Environmental chemicals and thyroid function. European J Endocr. 2006;154 : 599-611.
7. Gutteridge JM, Halliwell B. Free radicals and antioxidants in the year 2000: a historical look to the future. Ann N Y Acad Sci 2000; 899: 136-147.

8. Alm H, Tiemann U, Torner H. Influence of organochlorine pesticides on development of mouse embryos *in vitro*. Reprod Toxicol 1996;10 : 321-326.
9. Sharpe RM, Skakkebaek NE. Are oestrogens involved in falling sperm counts and disorders of the male reproductive tract ? The Lancet 1993; 341: 1392-1395.
10. Oschsendorf FR. Infections in the male genital tract and reactive oxygen species. Human Reproduction Update 1999; 5: 399-420.
11. Lenzi A. Lipoperoxidation damage of spermatozoa polyunsaturated fatty acids (PUFA) : Scavenger mechanisms and possible scavenger therapies. Front. Biosc 2000; 5 : 1-15.
12. Ellenhorn MJ, Schanwold S, Ordog G, *et al*. Diagnosis and treatment of human poisoning. 2nd ed., William & Wilkans, pp. 1997;1614-1629.
13. Jadaramkunti UC, Kaliwal BB. Effect of dicofol formulation on estrous cycle and follicular dynamics in albino rats. J. Basi Clin Physiol Pharmacol 1999;1014: 305-314.
14. Jadaramkunti UC, Kaliwal BB. Dicofol formulation induced toxicity on tests and accessory reproductive organs in albino rats. Bull Environ Contam Toxicol 2002 ;69 : 741-748.
15. Sinha N, Narayan R, Shanker R, *et al*. Endosulfan-induced biochemical changes in the testis of rats. Vet Hum Toxicol 1995; 37 (6) : 547-549.
16. Chitra KC, Latchoumycandane C, Mathur PP. Chronic effect of endosulfan on the testicular functions of rat. Asian J. Andrology 1999;1: 203-206.
17. Larson PS. Two-year study on the effect of adding Kelthane to the diet of rats. Medical College of Virginia. Unpublished report submitted to WHO 1957
18. Hazelton GA, Harris JC. Dicofol (Kelthane technical miticide) 24-month dietary chronic/oncogenic study in rats. Unpublished report, No. 89R-190, from Rhom and Haas Company, Spring House, PA, U.S.A., submitted to WHO by Rohm and Haas Company, Spring House, PA, U.S.A. 1989
19. Schalm OW, Veterinary Haematology. 4th Ed. 1986 Lea and Febiger, Philadelphia, pp. 21-86.
20. Banchraft JD, Stevens A, Turner DR. Theory and practice of histological techniques. 4th Ed., Churchill Livingstone, New York, London, San Francisco, Tokyo. 1996
21. Feustan MH, Bodnai KR, Kerstetter SL. Reproductive toxicity of 2-methoxy ethanol applied dermally to occluded and non-occluded sides in male rats. Toxicol. Appl. Pharmacol., 1989 ;100: 145-165.
22. Linder RE, Strader LE, McElroy WK. Measurement of epididymal sperm motility as a test variable in the rat. Bull Environ Contam Toxicol, 1986;36 : 317-324.
23. Krzanowska H, Styrna J, Wabik-Silz B. Analysis of sperm quality in recombinant in bred mouse stain: Correlation of sperm head shape with sperm abnormalities and with the incidence of supplementary spermatozoa in the perivitelline space. J. Reprod Fertil 1995;104 : 347-354.
24. Morel BS, Mercier S, Roux C, *et al*. Inter individual variations in the disomy frequencies of human spermatozoa and their correlation with nuclear maturity as evaluated by aniline blue staining. Fertil. Steril, 1998; 69 : 1122-1127.
25. Jaffe BM, Behrman NR. Method of Hormone Radioimmunoassay. Academic Press 1974.
26. Xing S, Cekan SZ, Diczfalusy UE. Validation of radioimmunoassay for estradiol 17-B by isotope dilution-mass spectrometry and by a test of radiochemical purity. Clinica Chimica Acta 1983;135 : 189-201.
27. Yalow R, Berson S. Principles of competitive protein binding assays. Odell, W. and Daughaday, W. (eds.); J.B. Lippincott Co., Philadelphia, U.S.A. 1971.
28. Santner S, Santen R, Kulin H, *et al*. A model for validation of radioimmunoassay kit reagents : measurement of follotropin and lutropin in blood and urine. Clin Chem 1981; 27: 1892-1895.
29. Britton KF, Guinna V, Brown BL, *et al*. A strategy for thyroid function tests. Br. Med. J., 1975;3: 350-352.
30. Ohkawa H, Ohishi N, Yagi K. Assay for lipid peroxides in animal tissues by thiobarbituric acid reaction. Anal Biochem 1979; 95 : 351-358.
31. Bergmeyer J, Graßl M, Glutathione and Glutathione Disulfide. 3rd Ed. "Methods of Enzymatic Analysis", Vol. III- Metabolites. 3- Lipids, Amino Acids and Related Compounds, pp. 1995; 521-529.
32. Bradford MM. A rapid and sensitive method for the quantitation of microgram quantities of protein utilizing the principle of protein-dye binding. Analyt Biochem 1976 ;72 : 248-254.
33. Babson LA. Phenolphalein monophosphate methods for the determination of alkaline phosphatase. Clin Chem 1965 ;11:789.
34. Babson AL, Ready AP. Colourimetric method for the determination of total and prostatic acid phosphatase. Am J Clin Path 1959;32: 89-91.
35. Moss DW, Henderson AR, Lactate Dehydrogenase. 2nd Ed., Textbook of Clinical Chemistry, Chapter 20, Enzymes, pp. 1994;812-818.

36. Jackson H, Ericsson RJ. Bibliography on effect of chemical agents and hormones on spermatogenesis and the epididymus. Bibliogr. Reprod. 1970;14: 435-600.
37. Jackson H, Chemical methods of male contraception. Amer Sci 1973;61: 188-193.
38. Gomes WR. Pharmacological agents and male fertility in the testes.Vol. IV, pp. 605-628, Johnson, A.D.; Gomes, W.R. (eds.), Academic Press, New York 1977
39. Ben Rhoum K, Tebourbi O, Krichah R, *et al*. Reproductive toxicity of DDT in adult male rats. Hum. Exp. Toxicol, 2001 ;20 (8): 393-397.
40. Chitra KC, Sujatha R, Latchoumycandane C, *et al*. Effect of lindane on antioxidant enzymes in epididymus and epididymal sperm of adult rats. Asian J Androl 2001; 3: 205-208.
41. Sujatha R, Chitra KC, Latchoumycandane C, *et al*. Effect of lindane on testicular antioxidant system and steroidogenic enzymes in adult rats. Asian J Androl 2001; 3: 135-138.
42. Choudhary N, Joshi SC. Reproductive toxicity of endosulfan in male albino rats. Bull Environ Contam Toxicol 2003;70:285-289.
43. Brown M, Casida JE. Metabolism of a dicofol impurity alpha-chloro-DDT, but not dicofol or dechlorodicofol, to DDE in mice and a liver microsomal sytem. Xenobiotica 1987 ;17: 1169-1174.
44. Kaur C, Mangat HK. Effects of estradiol dipropionate on the biochemical composition of testes and accessory sex organs of adult rats. Andrologia, 1980 ;12 (4): 373-378.
45. Takizawa S, Horii I. Endocrinological assessment of toxic effects on the male reproductive system in rats treated with 5-fluorouracil for 2 or 4 weeks. J Toxicol Sci 2002; 27 (1): 49-56.
46. Mann T. Secretory function of the prostate, seminal vesicle and other male accessory organs of reproduction. J Reprod Fertil 1974; 37: 179-188.
47. Mathur PP, Chattopadhyay S. Involvement of lysosomal enzymes in flutamide-induced stimulation of rat testis. Andrologia 1982; 14: 171-176.
48. Prasad RS, Vijayan E. A new non-hormonal antifertility drug DL-204. I- Effects on testes and accessory glands of reproduction in male rats. Contraception 1987;36 (5): 557-566.
49. Bjorndahl L, Söderlund I, Kvist U. Evaluation of the one-step eosin-higrosin staining technique for human sperm vitality assessement. Human Reproduction 2003;18 (4): 813-816.
50. Singh SK, Pandey RS. Differential effects of chronic endosulfan exposure to male rats in relation to hepatic drug metabolism and androgen biotransformation. Indian J Biochem Biophys 1989; 26 : 262-267.
51. Reuber MD. The role of toxicity in the carcinogenicity of endosulfan. Sci Total Environ 1981; 20: 23-47.
52. Moosani N, Pattinson HA, Carter MD, *et al*. Chromosomal analysis of sperm from men with idiopathic infertility using sperm karyotyping and fluorescence in situ hybridization. Fertil. Steril. 1994; 64: 811-817
53. Tag El-Din HA, Abbas HE, El-Kashoury AA. Experimental studies of dicofol reproductive toxicity on male albino rats. Bull Fac Pharm Cairo Univ 2003; 41 (2): 179-188.
54. Rosiak KL, Seo BW, Chu I, *et al*. Effects of maternal exposure to chlorinated biphenyl ethers on thyroid hormone concentration in maternal and juvenile rats. J. Environ Sci Health 1997; 37 (3): 377-393.
55. Hoekstra PF, Burnison BK, Garrison AW. Estrogenic activity of dicofol : Isomer-and enantiomer-specific implications. Chemosphere 2006;64 (1) : 174-177.
56. Mantovani A, Hazard identification and risk assessment of endocrine disrupting chemicals with regard to development effects. Toxicology 2002; 181-182: 367-370.
57. Figà-Talamanca I, Traina ME, Urbani E. Occupational exposures to metals, solvents and pesticides: recent evidence on male reproductive effects and biological markers. Occup Med 2001; 51: 174-188.
58. Gornall AG, Goldbery DM. Hepatobiliary Disorders. In: Applied Biochemistry of Clinical Disorders. Allan G. Gornall, Inc. Virginia Venue, Hagerstown, Maryland, pp. 1980; 164-192.
59. Robinson WF, Huntable CR. Clinicopathological principles for veterinary medicine. Cambridge Univ. Press, New York, Sydney 1988
60. Krause W. Influence of DDT, DDVP and malathion on FSH, LH and testosterone serum levels and testosterone concentration in testes. Bull Environ Contam Toxicol 1977; 18 (2) : 231-242.
61. Desaulniers D, Leingartner K, Wade M. Effects of acute exposure to PCBs 126 and 153 on anterior pituitary and thyroid hormones and FSH isoforms in adult Sprague Dawley male rats. Toxicol Sci 1999; 47(2): 158-169.
62. Lafuente A, Marquez N, Pousada Y, *et al*. Possible estrogenic and/or antiandrogenic effects of methoxychlor on prolactin release in male rats. Arch Toxicol 2000; 74(4-5): 270-275.

63. Foster WG, Desaulniers D, Leingartner K, *et al*. Reproductive effects of tris (4-chlorophenyl) methanol in the rat. Chemosphere 1999; 39 (5) : 709-724.

64. Desaulniers D, Poon R, Phan W, *et al*. Reproductive and thyroid hormone levels in -trichlorobiphenyl)rats following 90-day dietary exposure to PCB 28 (2, 4, 4 or PCB 77 (3, 3`, 4, 4`-tetrachlorobiphenyl). Toxicol Ind Health 1997;13(5) : 627-638.

65. March CM; Goebelsmann U, Nakamura RM, *et al*. Roles of estradiol and progesterone in eliciting the midcycle luteinizing hormone and follicle-stimulating hormone surges. J Clin Endocrinol Metab 1979; 49 : 507-512.

66. Ball HS. Effect of methoxychlor on reproductive systems of the rat. Proc Soc Exp Biol Med 1984; 176: 187-196.

67. Singh SK, Pandey RS. Effect of subchronic endosulfan exposure on plasma gonadotrophins, testosterone, testicular testosterone and enzymes of androgen biosynthesis in rat. Indian J Expt Biol 1990; 28:953-956.

68. Ahlborg UG, Lipworth L, Titus-ernustoff L, *et al*. Organochlorine compounds in relation to breast cancer, endometrial cancer, and endometriosis: an assessment of the biological and epidemiological evidence. Crit Rev Toxicol 1995; 25: 463-531.

69. Barton HA, Andersen ME. Endocrine active compounds: from biology to dose response assessment. Crit Rev Toxicol, 1998; 28:363-423.

70. Solomon HM, Kulwich BA. Dicofol: Two-generation study in rats. Unpublished report No. 89R-o28 from Rohm and Haas Company, Spring House, PA, U.S.A. 1991.

71. Lindane B. The article on dicofol. Pesticides News 1999; 43: 20-21.

72. Stephen H. Hydroxylated polychlorinated Biphenyls (PCBs) and organochlorine pesticides as potential endocrine disruptors. The Handbook of Environ Chemis 2001; 3:155-160.

73. Wiebe JP, Salhanick AI, Myers KI. On the mechanism of action of lead in the testis : *In vitro* suppression of FSH receptors, Cyclic AMP and steroidogenesis. Life Sci1983; 32:1997-2005.

74. Vinggaard AM, Hnida C, Breinholt V. Screening of selected pesticides for inhibition of CYP19 aromatase activity *in vitro*. Toxicol *In vitro* 2000; 14 (3): 227-234.

75. Vanage GR, Dao B, Li XJ, *et al*. Effects of anordiol, an antiestrogen, on the reproductive organs of the male rat. Arch Androl 1997;3 8 (1):13-21.

76. Mably TA, Bjerke DL, Moore RW, *et al*. In utero and lactation exposure of male rats to 2, 3, 7, 8 tetrachloro dibenzo-p-dioxin. Toxicol Appl Pharmacol 1992; 114:118-126.

77. Caroll RS, KowashM, Lofgren JA. *In vivo* regulation of FSH synthesis by inhibin and activin. Endocrinol 1991 ; 129:3299-3304.

78. Hill RN; Erdreich LS, Paynter OE, *et al*. Thyroid follicular cell carcinogenesis. Fundam Appl Toxicol 1989;12: 629-697.

79. Capen CC. Toxic responses of the endocrine system. In: Casarett and Doull's Toxicology : The Basic Science of Poisons, Klaassen, C.D. (Ed.), McGraw-Hill, New York.1996;617-640

80. Maran RR, Aruldhas MM. Adverse effects of neonatal hypothyroidism on Wistar rat spermatogenesis. Endocr Res 2002;28 (3) :141-154.

81. El-Kashoury AA, Mansour MK. Chronic exposure to organochlorine pesticide, dicofol, induced oxidative stress in testes of albino rats. Bull Fac Pharm Cairo Univ 200745 (3):245-252.

82. Hotz KJ, Wilson AG, Thake DC, *et al*. Mechanism of thiazopyr induced effects of thyroid hormone homeostasis in male Sprague-Dawley rats. Toxicol Appl Pharmacol 1997;142 (1) :133-142.

83. Heussen GA, Schefferlie GJ, Talsma MJ. Effect on thyroid hormone metabolism and depletion of lung vitamin A in rats by airborne particulate mater. J Toxicol Environ Health 1993;38 (4):419-434.

84. Van den Bery KJ, Van Raaj JA, Bragt PC. Interactions of halogenated industrial chemicals with transthyretin and effects on thyroid hormone levels *in vivo*. Arch. Toxicol., 1991; 56 (1):15-19.

85. Fisher JW, Campell J, Muralidhara S, *et al*. Effect of PCB126 on hepatic metabolism of thyroxin and perturbations in the hypothalamic-pituitary-thyroid axis in the rat. Toxicol Sci 2006; 90 :87-95.

86. Villa R, Bonetti E, Penza ML, *et al*. Target specific action of organochlorine compounds in reproductive and non-reproductive tissues of estrogen reporter male mice. Toxicol Appl Pharmacol 2004; 1 (2):137-148.

87. Martinez JM, Afshari CA, Buskel, PR, *et al*. Differential toxiciogenamic responses to 2,3,7,8 tetra-hydrochloro dibenzo-p-dioxin in malignant and non malignant human airway epithelial cells. Toxicol. Sci., 2002;69:409-423.

88. Lund J, Devereux T, Glaumann H, *et al*. Cellular and subcellular localization of a binding protein of PCB in rat lung. Drug Metab Perspect 1988; 109: 105-106.

89. Dacroix M, Hantella A. The organochlorine DDD disrupts the adrenal straidogenesis signaling pathway in rainbow trout. Toxicol. Appl. Pharmacol., 2003; 190(3):33-39.

90. Mansour S.A. Pesticides exposure. Egypt Sci Toxicol 2004;198 (1-3):91-115.

91. Ahmed R.S, Seth V, Pasha S.T. Influence of dietary ginger (*Zingiber officinale* rose) on oxidative stress induced by malathion in rats. Food and Chem Toxicol 2000; 38:443-450.

92. Ichikawa T, Oeda T, Ohmori H, *et al*. Reactive oxygen species influence the acrosome reaction but not acrosin activity in human spermatozoa. Int J Androl 1999; 22:37-42.

93. Verma RS, Mehta A, Srivastava N. *In vivo* chlorpyrifos induced oxidative stress: Attenuation by antioxidant vitamins. Pestic Biochem and Physiol 2007; 88:191-196.

94. Kale M, Rathore N, John S, *et al*. Lipid peroxidative damage on pyrethroid exposure and alterations in antioxidant status in rat erythrocytes : a possible involvement of reactive oxygen species. Toxicology letters 1999;105:197-205.

95. Sharma Y, Bashir S, Irshad M, *et al*. Dimethoate-induced effects on antioxidant status of liver and brain of rats following subchronic exposure. Toxicology, 2005; 215:173-181.

96. Latchoumycandane C, Chitra KC, Mathur PP. The effect of methoxychlor on the epididymal antioxidant system of adult rats. Reprod Toxicol 2002;16(2) :161-172.

97. Latchoumycandane C, Mathur PP. Effect of methoxychlor on the antioxidant system in mitochondrial and microsome-rich fractions of rat testes. Toxicology 2002;176 (1-2):67-75.

98. Kwon GS, Sohn HY, Shin KS, *et al*. Biodegradation of organochlorine insecticide, endosulfan and the toxic metabolite endosulfan sulfate by Kelbsiella oxytoca. App Microbiol Biol, 2005;67 (6):845-856

99. Latchoumycandane C, Chitra KC, Mathur PP. 2, 3, 7, 8-tetrachlorodibenzo-p-dioxin (TCDD) induces oxidative stress in the epididymus and epididymal sperm of adult rats. Arch Toxicol, 2003; 77 (5):280-284.

100. Fernandez A, Kiefer J, Fosdick L, *et al*. Oxygen radical production and thiol depletion are required for Ca (2+)-mediated endogenous endonuclease activation in apoptotic thymocyt. J Immunol, 1995;155:5133-5139.

101. Younes M, Siegers CP. Mechanistic aspects of enhanced lipid peroxidation following glutathione depletion *in vivo*. Chem. Biol. Interact, 1981; 34: 257-266.

102. Goel A, Dina V, Dhawan DK. Protective effects of zinc on lipid peroxidation, antioxidant enzymes and hepatic histoarchitecture in chlorpyrifos-induced toxicity. Chem Biol Inter 2005 ;156:131-140.

103. Tithof RK, Oliver J, Ruehle K. Activation of neutrophil calcium dependent and independent phospholipase A_2 by organochlorine compounds. Toxicol Sci 2000; 53 (1): 40-47.

104. Selzak BP, Hatch GE, Devito M, *et al*. Oxidative stress in female B6C3 FI mice following acute and subchronic exposure of TCDD. Toxicol Sci 2000; 54:390-398.

105. Luna Samanta, GBN Chainy. Response of testicular antioxidant enzymes to hexachlorocyclohexane is species specific. Asian J Androl 2002; 4: 191-194.

106. Saradha B, Mathur PP. Induction of oxidative stress by lindane in epididymis of adult male rats. Environ. Toxicol and Pharmacol 2006; 22: 90-96.

107. Wei YH, Lee H. Oxidative stress, mitochondrial DNA mutation and impairment of antioxidant enzymes in aging. Exp Biol Med 2001; 227:671-682.

108. Holmes GE, Bernstein C, Bernstein H. Oxidative and other DNA damages as the basis of aging : a review. Mutat Res 1992; 275: 305-315.

109. Sanz N, Diez-Fernandez C, Alvarez A, *et al*. Age-dependent modifications in the rat hepatocyte antioxidant defense systems. J Hepatol 1997; 27:525-534.

110. Brooks DE. Effect of androgen on protein synthesis and secretion in various regions of the rat epididymis, as analysed by two dimensional gel electrophoresis. Mol Cell Endocrinol 1983;29:255-270.

111. Shivanandappa T, Krishnakumari MK. Histochemical and biochemical changes in rats fed dietary Benzene hexachloride. Indian J Exp, 1981; 19:1163-1168.

112. Bhatnagar VK, Malviya AN. Changes in some biochemical indices in rat upon pesticide toxicity. Indian J Biochem Biophys, 1986;15 : 78-81.

113. Rao MV, Chinoy NJ. Effect of estradiol benzoate on reproductive organs and fertility in the male rat. Eur J Obstet Gynecol Reprod Biol, 1983; 15 (3) :189-198.

114. Yousef GM, Diamandis M, Jung K. Molecular cloning of a novel human acid phoshatase gene that is highly expressed in the testes. Genomics, 2001;74 (3):385-395.

115. Latchoumycandane C, Gupta S.K, Mathur P.P. Inhibitory effects of hypothyrodism on the testicular functions of postnatal rats. Biomed Lett, 1997; 56 : 171-177.

116. Mollenhauer HH, Morre DJ, Rowe LD. Alteration of intracellular traffic by monensin: mechanism, specificity and relationship to toxicity. Biochem Biophys Acta, 1990; 1031: 225-246.

117. Kamp G, Büsselmann G, Lauterwein J. Spermatozoa : models for studying regulatory aspects of energy metabolism. Experientia, 1996 ;52 :487-494.

118. Petrie A. Watson p Statistics for veterinary and animal science. 1st Ed., pp90-99, the Blackwell Science Ltd, United Kingdom. 1999.

Antifungal Properties and Phytochemical Screening of Crude Extract of *Lemna pauciscostata* (Helgelm) Against Fish Feed Spoilage Fungi

Effiong BN[1] , Sanni A[2]

[1]*Dept of Fisheries Technology, Federal College of Freshwater Fisheries Technology, P.M.B 1500,New Bussa, Nigeria.*
[2]*Dept of Microbiology, University of Ilorin, Ilorin, Nigeria.*

Received Febrary 21, 2009

Abstract

Aqueous and ethanolic extracts of duckweed (*Lemna pauciscostata*) meal was tested on fungal isolates from stored pelleted fish feeds to ascertain its efficacy as an antifungal agent against feed spoilage fungi. Test organisms used were *Fusarium oxysporium, Penicillium digitatum, A. niger, A.flavus, A.fumigatus, Rhizopus oryzae and .stolonifer* .Phytochemical analysis of the crude extract was also conducted to determine the active ingredients in duckweed meal. Proximate nutrient composition and amino acid analysis to determine the suitability or otherwise of duckweed meal as a feed additive was also carried out. Results showed that ethanolic extracts exhibited higher antifungal properties with total growth inhibition in some test organisms than the aqueous extract. However the efficacy of the extracts against fungal growth increased with increase in concentration. Result of the phytochemical analysis of duckweed meal revealed the presence of tannins and steroids. Determination of the proximate nutrient composition and amino acid analysis also showed that duckweed meal is rich in essential nutrients. [Life Science Journal. 2009; 6(3): 19 – 22] (ISSN: 1097 – 8135)

Keywords: duckweed meal; antifungal; extract; ethanolic; aqueous

1. Introduction

Antimicrobial agents, including food preservatives have been used to inhibit food borne fungi and extend shelf life of processed food for many centuries. Many naturally occurring compounds found in edible and medicinal plants, herbs and spices have been shown to posses' antimicrobial functions and could serve as agents against food spoilage micro-organisms[1,2]. Tannins and steroids have been shown to possess antimicrobial ability against several food spoilage fungi [3,4].

Lemna, a group of tiny, free-floating vascular plants with worldwide distribution are found in small water bodies such as fishponds, ditches and lagoons, which are nutrient rich. Their ability to bloom within days after cultivation with high nutrient content has made them a rich source of food nutrients in the diet of fishes and animals alike. Lemna have been shown to exhibit antimicrobial activity[5,6].

A major problem in fish feed production is associated with storage. A lot of losses occur in feedstuff during storage. Fungal attacks along with other kinds of storage problems are responsible for unreasonable losses occurring in feedstuff during storage. Such losses are loss in weight, loss in quality of feed and health risks to fish that feed on infected feed.

The addition of some fungicides could suppress the growth of fungi in feed, however as with all pesticides, these chemicals are likely to have side effects which may be hazardous to fish health. Therefore if a non-hazardous process could be found capable of suppressing or even eliminating fungal growth in stored compound feed, it would be of immense practical and economic benefits to the aquaculture industry in Nigeria.

Fungal isolates from stored pelleted fish feeds were therefore utilized as test organisms on extracts of *Lemna pauciscostata* used directly as fish feed.

2. Materials and Method

Samples of duckweed (*Lemna pauciscostata*) were harvested from the outdoor concrete tanks of National Institute of Freshwater Fisheries Research Hatchery Complex, New Bussa, Nigeria. They were thoroughly rinsed with clean water and evenly spread on a mosquito net-size mesh to dry and thereafter dried in a forced air oven at 65℃ for 48 hours before being grounded to powder with a milling machine[7]. The powder was exhaustively extracted with 95% Ethanol and sterile distilled water at room temperature for 2 days.

Extracts were filtered and the solvent removed under reduced pressure at 40℃[8]. Preliminary antifungal assays were performed using seven test organisms and extracts at concentrations of 5% and 10% respectively. Control plates had 95% ethanol and sterile distilled water without extracts. Mycelial plugs of the test organisms measuring 5.0 mm in diameter were cut with sterile cork borer from the advancing margin of the fungal colonies and placed at the centre of Potato Dextrose Agar[9].All plates were incubated at 25℃ and radial mycelial growth recorded.

Dried duckweed was ground using Automatic weed Grinder (Scientific Instrument, Yoshida Seikusho Co. Ltd, Tokyo, Japan, No. 5678). Extracts for phytochemical analysis were concentrated to dryness in hot air oven at 45℃[10]. The dried extracts were tested for alkaloids, saponins, tannins, anthraquinones, flavonoids, steroids and phlobatannins[11]. Proximate composition of the following nutrients was determined using standard procedures of AOAC[12]: moisture, crude protein, lipid, crude fiber and Nitrogen free extract (NFE). Amino acid profile of duckweed meal was determined using the method of Abdullahi[13].

3. Results and Discussion

Differential efficacy on the test organisms was noted between the aqueous and ethanolic extracts of *Lemna pauciscostata* (Table 1). Ethanol appeared a better

extractant judging from the wider activity spectrum and the effect of its extract on isolates. This observation perhaps suggests the possibility of the occurrence of bioactive substances that are not only soluble in water but also in organic solvent in the plant material.

Majekodunmi *et al*.[14] and Martinez *et al*.[15] reported that a higher activity of extractable natural products was obtained in ethanol compared with aqueous extracts. Ahmed *et al*.[16] also observed that alcoholic extracts showed greater activity than the aqueous and hexane extract of some Indian medicinal plants with antimicrobial properties. While ethanolic extracts showed total growth inhibition on some organisms even at 5% concentration, aqueous extract showed none although; growth rate was slower at the 10% aqueous than 5% aqueous extract. The most susceptible isolates to both the aqueous and ethanolic extracts were *Aspergillus fumigatus* and *Fusarium oxysporium* where total growth inhibition was observed.

Several authors have reported on the antimicrobial activity of various plant extracts using different means of extraction on various plants materials. Natarajan *et al*.[17] reported the antifungal properties of three medicinal plant extracts against *Cercospora arachidicola*. They reported that fungal growth was gradually suppressed with increasing extract concentration. Similar findings have been reported by Lucia *et al*.[3] on the antifungal properties of Brazilian cerrado plants. They stated that ethanolic extracts of the plants showed higher antifungal activity.

Silva *et al*.[18] and Costa *et a.l*[4] also reported the antifungal activity of extracts of *Eugenia dysentrica* and *Annora crassiflora* against some pathogenic fungi. The findings from this study are similar to the report of these authors.

Adekunle and Ikunmapayi (2006) working on the antifungal properties and phytochemical screening of the crude extracts of *Funtumia elastica* and *Mallotus oppositifolius* reported varying degrees of antifungal activity of the plant extracts on some test organisms including *Aspergillus flavus* and *Penicillium* species. The same authors reported that the ethanolic extracts of the plants showed higher antifungal activity on the test organisms than the aqueous extracts.

The result of the phytochemical screening of the *Lemna pauciscostata* extracts (Table 2) revealed the presence of tannins and steroids. Research findings from several authors have shown that both tannins and steroids possess antimicrobial ability. Bairagi *et al*.[19] reported the presence of tannins and phytic acid in duckweed meal. Baba Moussa *et al.* [20] reported antifungal activities of seven West African combretaceae extracts used in traditional medicine against several fungal species. The result of the phytochemical screening of these plant extracts showed that they were rich in tannins and saponins.

Table 1: Efficacy of duckweed extracts on the mycelial growth of fungal isolates after 72 Hours.

TEST ORGANISMS	MYCELIAL GROWTH IN MM					
	AQUEOUS EXTRACT			ETHANOLIC EXTRACTS		
	0%	5%	10%	0 %	5%	10%
Fusarium oxysporium	46	21	10	10	-	-
Penicillium digitatum	50	35	24	9	5	-
Aspergillus niger	47	27	18	16	7	2
Aspergillus fumigatus	38	18	12	4	-	-
Aspergillus flavus	50	38	20	16	-	-
Rhizopus oryzae	36	29	16	14	-	-
Rhizopus stolonifer	42	21	13	22	10	4

Table 2:Phytochemical analysis of duckweed meal.

Test	Result
Alkaloids	-
Saponins	-
Tannins	+
Anthraquinones	-
Flavonoids	-
Phlobatannins	-
Steroids	+

Table 3: Proximate composition of duckweed (*Lemna pauciscostata*) meal

Sample	% Crude Protein	% Ether Extract	% Ash Content	% Moisture Content	% Crude Fiber
Duckweed	34.18	5.3	13.55	2.8	14.28

Adekunle and Ikunimapayi (2006) reported the presence of tannins,, saponins and steroids among other substances from the extracts of *Funtumia_elastica* and *Mallotus oppositifolius* which they inferred were likely to be responsible for the antifungal activity exhibited by these plants. Other authors have also reported similar findings[21-25]. Burapedjo and Bunchoo[26] implicated these phytochemicals to inhibit cell wall formation in fungi leading to the death of the organisms. The findings of this experiment are similar to the report of these authors.

The results of the proximate composition of nutrients as well as that of amino acid profile in Tables 3 and 4 respectively showed that duckweed meal is rich in essential nutrients. Therefore, incorporating it into fish feed formulation will not cause any negative effect to fish growth and survival. Several authors have reported the use of duckweed as fish feed ingredient[27-31].

Table 4: Amino acid analysis of duckweed meal.

AMINO ACID	AMOUNT
LYSINE	5.30
HISTIDINE	2.03

4. Conclusion

From the findings of this experiment, there are indications that duckweed meal could be incorporated into formulated fish feeds to serve as antifungal agent against feed spoilage fungi. This will be of immense benefit to the local fish farmers and therefore improvement in the fisheries aquaculture practice in Nigeria.

References

1. Deans SG, Ritchie GA. Antimicrobial properties of plants essential oils. Int. J. Food Microbio. 1987; l (5): 165– 180.
2. Janssen AM, Scheffer JJC, Svendsen A, *et al*. Composition and antimicrobial activity of essential oil of Ducrosia anethifolia. In Essential oils and Aromatic plants; Svendsen, A. B, Scheffer, J .J.C; Eds; Martinus Nijloff Publishers: Dordrecht. The Netherlands Pp. 1985:213 – 216.
3. Lucia KHS, Cecilia ADO, Pedro NF, *et al*. Antifungal properties of Brazillian carrado plants. Braz. J. Microbiology. 2002; 33(3): 102-107.
4. Costa TR, Fernandes OFL, Santos SC, *et al*. Antifungal activity of volatile constituents of *Euglenia dysentrica* leaf oil J. Ethno Pharmacol. 2000; 72: 111-117.
5. Skilicorn P, Spirar W, Journey W. Duckweed Aquaculture: A new Aquatic farming system for Developing countries. A World Bank Publication 76P. National Agricultural Research Project (NARP), Nigeria. 1993;309.
6. Mbagwu IG. The effect of long-term storage on the nutrient characteristics of duckweed (*Lemna pauciscostata* Helgelm) J.Arid Agric. 2001; 11:147-149.
7. Mbagwu IG, Adeniyi HA. The nutritional content of Duckweed (*Lemna pauciscostata* helgelm) in the Kainji Lake Area - Nigeria. Aquatic Botany 1988; 375-366.
8. Souza LKH, Oliveira CMA, Ferri PH, *et al*. Antifungal properties of Brazilian cerrado plants. Braz. J. Microbiology.2002; 33(3) 121-124.
9. Adedayo O, Kolawole DO. Resistance of mouse-virulent encapsulated nasal isolates of *Staphylococcus aureus* to disinfectant and antiseptics. Biomedical letters 1994; 50: 151 -156.
10. Odebiyi OO, Sofowora EA. Phytochemical screening of Nigerian Medicinal plants II. Lloydia. 1978; 41(3): 234-236.
11. Harbone JB. Phytochemical methods: A guide to modern techniques of plant analysis. 2nd Edition. Chapman and Hall. 1984; 4-18, 288.
12. AOAC."Official Methods of Analysis" 17th Ed;Association of of official Analytical chemists, 2000;Washington, D.C
13. Abdullahi SA. Investigation of Nutritional status of *Chrysichthys nigrodigitatus*, *Barus filamentous* and *Auchenoglanis occidentalis*: Family Barigdae. Journal of Arid Zone Fisheries 2001; 1:39-50.
14. Majekodunmi OF, Zany L, Ohayaga IE, *et al*. Selective cytotoxic diterpene from Euphorbia poisonic. Journal of Medicinal Chemistry 1996; 39(4): 1005-1008.
15. Martinez MJ, Betancant I, Alonso-Gonzalez N, *et al*. Screening of some Cuban medicinal plants for antimicrobial activity. Journal of Ethano-Pharmacology. 1996;52: 171-174.
16. Ahmad I, Mechmood Z, Mohammed F. Screening of some Indian Medicinal plants for antimicrobial properties. Journal of Ethano Pharmacology. 1998;62(2):183-193.
17. Natajaran D, Srinivasan K, Mohanasoundari C *et al*. Antifungal properties of three medicinal plant extracts against *Cercospora arachicola*. Advances in plant Sciences. 2005;18(1): 45-47.
18. Silva MV, Costa TR, Costa MR, *et al*. Growth inhibition effect of Brazillian cerrado plant extracts on candida species. Pharm. Biol. 2001;39: 138-141.
19. Bairagi A, SarkarGhosh K, Sen SK. *et al*. Duckweed (*Lemna polyrrhiza*) leaf meal as a source of feedstuff in formulated diets for rohu (*Labeo rohita* Ham) fingerlings after formulation with a fish intestinal bacterium. Bio resour-Technol. 2002;85(1): 17-23.
20. Baba Moussa F, Akpagana K, Bouchet P. Antifungal activities of seven West African combretaceae used in traditional medicine.Journal of Ethno pharmacology. 1999; 66(3): 335 – 338.
21. Onadapo A. Owonubi CA. The antimicrobial properties of Tremaguineensis. In: 1st NAAP Proceedings. Faculty of Pharmaceutical Science ABU, Zaria. 1993;139-144.
22. Barnabas CG. Nagarajan S. Antimicrobial flavonoids of some medicinal plants.Fitoterapia 1988;3: 508-510.
23. Adekunle AA, Duru C, Odufuwa OM. Antifungal activity and phytochemical screening of the crude extracts of *Khaya ivorensis* Juss (meliaceae) and *Tetracera potabria* L. (Dileniaceae) South African Journal of Botany. 2003;69: 568-571.
24. Subhisha S, Subramoniam A. Steroid screened from Pallavicinia Iyelli against four test organisms. Indian Journal of Pharmaceutics. 2005 ;37(5): 304-208.
25. Adio AM, Paul C, Kloth P, *et al*. Sesquisterpenes of the liverwort, *Scapania undulata*. Phytochemistry. 2004;65: 199-206.

26. Burapedjo S, Bunchoo A. Antimicrobial activity of tannins from *Terminalia citrina.* Plant medica.1995; 61:365-366.
27. Fasakin EA, Balogun AM. Evaluation of dried water fern (*Azolla-pinnata*) as a replacer for soybean dietary components for *Clarias gariepinus* fingerlings. Journal of Aquaculture in the Tropics. 1998;13(1):57-64.
28. Fasakin EA, Balogun AM, Fagbenro OA. Evaluation of sun dried water fern *Azolla africana*, and Duckweed, *Spirodela polyrrhiza*, in practical diets for Nile Tilapia, Orechromis niloticus fingerlings. Journal of Applied Aquaculture.2001; 11(4):83-92.
29. Fasakin EA, Balogun AM, Fasuru. Use of Duckweed, Spirodela polyrrhiza L.Schleiden, as a protein feedstuff in practical diets for Tilapia, *Orechromis niloticus* L. Aquaculture Research.1999; 30(5):313-318.
30. Edwards P. Food potential of Aquatic Macrophytes, ICLARM Studies and Reviews. The International Centre for Living Resources Management, Makati, Metro Manila, Philippines.1980;261-265.
31. Robinette HR, Brunson MW, Day EJ. Use of duckweed in diets of channel catfish. Mississippi Agricultural Experiment Station. Publication No. 4532. Mississippi State University, Mississippi State, Miss. 1980;13.

Clinical Application of ABCD^2 Score System

Tan Song, Zhao Lu, Song Bo, Li Zhuo, Zhang Rui, Gao Yuan, Xu Yuming*

Department of neurology, the First Affiliated Hospital of Zhengzhou University, Zhengzhou, Henan 450052, China

Received March 10, 2009

Abstract

There is a high early risk of stroke after a transient ischemic attack (TIA). ABCD^2 score system is a useful tool to predict the risk of stroke for the patients with TIA. It's necessary to make validation in different ethnic groups. In this study, we prospectively recruited 136 TIA patients in Henan province. Nine patients with ischemic stroke at 2-day follow-up and sixteen patients at 7-day follow-up were recorded. The risk of stroke increases with the increasing of the score. 2-day and 7-day Area Under Receiver Operating Characteristic Curve (AUROCC) of ABCD^2 score is 0.804 and 0.764 respectively. The cut-off point is at 4. The sensitivity of ABCD^2 score at 2-day and 7-day was 88.9% and 87.5% respectively. The specificity of ABCD^2 score at 2-day and 7-day was 55.9% and 58.3%. Multivariate Logistic regression analyses demonstrated that ABCD^2 score of 4 to7 was the independent predictive factor of stroke after TIA (2-day multivariate Logistic regression analyses: OR9.578, 95%C.I. 1.146-80.059, P=0.037; 7-day multivariate Logistic regression analyses: OR13.458, 95%C.I. 2.516-71.978, P=0.002). Thus, ABCD^2 score could be validated in identifying patients at high risk of stroke after TIA in Henan Chinese population. [Life Science Journal. 2009; 6(3): 23 – 26] (ISSN: 1097 – 8135).

Key Words: ABCD^2 score; transient ischemic attack; stroke; risk

1 Introduction

High early risk of stroke after a transient ischemic attack (TIA) has been reported[1,2,3]. Johnston et al proposed ABCD^2 Score to predict well of the risk of stroke in 2 days after TIA[4]. Since the ABCD^2 Score was published in January 2007, validation for different ethnic group is not completed yet. To validate ABCD^2 score in identifying high early risk of stroke in China, we studied the patients prospectively with ABCD^2 score by 2-day and 7-day follow-up after TIA being registered outpatient and inpatient in neurology department of the First Affiliated Hospital of Zhengzhou University..

2 Methods

The TIA diagnosis is based on the TIA diagnostic criteria of World Health Organization 1976 [5]. The elapsed time from last episode to registry was less than 48 hours. Patients who could not describe the situation of the attack or provide the past history due to cognition impairment or other causes and patients who rejected participating in the research as well as patients who could not cooperate to accomplish the follow-up were excluded.

Consecutive TIA patients were registered prospectively. ABCD^2 scores were documented. Meanwhile, TIA registry forms were filled by neurological physicians with unified training. ABCD^2 score is graded by the following: Age (≥60 years=1, ＜60years=0 ; Blood pressure(systolic≥140mmHg and/or diastolic≥90 mmHg=1, systolic＜140 mmHg and diastolic＜90 mmHg=0; Clinical manifestation(unilateral weakness=2, speech impairment without weakness=1, other symptom=0); duration of symptom(≥60minutes=2, 10 to 59minutes=1, ＜60minutes=0; diabetes(yes=1, no=0). Patients were followed-up to document subsequent stroke and medication at 2 and 7 days respectively.

First authors: Tan Song, Zhao Lu

*Corresponding author. Email: xuyuming@zzu.edu.cn

The study is supported by Natrual Science Program of Education Department of Henan province (Grant No. 2008A320028)

Differences in stroke-free survival between groups stratified by $ABCD^2$ score were assessed for statistical significance with the log-rank test. Sensitivities and specificities of prediction were determined at each cut-off of the score and the receiver operating characteristic curve (ROC) was plotted. Logistic regression analysis was used to identify factors that increased the risk of subsequent stroke after TIA. Factors that contributed to the outcome in the initial univariate analyses at $P<0.1$ were included in the multivariate model. In the final multivariate analyses, statistical significance was achieved if $P<0.05$. The Statistic Package for Social Science version 10.0 was used for statistical analysis.

3 Results

136 TIA patients participated in the study. The distribution of the $ABCD^2$ score was shown in Table 1. Within 2 days of TIA, 9 (6.6%) patients had a subsequent ischemic stroke and within 7 days of TIA, 16 (11.8%) patients had a subsequent ischemic stroke.

The 2- and 7-day risk of stroke stratified according to $ABCD^2$ score were presented in Table 1. The risk of stroke increased according to the increase of the score.

Table 1. 2- and 7-day risk of stroke stratified according to $ABCD^2$ score

$ABCD^2$ score	Patients	2 days		7 days	
		Strokes	Risk * (%，95%CI)	Strokes	Risk * * (%，95%CI)
0	4	0	0	0	0
1	12	0	0	0	0
2	20	0	0	1	5.0(0-25.0)
3	36	1	2.8(0-15.0)	1	2.8(0-15.0)
4	40	3	7.5(2.0-21.0)	8	20.0(9.0-35.0)
5	18	3	16.7(4.0-41.0)	4	22.2(6.0-48.0)
6	4	1	25.0(1.0-81.0)	1	25.0(1.0-81.0)
7	2	1	50.0(1.0-99.0)	1	50.0(1.0-99.0)
合计	136	9	6.6(2.4-10.8)	16	11.8（6.4-17.2）

* Log-rank test=16.57，df=7，P=0.0204; * * Log-rank test=15.87，df=7，P=0.0263

The receiver operating characteristic curves were plotted (Figure 1 and 2).2- and 7-day area under receiver operating characteristic curve (AUROCC) of $ABCD^2$ score is 0.804 and 0.764 respectively. The cut-off point was determined by presetting the sensitivity (low limit is 80%) and the cut-off point is 4. Validation of the cut-off point was seen in table 2.

.

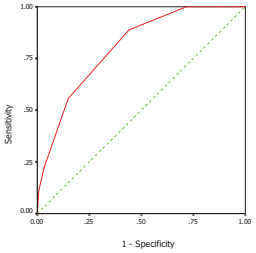

Figure 1. 2-day ROC

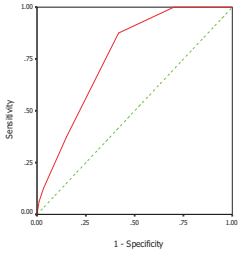

Figure 2. 7-day ROC

Table 2. Validation of the cut-off point

	2-day	7-day
sensetivity	88.9%	87.5%
false negative rate	11.1%	12.5%
specifity	55.9%	58.3%
false positive rate	44.1%	41.7%

The association of the gender, ABCD^2 score (4-7 versus 0-3), stroke risk factors and secondary prevention therapies with the risk of subsequent stroke was evaluated using univariate Logistic regression analyses. The variables which were significantly (P<0.1) related to subsequent stroke were selected for entry into the final multiple-variable model. The results of multivariate Logistic regression analyses were seen in table 3 and 4.

Table 3. 2-day Logistic regression analyses

	B	SE	Wald	Sig	Exp(B)	95%C.I.for Exp(B)	
						Lower	Upper
ABCD^{2}score	2.259	1.083	4.350	0.037	9.578	1.146	80.059

Table 4. 7-day Logistic regression analyses

	B	SE	Wald	Sig	Exp(B)	95%C.I.for Exp(B)	
						Lower	Upper
ABCD^{2}score	2.600	0.856	9.233	0.002	13.458	2.516	71.978
hypertension	1.531	0.719	4.536	0.033	4.624	1.130	18.921
hyperlipidemia	1.739	0.804	4.683	0.030	5.691	1.178	27.487

4 Discussion

The short-term stroke risk after a TIA is very high. The research of the Oxfordshire Community Stroke Project reported a 7-day stroke risk of 8.6% and a 30-day stroke risk of 12.0% in patients with TIA. Analyses of the Greater Cincinnati/Northern Kentucky stroke study found the risk of stroke after TIA was 3.9% at 2days, 7.0% at 7days, and 14.6% at 90 days. This study showed a 6.6% risk of stroke at 2 days and an 11.8% risk at 7 days, revealing a high early risk of stroke after a TIA. Therefore TIA should be considered as “minor stroke, high risk”.

The risk of stroke was higher according to the increase of the score. 2-day and 7-day AUROCC of ABCD^2 score was in the range from 0.7 to 0.9 which indicated moderate predictive value of ABCD^2 score. The sensitivity and specificity was about 85% and 56% respectively, and the high sensitivity met the principle of screening test. After adjustment for the other factors, an ABCD^2 score of 4 to 7 was independently associated with 9.5-fold and 13-fold greater 2-day and 7-day risk of stroke respectively.

Guideline recommendations for hospital admission of TIA are vague and practice is highly variable[6]. Some examinations and interventions for TIA patients are expensive and may not be cost effective if used in all TIA patients. ABCD^2 score might help clinicians to stratify TIA patients and determine which patients should be admitted, assessed and treated as soon as possible. A cost-utility analyses showed an ABCD^2 score of 4 to7 might justify 24h hospital admission on the basis of a greater chance to administer thrombolysis given the subsequent stroke[7]. Cut-off points of different interventions might vary. Same intervention also might has different cut-off in different regions. However, high risk TIA patients (ABCD^2 score: 6-7) benefit from urgent assessment and treatment. Low risk patients (ABCD^2

score: 0-3) are not need for hospital admission. And the need of admission for moderate risk patients ($ABCD^2$

score: 4-5) depends on specific individual conditions and medical system[4]. The stratification of TIA patients can decrease stroke risk and abuse of medical resources. $ABCD^2$ score is easy for clinical practice and helpful to identify the high risk TIA patients.

Reference

1. Johnston SC, Gress DR, Browner WS, et al. Short-term prognosis after emergency-department diagnosis of transient ischemic attack [J]. JAMA, 2000, 284: 2901–2906.
2. Lovett JK, Dennis MS,Sandercock PA, et al. Very early risk of stroke after a first transient ischemic attack [J]. Stroke, 2003, 34: 138–140.
3. Kleindorfer D, Panagos P, Pancioli A, et al. Incidence and short-term prognosis of transient ischemic attack in a population-based study [J]. Stroke, 2005, 36: 720–723.
4. Johnston SC, Rothwell PM, Nguyen-Huynh MN, et al. Validation and refinement of scores to predict very early stroke risk after transient ischemic attack [J]. Lancet, 2007, 369: 283–292.
5. Hatano S. Experience from a multicentre stroke register: a preliminary report [J]. Bull WHO, 1976, 56: 541–553.
6. Johnston SC, Smith WS. Practice variability in management of transient ischemic attacks [J]. Eur Neurol, 1999, 42: 105–108.
7. Nguyen-Huynh MN, Johnston SC. Is hospitalization after TIA cost-effective on the basis of treatment with tPA? [J] Neurology, 2005, 65: 1799–1801.

Research on the relationship between the polymorphisms of Methionine synthase (MS A2756G) gene and ischemic cerebrovascular disease

Li Aifan[1], Zheng Hong [2], Xu Yuming [3*], Zhang Xiaoman [1], Song Bo[3]

[1] Department of Neurology, the First People's Hospital of Zhengzhou city, Zheng zhou 450000, China; [2] Department of Cell Biology and Medical Genetics, College of Basic Medical Sciences, Zhengzhou University, Zheng zhou 450052, China ; [3] Department of Neurology, the First Affiliated Hospital, Zhengzhou University, Zheng zhou 450052, China

Abstract

Objective: To explore the relationship between the polymorphisms of Methionine synthase (MS A2756G) gene and ischemic cerebrovascular disease. *Methods*: The genotypes of MS A2756G were determined by PCR-RFLP, in 512 patients with ischemic cerebrovascular disease and 500 healthy controls in Henan Han population. *Result*: The distribution of genotype and allele in MS A2756G had no significant difference between the patient and the control groups, while the frequencies of MS A2756G mutations had significant differences between the Henan Han population and other races. *Conclusion*: Gene mutations as MS A2756G may not be independent risk factors for ischemic cardiovascular in Northern Chinese Han population. The prevalence of MS A2756G may vary among different ethnic groups or geographic regions. [Life Science Journal. 2009; 6(3): 27 – 31] (ISSN: 1097 – 8135)

Key words: Ischemic cerebrovascular disease, Methionine synthase, Polymorphism

1 Introduction

CVD, which has high incidence and mortality and disability, is a common and dangerous disease and now has become one of three most fatal diseases. Among them, ICVD is up to 80%. The etiology of ICVD is complicated and not understood completely until now. New researches have discovered that ICVD is related with both hereditary and environmental factors.

Recently, many researchers focus on the predisposing genes of the related risk factors of cerebral infarction. Several recent studies have shown that Hyperhomocysteinemia (HHcy) is increasingly one of the more important and independent risk factors for thrombotic vascular or arteriosclerotic diseases[1,2,3] . Therefore, the metabolism-relative enzyme of Hcy has become one of candidate genes. But the correlation between the mutations of MS A2756G and ischemic cerebrovascular disease remains controversial. The aim of the present study was to investigate the association between the polymorphism of MS A2756G gene and ischemic stroke in a case-control study in the Han population in Chinese of Henan.

This work was supported by the science foundation for prominent youth of Henan (No.0612001300) and Henan innovation project for university prominent research talents(No.2005KYCX020)

*Corresponding author: xuyuming@zzu.edu.cn

2 Methods

2.1 Subjects

The patient group were consisted of 512 consective patients with ischemic stroke (310 cases were male and 202 cases were female, mean age years 60±10.2 years) who were recruited to the Hospital of Henan province from December 2004 to July 2005 and the control group were consisted of 500 healthy volunteers (274 cases were male and 226 cases were female, mean age 56±9.8 years). Diagnosis of ICVD was made by clinical manifestations and CT or MRI scans. Severe systemic diseases such as epilepsy, neoplastic, liver or renal disease were in the range of exclusion both patient and control group. All of them were unrelated, and were from the Chinese Han population.

2.2 Genotyping of MS A2756G polymorphism

Blood samples were drawn from cases and controls in the fasting state and collected in EDTA tubes. Genomic DNA were extracted from peripheral-blood lymphocytes

by the standard phenol-chloroform method. The MS gene A2756G polymorphism was identified after amplification with primers (5'-CATGGAAGAATATGAAGATATTAGAC-3' and 5'-GAACTAGAAGACAGAAATTCTCTA-3') according to the previously described by Leclerc et al [4] and the conditions of the PCR reaction were thirty-five cycles (92°C for 60 seconds, 56°C for 60 seconds, and 72°C for 90 seconds) were used to amplify 189-bp products. PCR reaction mixture 25μl contains 100ng genoMic DNA, 10μmol of the primer, 1.5mol/L $MgCL_2$,50mol/L KCL, 10mol/L Tris-HCL(PH8.3), 0.2mol/L of each dNTP and 2.0U DNA polymerase. Following amplification, a restriction digestion was performed to detect the MS A2756G sequence polymorphism with the enzyme *Hae*III under the condition of 37℃during 16 hours. These products and PCR products were separated using electrophoresis through 2％ agarose gel and staining with ethidium bromide and visualized under UV light.

2.3 Statistical analysis

The frequencies of the alleles and genotypes were counted and compared by the Chi-square test. Odds Ratios(OR) and their 95％ confidence intervals (95％CI) were used to estimate the risk association to the genotype. All statistical procedures were performed with SPSS 11.0 software package. *P* values below 0.05 were considered statistically significant.

3 Results

3.1 Mutation Identification

The pattern of heterozygous MS A2756G mutation (AG) showed three bands of 189, 159 and 30bp. The mutant homozygote (GG) showed two bands of 159 and 30 bp; the wild type (AA) showed only one band of 189 bp (fig1. the 23-bp band was out of gel).

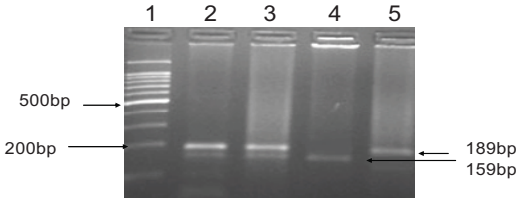

Fig.1 Genotyping of the MS A2756G gene

Lane 1:100bp DNA ladder

Lane 2,3:AG heterozygous

Lane 4:GG honozygous

Lane 5:AA honozygous

3.2 Genotype distributions and allele frequencies

The genotype distribution for both patients and controls was consistent with Hardy-Weinberg equilibrium by Chi-square test (*P*>0.05) (Tab1). The frequency of MS A2756G genotypes in study and control is shown in (Tab2). As can be seen, the frequency of genotypes and G alleles was no significantly difference in the study group compared with controls.

The data summarized in Table 3 demonstrate that the genotypes and allele distribution of MS A2756G in Henan Han population was consistent with the other areas in Chinese and differences with most foreigner of white races .

Table 1. The Hardy-Weinberg equilibrium of MS A2756G genotypes in patients and controls

genotypes	Patient group		Control group	
	object	expect	object	expect
AA	455	452	423	423.2
AG	55	57.8	75	73.6
GG	2	1.8	2	3.2
	χ^2=0.090 P=0.75		χ^2=0.207 P=0.825	

Table 2. Prevalence of the MS A2756G genotypes and allele frequency in patients and controls

groups	subjects(n)	Genotype frequency n (%)			allele frequency (%)	
		AA	AG	GG	A	G
Patient	512	455(88.9)	55(10.7)	2(0.39)	965(94.2)	59(5.8)
control	500	423(84.6)	75(15)	2(0.4)	921(92.1)	79(7.9)
		χ^2=4.101 P > 0.05			χ^2=3.64 P > 0.05	

Table 3. Methionine Synthase A2756G Genotypes and alleles in Case-Control and Reference Panels

Genotype frequencies	China (Henan)	China [5] (Guangzhou)	China [5] (Hunan)	American[8]	Finnish [4]	Austrilian[6]	Spanish[7]
AA	84.6	80.09	82	70.88	59	62.75	66.87
AG	15	18.02	17	25.82	38	33.22	30.12
GG	0.4	1.89	1	3.38	3	4.03	3.01
		χ^2=2.424 P＞0.05	χ^2=1.179 P＞0.05	χ^2=7.208 P＜0.05	χ^2=17.64 P＜0.001	χ^2=14.020 P＜0.001	χ^2=10.13 P＜0.001
Allele frequencies							
A(%)	92.1	89.10	90.50	83.79	78.39	79.36	81.93
G(%)	7.9	10.90	9.5	16.21	21.62	20.64	18.07
		χ^2=0.523 P＞0.05	χ^2=0.223 P＞0.05	χ^2=3.93 P＜0.05	χ^2=7.686 P＜0.01	χ^2=5.413 P＜0.05	χ^2=4.423 P＜0.05

3.3 Risk estimation

In subjects with the methionine synthase (AG+GG) genotype, the odds ratio (OR) and 95% confidence interval (*CI*) for patients with ischemic cerebrovascular diseases to controls were 0.682(0.47-0.98) and 0.93(0.13-6.63), respectively (P>0.05).

4. Discussion

Epidemiological evidence suggested that ischemic cerebrovascular disease (ICVD) shares many risk factors, such as age, hypertension, and smoking, et al. Recently, Cattaneo et al[3] reported that Hyperhomocysteinemia, which corresponds to the C677T mutation in the MTHFR gene, may be an inherited risk factor for coronary artery disease and ischemic cerebrovascular diseases. It is also possible that the features of the hemostastic system may influence the development of ICVD, as has been suggested for IHD. Genetic variations play a role in the ICVD.

Homocysteine is a sulfur amino acid generated as an intermediate product in methionine metabolism and occurs at the intersection of two metabolic pathways, remethylation and transsulfuration. These pathways are known to be regulated by 3 key enzymes: cystathionine ß-synthase, homocysteine methyltransferase (methionine synthase), and 5, 10-methylenetetrahydrofolate reductase (MTHFR), as well as by the cofactors folate, vitamin B6, and vitamin B12.

Methionine synthase is an key enzyme in molulation of plasma homocysteine by converting it into methionine. The mutation of Methionine synthase (MS A2756G) leads to a reduction in enzyme activity and subsequent elevation of plasma homocysteine. Leclerc et al[4] Interestingly, they also showed that this mutation is common in the general population and inferred that it might lead to mild hyperhomocysteinemia with a consequent impact on vascular disease. Thus, analysis of the genetic polymorphism of methionine synthase might provide us with an explanation for elevated homocyst(e)ine levels in those cases that cannot be explained by other causes, such as MTHFR genotype. The most prevalent mutation of the MS gene is the

A2756G transition, which results in the substitution of aspartic acid by glycine [8]. Leclerc et al[4] found 3 mutations in Canadian patients with deficiencies in methionine synthase activity and among Western Caucasian populations, the prevalence of heterozygous and homozygous MS A2756G carriers has been reported to be around 32% and 4%, respectively. In our study, prevalence of the MS A2756G AG and GG genotypes in patients and controls is 57 and 79 relatively, while the allele frequency of G in patients is 59 and in controls is 79, which does not exhibit a significant difference between patients with ICVD patients and healthy controls. we found no evidence to suggest an association between this methionine synthase mutation and ischemic cerebrovascular diseases .The information indicates that the MS A2756G gene may not be an independent risk factor for ischemic cerebrovascular diseases in the Henan Han population. Differences in allelic frequencies had been reported in difference ethnic groups. In our study, the frequency of G allele in cases and controls was 5.8％ and 7.9％, respectively. The G allele frequency of the MS A2756G polymorphism in Henan Han population was similar to that of Guangzhou and Hunan ($P > 0.05$)[8]significantly lower than that of the Americans ($P < 0.05$) . It was also lower than frequencies of the Spanish and Australian($P < 0.05$)[4,6], which suggested that the prevalence of gene mutation of MS A2756G varied with different ethnic group or geographic regions.

We didn't measure plasma levels of homocyst(e)ine and folate in the participants with ischemic cerebrovascular disease, which is thought to be another limitation of this study.

5 Conclusion

0ur preliminary data indicates lack of significant association between MS A2756G polymorphism with ICVD; MS A2756G gene mutation may not be an independent risk factor for ischemic cerebrovascular disease. The polymorphisms of MS A2756G display an ethnic or geographic difference.

Acknowledgments

The authors express their appreciation to the Henan Key Laboratory of Molecular Medicine, for the financial support of this study.

References

1. Temple ME,Luzier AB,Kaziered DJ.Homocysteine as a risk factor for atheroaclerosis .Am Pharmacother ,2000,34(1):57-65.
2. Selhu J, d'Angelo A. Relationship between homocysteine and thrombotic disease. Am J Med Sci 1998;316:129–140.
3. Cattaneo M. Hyperhomocysteinemia, atherosclerosis and thrombosis. Thromb Haemostasis, 1999; 81:165–176.
4. Leclerc D,Campeau E,Goyette P,et al.Human methionoine synthase:cDNA cloning and identification of mutations in patients of the cblG complementation group of folate /cobalamin disorders.Hum Mol Genet,1996,5(12):1867-1874.
5. Li YN, Gulati S, Baker PJ, Brody LC, Banerjee R, Kruger WE. Cloning, mapping and RNA analysis of the human methionine synthase gene. Hum Mol Genet 1996;5:1851–8.
6. Gulati S, Baker P, Li YN, Fower B, Kruger W, Brody LC, Banerjee R. Deffects in human methionine synthase in cblG patients. Hum Mol Genet 1996;5:1859–65.
7. Chen LH, Lin M-L, Hwang H-Y, Chen L-S, Korenberg J, Shane B. Human methionine synthase: cDNA cloning, gene location and expression. J Bio Chem 1997;273:3628–34.
8. Yates Z,Lucock M.Methionine synthase polymorphism A2756G is associated with susceptibility for thromboembolism events and altered B vitamin /thiol metabolism .Haematologica, 2002,87(7):751-756.
9. Alessio AC,Annichino-Bizzacchi JM, Bydlowski SP ,et al . Polymorphism in the methylenetetrahydrofolate reductase and methionine synthase reductase gene and homocysteine levels in Brazilian children.Am J Med Genet A.2004,128 (3):256-60.

10. Temple ME,Luzier AB,Kaziered DJ.Homocysteine as a risk factor for atheroaclerosis .Am Pharmacother ,2000,34(1):57-65.
11. Finkelstein JD. The metabolism of homocysteine:pathways and regulation.Eur J Pediatr,1998;157[suppl 2]:40-44.
12. Wang XL, Duarte N, Cai H, Adchi T, Sim AS, Cranney G, Wilcken DEL. Relationship between total plasma homocysteine, polymorphisms of homocysteine metabolism related enzymes, risk factors and coronary artery disease in the Australian hospitalbased population. Atherosclerosis 1999; 146:133–40.
13. Zhang G,Dai C.Correlation analysis between plasma homocysteine level and polymorphism of homocysteine metabolism related enzymes in ischemic cerebrovascular or cardiovascular diseases.Zhonghua Xue Ye Xue ZaZhi.2002,23(3):126-129.

Cloning and Higher Expression of Recombinant Human Insulin-like Growth Factor-1

Yan Yuqing*[1], Xiao Minghui[2], Sun Hongmei[1], Zhu Hongjie[2]

[1]College of Life Science and Technology in Harbin Normal University 150080; [2]Harbin Pharmaceutical Group Bioengineering Co., LTD

Received April 24, 2009

Abstract

Insulin-like Growth Factor (IGF) is a type of important growth factor, of which chemical structure is similar to proinsulin. There are two relative polypeptides - IGF-1 and IGF-2. This study aims to produce high yield viable IGF-1 using genetic modification and various other methods. [Life Science Journal. 2009; 6(3): 32– 36] (ISSN: 1097 – 8135)

Key words: IGF-1; fusion protein; higher expression; serum free culture medium

1. Introduction

IGF-1and IGF-2 which belongs to the IGF family play a significant role in the proliferation, differentiation, apoptosis, and growth of tissues, generated and developed of tumor cells. IGF-1 in particular has a special role in influencing cell growth. It correlates with the occurring of diseases such as cardiovascular disease, metabolic syndrome, diabetes, insulin antagonistic. Due to the fact that IGF has properties that low protein expression and difficulty to isolated.

In 1957, Salmon and Daughaday[1] first found that IGF-1 and IGF-2 could promote the cartilage to absorb 35s in sulphate. They named them as sulphation factors [2]. In 1963, Froesch[3] described them as NSILA1 and 2.

In 1972, they were named as Somatomedin [4]. In 1976, Rinderknecht and Humbel [5] isolated two active factors. They shared high degree of structural homology with insulin. They renamed them as insulin-like growth factor-1 and insulin-like growth factor-2 (IGF-1 and IGF-2) [6]. In 1978, Rinderknecht and Humbel identified the structure and characteristic of IGF-1 and IGF-2[7].

In this research we isolate the total RNA from healthy human placenta tissues. Based on the records of IGF-1 from GenBank, reference number A29117, the primers were designed and a 227bp IGF-1 segment was gotten through Reverse Transcription PCR methods. After sequence identification, the homologous was 99% compare with A29117 coden region of IGF-1 polypeptide. The experiment constructed pET-32a-IGF-1 Fusion Protein Expression Vector, and uses Ampicillin resistance selection, PCR amplification and enzyme cutting to confirm linkage. IPTG was then used to induce the expression of target protein. Analysis of the sequence showed that the target protein didn't express well was due to rare codons interference. Hence, using contig PCR methods to get a gene and constructed a pET-32a-rIGF-1, inducing higher expression after transformation, expression level up to 38%. The protein was purified using his-tag affinity column chromatography, then putted it into CHO cells culture and confirmed its bioactivity in cells. It has an activity to stimulate cell proliferation.

2. Materials and Reagents

E.coli JM109, *E.coli* BL21 bought from TAKARA biotechnology (Dalian) Co. Ltd. Plasmid: pMD18-T form TAKARA biotechnology (Dalian) Co. Ltd. pET-32a (+) bought from Novagen Company. Cell: CHO cell system supplied by Company: Harbin Pharmaceutical Group Biological Engineering Co., Ltd.

Cloning and expression of hIGF-1

We isolated the total RNA from healthy human placenta tissues. The primers were designed and a

227bp IGF-1 segment was gotten through Reverse Transcription PCR methods.Primers:

P1:CCATGG GGACCGGAGACGCTCTGCGGGGCTG
Nco Ⅰ
P2: CTCGAG CTAAGCTGACTTGGCAGGCTTGAGG
Xho Ⅰ

Reaction conditions:

10×ExBuffer	2.5μl
dNTPs （2.5mmol/L）	2.0μl
P1 （10μM）	1.0μl
P2 （10μM）	1.0μl
Ex Taq （5U/μl）	0.5μl
Template（ < 1μg/μl）	1.0μl
ddH_2O	17μl
total volume	25μl

94℃	5min	
94℃	30s	30 circles
60℃	30s	
72℃	30s	
72℃	10min	
4℃	∞	

Linked the gene with pMD18-T vector, then transformed into *E.coli*JM109.

Constructed pET-32a-IGF-1 Fusion Protein Expression Vector used Ampicillin resistance selection, PCR amplification and enzyme cutting to confirm linkage.

SDS-Polyacrylamide Gel Electrophoresis

Preparation of the separate solution and condensable solution

Separate solution: Table 1-1 component of the 12% polyacrylamid separate solution.

Condensable solution: Table 1-2 component of the polyacrylamid condensable solution.

Electrophoresis buffer:

5 x Tris- Glycin electrophoresis buffer:

Tris-base	15.1g
Glycine	94g
10%SDS	50ml
pH 8.3	
Water	till 1000ml

Modification, clone and expression of IGF-1 gene

After small amount of the gene expression, it was found that the low expression of the target gene even changed the express condition. Through the rare codons analyses, we designed and synthesized 3 DNA single strands and called IGFa, IGFb, IGFc and 2 PCR primers: Pup, Plow. Used contig PCR methods to get a gene and called it rIGF-1.

IGFa：
5’-GGCCCGGAAACCCTGTGCGGCGCAGAACTGG TGGATGCACTGCAGTTTGTGTGCGGCGATCGCG GCTTTTATTTCAACAAACC-3’

IGFb：
5’-AGCTGCGAAAGCAGCATTCATCCACAATGCC GGTCTGCGGCGCGCGGCGACTGCTGGAGCCATA GCCGGTCGGTTTGTTGAAAT-3’

IGFc：
5’-AATGCTGCTTTCGCAGCTGTGATCTGCGCCGC CTGGAAATGTATTGCGCGCCGCTGAAACCGGCG AAGTCAGCA-3’

Pup: CCATGG GCCCGGAAACCCTGTGCGGCGCAG
Plow:CTCGAGCTATGCTGACTTCGCCGGTTTCAG

Dissolved the synthetic gene segment with the sterile water to run PCR reaction, then after enzyme cutting identification, we constructed the expression vector to express the gene.

Bioactivity Test of rIGF-1

Purified the target protein

Processing the cell break, inclusion body washing, dissolving, renaturation and then purified the fusion protein. Take out the renaturation solution from 4℃. Centrifuge in 30mins with 5000rpm and removal the hybridprotein. Put the supernatant into a clean triangular flask to process the His-tag column purification.

Balanced solution: 20mM sodium phosphate, 0.5M NaCl, 5 mM imidazole (pH 7.4).

Elutriant solution: 20mM sodium phosphate, 0.5M NaCl, 0.5 mM imidazole (pH 7.4).

Filtrating with 0.45μm filter membrane after prepare of the solution. Obtain the target protein through enzyme cutting and process the serum-free cell culture.

Bioactivity test of IGF-1

The concentration of the IGF-1 is 0.76mg/ml through the testing of UV spectrophotometer. Prepared the serum-free medium with the final concentration as 100μg/ml、50μg/ml、25μg/ml to test the activity of insulin.

Put the serum-free DMEM as negative control, and the DMEM with 25μg/ml IGF-1 as the positive control.

Table 1-1 component of the 12% polyacrylamid separate solution

Content	water	30% acrylamide	1.5M Tris-HCl (pH8.8)	10%SDS	10% Ammonium Persulfate	TEMED
（ml）	1.28	1.6	1.04	0.04	0.04	0.004

Table 1-2 component of the polyacrylamid condensable solution

Content	water	30% acrylamide	1.0M Tris-HCl (Ph6.8)	10%SDS	10% Ammonium Persulfate	TEMED
（ml）	1.4	0.33	0.25	0.02	0.02	0.002

Preparation of the medium:

DMEM basic medium

DMEM+100μg/mlIGF-1

DMEM+50μg/mlIGF-1

DMEM+25μg/mlIGF-1

DMEM+25μg/ml insulin.

Adherent culturing the CHO cell with 3-4 generation with good cell shape and stable condition, then digest the cell from 24 pores plate, and removal the digestive juice. Culturing the cell with the five different medium, observe the cell with micro. Use the blood cell counting chamber to calculate the cell amount per ml and the motility rate of the cell.

3. Result and Analysis

Cloning and Expression of hIGF-1

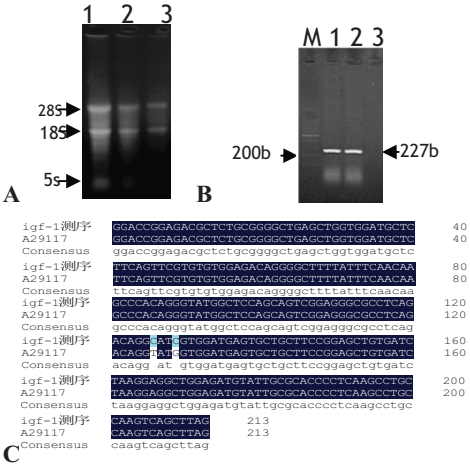

Figure 1-A. Isolation of total RNA from placenta. B. PCR Agarose gel electrophoresis analysis of IGF-1 gene. M: 100 ladder, 1-2: DNA strip, 3: Blank. C. Comparison of nucleotide sequence of IGF-1.

SDS-PAGE of the IGF-1

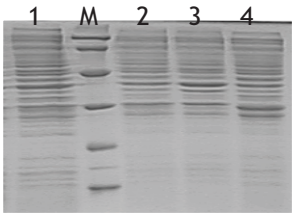

Figure 2. pET-32a-IGF-1SDS-PAGE.
1: Un-induced, M: LMAP Maker, 2: Induced for 2h, 3: Induced for 3h, 4:Induced for 4h.

Modification, Clone and Expression of IGF-1

Modification of the gene sequence

Sequence after the modification:

GGC CCG GAA ACC CTG TGG GGC GCA GAA CTG GTG GAT GCA CTG CAG TTT GTG TGG GGC GAT CGC GGC TTT TAT TTC AAC AAA CCG ACC GGC TAT GGC TCC AGC AGT CGC CGC GCG CCG CAG ACC GGC ATT GTG GAT GAA TGG TGG TTT CGC AGC TGG GAT CTG CGC CGC CTG GAA ATG TAT TGG GCG CCG CTG AAA CCG GCG AAG TCA GCA TAG

Figure 3-A. Comparison the nucleotide sequence of rIGF-1 and IGF-1. 3-B. Comparison of the amino acid sequence of rIGF-1 and IGF-1.

Cloning and Expression of the Modified Gene

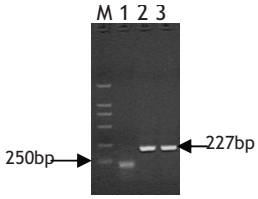

Figure 4.Slipcing PCR of E.coli preference. M: DL2000, 1: Blank, 2 and 3: PCR result.

```
rigf-1基因  GGCCCGGAAACCCTGTGGGGCGCAGAACTGGTGGATGCAC   40
测序结果    GGCCCGGAAACCCTGTGGGGCGCAGAACTGGTGGATGCAC   40
Consensus   ggcccggaaaccctgtggggcgcagaactggtggatgcac
rigf-1基因  TGCAGTTTGTGTGGGGCGATCGCGGCTTTTATTTCAACAA   80
测序结果    TGCAGTTTGTGTGGGGCGATCGCGGCTTTTATTTCAACAA   80
Consensus   tgcagtttgtgtggggcgatcgcggcttttatttcaacaa
rigf-1基因  ACCGACCGGCTATGGCTCCAGCAGTCGCCGCGCGCCGCAG   120
测序结果    ACCGACCGGCTATGGCTCCAGCAGTCGCCGCGCGCCGCAG   120
Consensus   accgaccggctatggctccagcagtcgccgcgcgccgcag
测序结果    ACCGGCATTGTGGATGAATGCTGCTTCGCCAGCTGTGATC   160
rigf-1基因  ACCGGCATTGTGGATGAATGCTGCTTTCGCAGCTGTGATC   160
Consensus   accggcattgtggatgaatgctgctt cgcagctgtgatc
测序结果    TGCGCCGCCTGGAAATGTATTGCGCGCCGCTGAAACCGGC   200
rigf-1基因  TGCGCCGCCTGGAAATGTATTGCGCGCCGCTGAAACCGGC   200
Consensus   tgcgccgcctggaaatgtattgcgcgccgctgaaaccggc
rigf-1基因  GAAGTCAGCATAG   213
测序结果    GAAGTCAGCATAG   213
Consensus   gaagtcagcatag
```

Figure 5. Comparison of the sequence of rIGF-1

SDS-PAGE of the Expressed Modified Gene

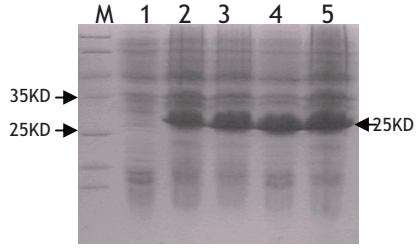

Figure 6. pET-32a-rIGF-1 SDS-PAGE. M: LMWP Maker, 1: Un-induced, 2-5: Expressed protein.

Bioactivity Test of rIGF-1

Purification of the fusion protein.

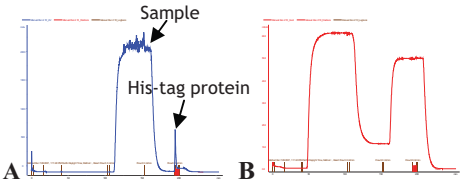

Figure 7-A. Optical absorption. B. Conduction.

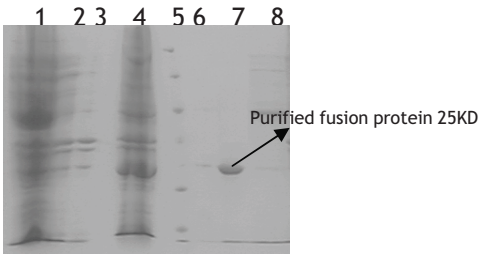

Figure 8. Product detection of purification of fusion protein by SDS-PAGE.

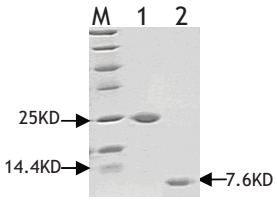

Figure 9. SDS-PAGE after purification. M: LMWP Marker, 1: Fusion protein before cutting, 2: Target IGF-1.

Bioactivity test

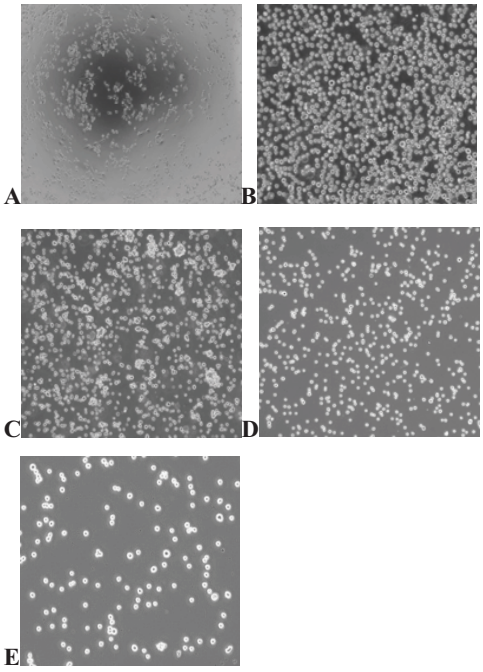

Figure 10-A. Negative control:Dead cell.B.Positive control.

C.DMEM+100μg/mlIGF-1.

D.DMEM+50μg/mlIGF-1.

E. DMEM+ 25μg/mlIGF-1.

4. Discussion

With the rapid develop of biotechnology, the shortage of the prokaryotic expression is coming out. For instance, most of the expressed protein is inclusion body of which has the difficult renaturation and purification. The target cannot process the glycosylation modifications which will influent the function of the protein. More and more researches start to use the eukaryotic cell. And the serum-free medium is the trend of the cell culture.

In this study we obtained the recombinant and high expressed IGF-1 polypeptide which has given the contribution to the serum-free culture.

References:

1. Salmon W D, J Daughaday W. A hormonally controlled serum factor which stimulates sulfate incorporation by cartilage in vitro. J Lab Clin Mwd, 1957,49:825-836
2. 张应华.核基质结合区 MAR 调控的胰岛素样生长因子-1 表达载体与转化甘蓝的研究.2004.云南农业大学
3. Froesch E R , Burgi H. Antibody-suppressible and nonsuppressible insulin-like activities in human serum and their physiologic significance. An insulin assay with adipose tissue of increased precision and specificity[J] . J Clin Invest , 1963 ,42 :1816 - 1834.
4. Daughaday WH ,Hallk. Somatomedin :a proposed designation for the sulfation factor[J] . Nature , 1972 ,235 :107.
5. Rinderknecht E , Humbel R E. Polypeptides with nonsuppressible insulin-like and cell growth promoting activities in human serum: isolation ,chemical characterization and some biological properties of forms1 and Proc Natl Acad Sci, 1976 ,73 :2365-2369.
6. 贺淹才. 胰岛素样生长因子的发现及其生理作用. 生命的化学, 1994, 14(3):23-24.
7. Rinderknecht E, Humbel R E. The amino acid sequence of human insulin-like growth factor 1 and its structural homology with proinsulin. J Biol Chem, 1978 ,253 :2769 - 2776.

Gustatory Afferents from the Locust Ovipositor: Integration at the Interneuron Level

Tousson, Ehab[1] and Hustert, Reinhold[2]

[1] *Department of Zoology, Faculty of Science, Tanta University, Egypt.*
[2] *Institute of Zoology and Anthropology, Georg August Univ., Göttingen, Germany*

Received March 25, 2009

Abstract

Sensory afferents from the ovipositors influence the behaviour of locusts before and during egg-laying. Their contact chemoreceptors have only one terminal porous (basiconic sensilla) and five sensory neurons at their base, with one responding to mechanical contact and the others to different classes of attractant or repellent chemicals. Responses to aqueous solutions of salts (NaCl), sugars (glucose), acids (citric acid), oviposition aggregation pheromones (veratrole and acetophenone), alkaloids (quinine and tomatine), and phenolic compounds (salicin) were seen. Higher order processing occurs in local and ascending interneurones of the terminal abdominal ganglion. They are excited or inhibited when purely aqueous solutions of a single chemical are applied to the ovipositor taste receptors. We focussed on a cluster of interneurons extending in the anterolateral region of the eighth abdominal neuromere. Several have ascending collaterals to more anterior abdominal ganglia. Projecting interneurons respond only to one or two chemical substances (sugars or salts, or salts and acids together). The physiological and morphological differences between the chemosensory interneurons suggest that there is no specific centre for processing taste information in the locust terminal ganglion. [Life Science Journal. 2009; 6(3): 37 – 45] (ISSN: 1097 – 8135).

Key words: Taste sensilla, locust ovipositor, local and ascending interneurons, chemical stimulants.

1 Introduction

Most insects have contact chemoreceptors on various surfaces of their body. This sense of taste can be involved in a number of behaviours, including avoidance [1-11], detection and the selection of food[5, 12-14], and selection of egg-laying sites[4, 9, 10, 15-17] . Suitable substrates for starting oviposition are detected first by the tarsal contact chemoreceptors of fore- and middle legs[1, 14, 18-20]. Consecutively, further chemical cues are given for starting and maintenance of digging as well as egg-laying by the contact chemoreceptors of the genital segments and ovipositor valves of the abdomen.

Many locust contact chemoreceptors are distributed "randomly" on the body and extremities. Their central projections do not sort out or converge in specific glomeruli in the CNS according to typical sensory classes of taste (e.g. salts, acids, sugar, water and others). The afferents branch more or less position- specific like mechanosensory afferents even if they originate from areas of increased body contact with the substrate as the tarsi [18, 21] or genital segments of females [6, 8, 9, 22-25]. Chemosensory projections develop no specific gustatory centers with specific interneurons that might ease integration and extracting specific chemosensory information in the terminal ganglion.

Neural responses from the tips of insect taste sensilla were first recorded with the technique of Hodgson *et al* [26] that allows studying chemosensory specificity of the different afferents from single basiconic contact chemoreceptors. In the fly for example, different chemosensory afferents in one sensillum respond selectively to water, anions, salts and sugars[12]. Stimulation of their contact chemoreceptors on the tarsi leads to extension of the proboscis[12]. In locusts, stimulation of tarsal chemoreceptors with an antifeedant (sodium nicotine tartrate) elicits aversive leg waving[1, 27]. Natural stimuli, such as plant extracts, appear to be encoded in an across fibre pattern in the responses of many chemosensory afferents and elicit various feeding behaviours[4, 10, 28, 29] .

Neuronal pathways for processing tastes are poorly understood in insects. We know little of how the taste of different chemicals is coded and represented in the central nervous system or which interneurones are responsible for their processing [2, 3, 4, 9, 21, 30]. Part of the underlying problem is the relative inaccessibility and small size of the taste cells, of the integrating neurones that process their signals [31] and their physiological properties. The contact chemoreceptors on the ovipositor of locusts are innervated regularly by five sensory afferent neurones that project intersegmentally in the terminal abdominal ganglion and further into the seventh abdominal ganglion [9, 23, 25]. This system offers the chance of understanding chemoreception systems at the level projecting interneurons by recording extracellularly from their ascending axons in connectives to preceding ganglia. Which chemical cues are extracted from environmental contacts of the locust ovipositor and which are required to select suitable oviposition sites and subsequently control oviposition before and during digging and egg laying. Intracellular recording and staining of several chemosensory integrating interneurons from the locust terminal ganglion gave an insight into the

---

Email: ehabtousson@yahoo.com

integrative properties, the morphology types and the distribution of local and ascending taste sensitive interneurons.

2 Material and Methods

All experiments were performed on sexually mature females of *Locusta migratoria* taken from our crowded laboratory culture reared at 25 °C under a 12h light / 12h dark regime and fed mainly with fresh wheat. Prior to the dissection locusts were anaesthetised by cooling to 2-4°C and experiments were performed at 22-25 °C.

In order to record from the anterior connectives of the terminal ganglion the 7th and the terminal abdominal ganglia were first exposed by dorsal dissection removing internal genitals, fat and viscera. All nerves from the terminal abdominal ganglion (TG) were cut except for the terminal branch of the eighth ventral abdominal nerve (8V) that innervates the ventral ovipositor valve. Locust saline at 22-25°C was exchanged regularly throughout an experiment in the terminal abdominal segments.

2.1 Recording afferent responses

Electrophysiological recording of the activity of chemosensory neurones were obtained from the terminal pore of basiconic sensilla using a modified version of the tip recording technique [4]. For simultaneous stimulation and recording, contact was made with the meniscus of the salt solution at the end of the fine tapering plastic tip of a suction electrode. The recording and stimulating electrodes for the basiconic sensilla contained different concentrations of salts as NaCl (0.01 M to 3.0 M), sugar as glucose (0.01 M to 3.0 M), acids as citric acid (0.01M, 0.1M and 1.0 M), oviposition aggregation pheromones as veratrole and acetophenone (1.0% and 0.1%), alkaloids as quinine and tomatine (0.1%) and phenolic compounds as salicin (0.1%).

For specific stimulation, different chemicals were applied to a distinct single basiconic sensillum (contact chemosensitive sensillum) in the ventral region of the ipsilateral ventral ovipositor valve. Mechanical stimulation of other sensory neurons was avoided by immobilising all other sensilla in the terminal abdominal segments and on the ovipositor valves with Vaseline. In addition, large mechanosensitive sensilla near the basiconic sensillum selected for recording were shaved off. A ring of a soft, low temperature melting wax was applied to surround the basiconic sensillum in which drops of different chemical stimulants could be applied selectively during recording. Sometimes application of the stimulant solution deflected the basiconic sensillum initially and elicited spikes phasically for up to 20ms in its mechanosensory afferent**.** Each stimulus was repeated 8-10 times for each stimulant chemical. For testing the specific response of stimulants all basic classes of stimulating chemicals (salts, acids, sugar, alkaloids) diluted in water with electrolyte (0.01M NaCl) were applied consecutively with interspersed pauses of several minutes in each experiment. In contrast to chemical stimulation and recording simultaneously at the terminal pore of the gustatory sensilla, stimulation with just the specific chemical in water for recording from interneurons had the great advantage of being unbiased by an additional electrolyte.

2.2 Interneuron recording and staining

For extracellular recording from the left or right abdominal connective between the 7th and the terminal abdominal ganglia large diameter suction electrodes were used. For intracellular recordings from neurons of the terminal ganglion while stimulating a basiconic sensillum on the ventral ovipositor the last abdominal ganglia were isolated except for their connection with the ventral ovipositor valves and fixed dorsal side down in a Petri dish on non-toxic plasticine. The ovipositor apodemes were pinned down. On a wax-covered stainless steel platform the terminal ganglion was mounted and its sheath was treated with a solution of about 1% (Wt / Vl) of protease (Sigma XIV) to facilitate intracellular recording from the interneurons.

Intracellular microelectrodes were filled at their tips with a solution of about 4% Lucifer yellow CH (Molecular Probes, Inc.) in 1 M lithium chloride. The main shaft of the electrode was back-filled with 1.0 M lithium chloride. Electrode resistances ranged from 60 to 80 MV. Chemosensitive interneurons could be classified according to their specific responses to chemical stimuli and further identified morphologically with Lucifer Yellow dye injected into each recorded cell by passing depolarising current pulses 500 ms at 1 Hz for up to 20 minutes. The ganglia were then left in saline for 1 hour to allow the dye to diffuse into the arborizations and collaterals of the cell. Then the caudal ganglia (7th and terminal abdominal ganglia) were isolated from the preparation and fixed for 30 minutes in a buffered (pH 7.4) 4% formaldehyde solution, dehydrated, and cleared in methyl salicylate. Ganglia containing stained interneurones were viewed first as whole-mounts under an epifluorescence microscope (Leitz Aristoplan), photographed (35 mm or digital camera, Nikon Coolpix 950) and the interneuron was then either drawn directly by using a camera Lucida attachment on the compound microscope or reconstructed from negatives or computer printouts. For testing the specific response of the stimulants all basic classes of stimulating chemicals were applied consecutively with interspersed pauses of several minutes in each experiment. Before each stimulation by diluted substances, stimulation with plain water solution served as a test for presence or absence of water responsiveness of an interneuron.

3 Results

Afferent responses from gustatory receptors of locust female ovipositors were tested with the stimulation/recording electrode containing a minimum content of salt (0.1mM NaCl) for the conduction in water between the inner surfaces of the receptor. So at least the two potential stimulants water and salt are present and that can be coded by different receptor neurons of a single basiconic sensillum at contact with the electrode solution. Therefore, we could not test directly the afferent responses to pure water but rather at the postsynaptic level of afferents: from higher order interneurons of the terminal ganglion. Generally, identified taste receptors from a well described region of the ventral ovipositor were tested, both for their responses to different chemical

concentrations at the receptor level and at the interneuron integration level.

In the interneurons, either excitation or inhibition occurred in response to stimulation of the ovipositor contact chemoreceptors. The responses could be mono- or polysynaptic in the case of excitation and di- or polysynaptic for inhibited interneurons. The specific interneurons were identified by specific morphological features, mainly their soma positions (all near the ventral surface of the 8th abdominal neuromere); the arrays of their neurite branching patterns, and the path of their axons. Six interneurones were identified in the terminal abdominal ganglion [two local (ChSIN 1, 2) and four intersegmental (ChSIN 3-6) interneurons] due to their selective responses to chemical stimulation of gustatory sensilla (Fig.1). Several other identified interneurons were found perceiving chemosensory as well as other sensory input, but are not included here.

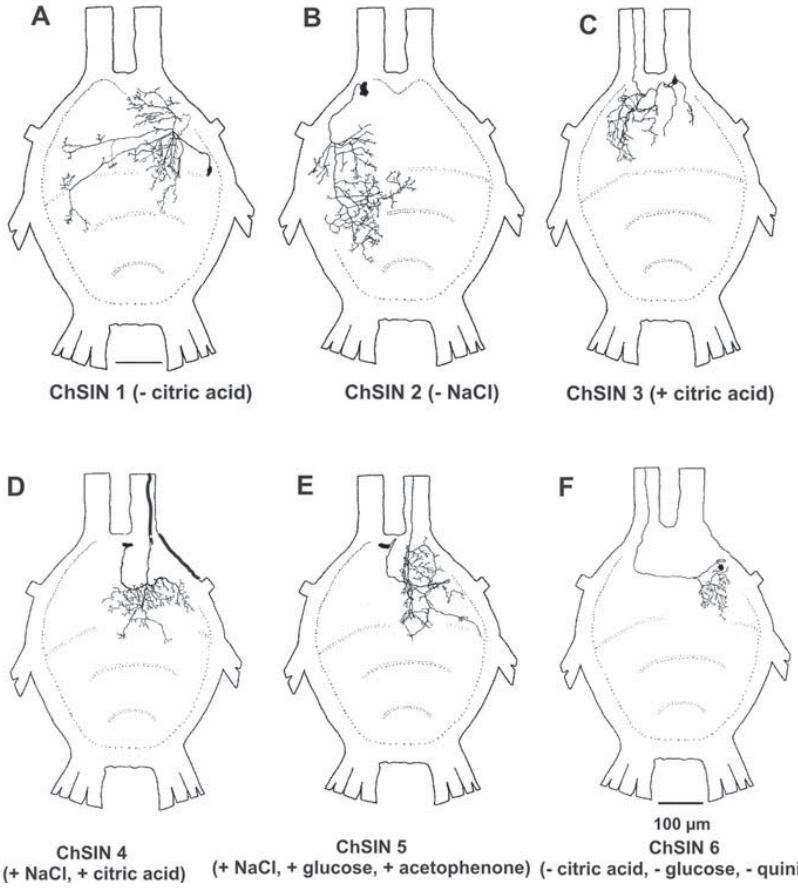

Figure 1. Morphological overview of interneurons that integrate chemosensory information (ChSIN) from the locust ovipositor, stained intracellularly with Lucifer yellow in the terminal ganglion (dorsal view).
A. ChSIN 1 (inhibited by glucose) is a local interneuron branching ipsilateral to the soma in the posterior 8th, the 9th and anterior 10th neuromere. A single contralateral branch also crosses the midline. B. ChSIN 2 (inhibited by NaCl) is an extensive local interneuron with a very lateral soma (in 9th neuromere) branching ipsi- and contralaterally in the 8th and the 9th neuromere. Two main branches cross the midline and extend there far into the contralateral neuropil. C. ChSIN 3 (excited by citric acid) is a projecting interneuron of with contralateral extensive neuropile branching in the 8th neuromere and a contralateral ascending axon. In the ipsilateral 8th neuromere only few branches extend from the primary neurite of the soma. D. ChSIN 4 (excitedby NaCl and citric acid) is a projecting interneuron with an almost median soma, extensive ipsilateral neuropile branching in the 8th neuromere and some branches in the 9th neuromere and across the ganglion midline. The ascending axon extends ipsilaterally. E. ChSIN 5 (excited by NaCl, glucose and acetophenone), with an almost median soma in the 8th neuromere and all other structures extending contralaterally, branches extensively in the 8th neuromere and sparse branching in the 10th while its axon ascends medially. F. ChSIN 6 (inhibited by citric acid, glucose and quinine) with a lateral soma and restricted neurite branching in the posterior 8th neuropile and with an ascending contralateral axon without branching.

3.1 Responses to water at the interneuron level

Responses to application of pure water to basiconic sensilla of the ventral ovipositor were only observed in several larger ascending interneurons (receptor tip recording not possible) (Fig. 2). Their summated extracellular responses are mainly phasic, but cannot be counted or separated as identifiable units. In spite of their intensity none of these could be identified with intracellular methods. It would be interesting to see whether they respond to chemically inert substrates containing different levels of moisture.

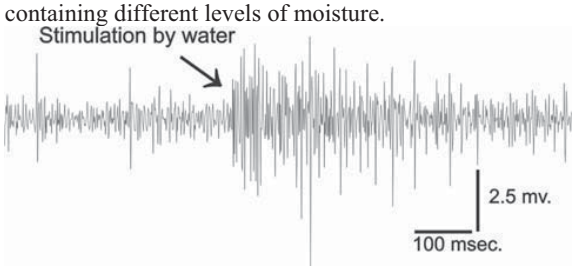

Figure 2. Interneuron responses recorded from the ascending connective of the terminal ganglion during stimulation of the ventral ovipositor with water. At least three units respond phasically.

3.2 Responses to salts

3.2.1 Receptor level

The response to salt in single basiconic sensilla of the ventral ovipositor is phasic with two main units, possibly one for salt and one for water at the concentration of 0,1M sodium chloride (Fig. 3A). Sometimes initially as a third class of afferent units, very large spikes arise (shortly after a contact artefact) from the mechanosensory neuron at the moment of contact.

3.2.2 Interneurons extracellularly

Responses of ascending interneurons to sodium chloride were tested at concentrations of 0.01M to 3.0M (Fig 4A - 4C). Typically, at least three interneurons responded, recognised from their three different unit amplitudes. It cannot be distinguished to which sensory cue contained in the stimulus (mechanosensory, salt and water) the responses are specific. The spiking frequency increases with stimulus concentration up to 1.0M sodium chloride (Fig. 4C). Beyond this concentration, the response by salt-sensitive interneurons remains at a constant level. Rapid adaptation within three seconds occurs at low concentrations while extended adaptation is typical for higher salt concentrations (six seconds for 1.5M sodium chloride).

3.2.3 Interneurons intracellularly

Excitatory responses to salt stimulation (0.1M NaCl) was seen in two ascending interneurons (ChSIN 4/5, Fig. 5 A/B) located in the 8th neuromere of the terminal ganglion with near-midline somata, one ipsi- and one contralateral to the ascending axon and neuropile branching, and only a few posterior branches extending into the ninth neuromere (Fig.1 D/E). The response to stimulating just one basiconic sensillum was phasic with a long tonic after-discharge in ChSIN5 and just phasic in ChSIN4. A third salt-responsive interneuron (ChSIN 2) responded with some inhibition of ongoing activity (Fig. 5C). This local interneuron (Fig.1B) it exhibits a completely different branching pattern extending from a very lateral soma: wide ipsilateral branching in the eighth and ninth neuromere and two separate contralateral neurites reaching far laterally into the ninth and eighth neuromere.

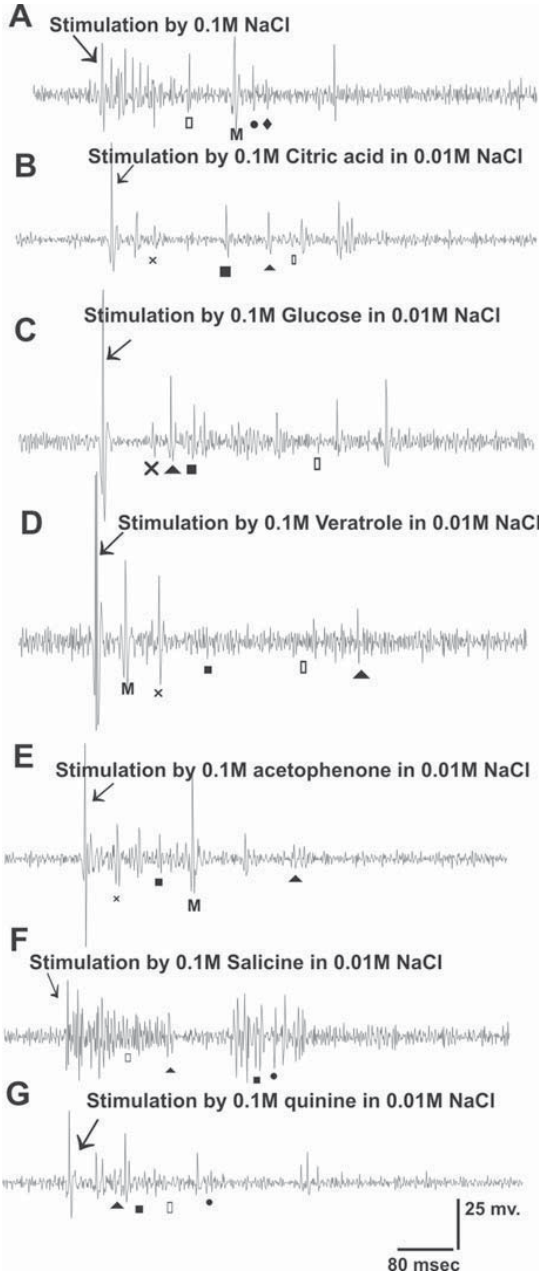

Figure 3. Extracellular responses (recording from the tip of the ventral valve basiconic sensillum) to ovipositor valve stimulation with different kind of chemical substances. A. Stimulation by 0.1M NaCl; B. Stimulation by 0.1M citric acid in 0.01M NaCl; C. Stimulation by 0.1M glucose in 0.01M NaCl; D. Stimulation by 0.1M veratrole in 0.01M NaCl; E. Stimulation by 0.1M acetophenone in 0.01M NaCl; F. Stimulation by 0.1M salicine in 0.01M NaCl; G. Stimulation by 0.1M quinine in 0.01M NaCl

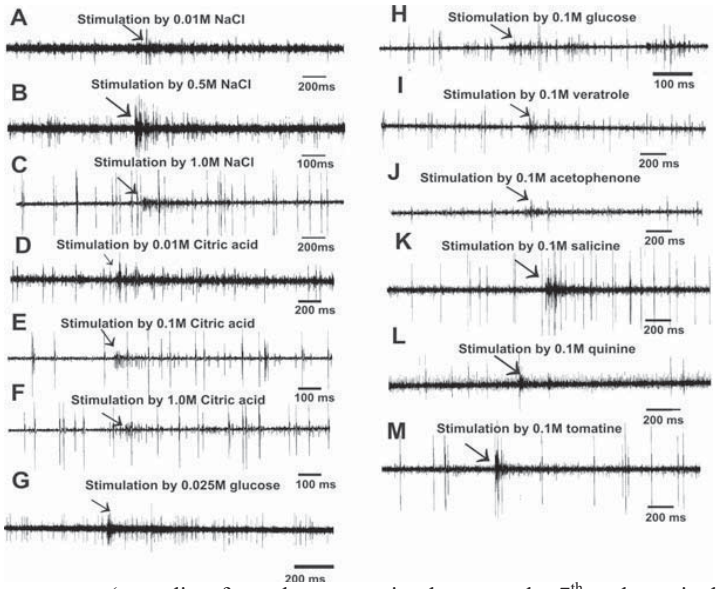

Figure 4. Extracellular responses (recording from the connective between the 7th and terminal abdominal ganglia) to single basiconic sensilla in ventral ovipositor valve stimulation with different concentration of chemical substances. A-C: Responses from interneurons in the ascending connective of the terminal ganglion after stimulation with different concentrations of NaCl (A. with 0.01M NaCl; B. with 0.1M NaCl, C. with 1M NaCL). D-F: Responses from interneurons in the ascending connective of the terminal ganglion after stimulation with different concentrations of citric acid in water (D. with 0.01M citric acid; E; with 0.1M citric acid; F. with 1M citric acid). G, H: Responses from interneurons in the ascending connective of the terminal ganglion after stimulation with different concentrations of glucose in water (G. with 0.025M glucose; H. with 0.1M glucose). Responses from interneurons in the ascending connective of the terminal ganglion after stimulation with 0.1M veratrole (I); 0.1M acetophenone (J); 0.1M salicine (K); 0.1M quinine (L); 0.1M tomatine (M).

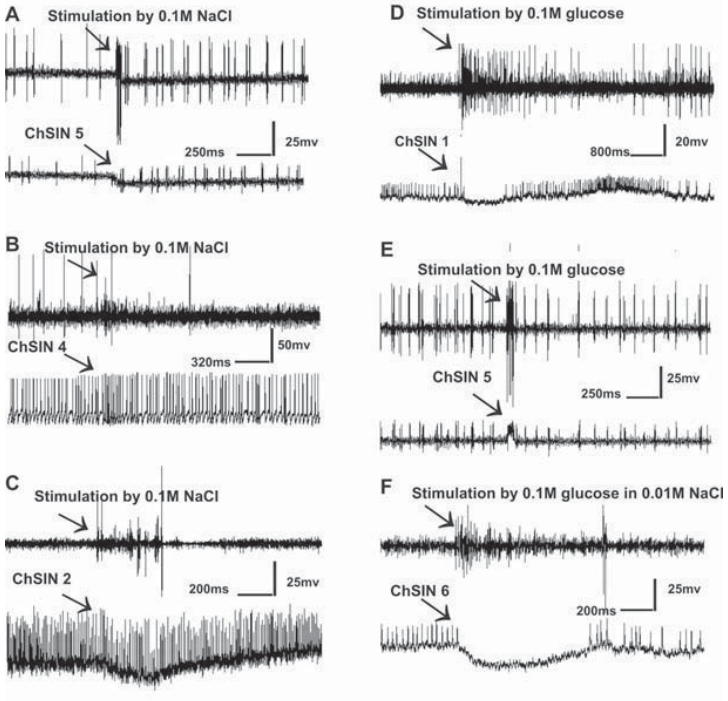

Figure 5A-5C Intracellular responses (lower traces) to ovipositor valve stimulation with 0.1M NaCl in water and extracellular response (upper traces) in 5A. from ChSIN 5, phasic and tonic excitation, 5B from ChSIN 4, phasic excitation; 5C; from ChSIN 2 transient inhibition. 5D-5F: Intracellular responses (lower traces) to ovipositor valve stimulation with 0.1M glucose in water and extracellular response (upper traces) in 5D. from ChSIN 1, transient inhibition; 5E. from ChSIN 5, phasic excitation; 5F. from ChSIN 6, pronounced inhibition

3.3 Responses to acids

3.3.1 Receptor level

The response to citric acid in single basiconic sensilla of the ventral ovipositor is phasic with two main units for citric acid and salt (0.01M sodium chloride serving as electrolyte) and a smaller unit possibly for water (Fig 3B). Initially, as a fourth class of afferent unit's very large spikes arise from the mechanosensory neuron at the moment of contact.

3.3.2 Interneurons extracellularly

Responses of interneurons to citric acid were tested at concentrations of 0.01M, 0.1M and 1.0M (Fig. 4D - 4F). Typical responses occurring from applying a concentration of 0.1M (Fig. 4E) indicate that only one slowly adapting, ascending interneuron is activated in this specific recording. At higher concentration, the interneurons respond less.

3.3.3 Interneurons intracellularly

The salt-responsive interneuron ChSIN 4 can also respond with increased pasic-tonic excitation to citric acid (0.1M) applied to a basiconic sensillum (Fig. 6A). A morphologically different interneuron (ChSIN 3, Fig. 1C, 6B) responds to the same stimulus concentration with prolonged excitation after a short phasic response. It is also an ascending interneuron with a contralateral ascending axon and an extensive branching area in the 8th neuromere, but some sparse branches extend also in the 8th neuromere ipsilateral to the soma.

A third ascending interneuron ChSIN 6 (Fig. 1F, 6C) responds with inhibition or lowered excitation to citric acid (0,1M) applied to the basiconic sensillum. Its soma is located very lateral and from its long primary neurite the only branching area extends ipsilaterally in the 8th neuromere.

3.4 Responses to sugars

3.4.1 Receptor level

The response to glucose solutions in single basiconic sensilla of the ventral ovipositor is phasic. The two larger units could respond to sugar and the electrolyte salt (0.01M sodium chloride) and a small third unit possibly responds to the water (Fig 3C). Initially, as a third class of afferent units' very large spikes arise from the mechanosensory neuron at the moment of contact.

3.4.2 Interneurons extracellularly

Responses of ascending interneurons to glucose were tested at concentrations between 0.25M and 3.0M. The reaction to glucose (Fig. 4G, 4H) indicates that several units of ascending interneurons respond, two of which can only be responses to sugar due to their concentration-related increase in spiking frequency. At 1.0M glucose applied, a maximum spike frequency was reached and adaptation was very slow (not shown). Beyond this concentration bursting of one neuron in response to glucose is typical.

3.4.3 Interneurons intracellularly

Excitation to glucose stimulation (0.1M) of a ventral ovipositor taste receptor was seen in ChSIN 5 (Fig. 1E; 5E), which responds to salts as well. The response is short and phasic in this multimodal interneuron. Pronounced inhibitory responses were seen in ChSIN 1 (Fig.1A; 5D), which is a local and mostly ipsilateral interneuron that extends from the eighth to the tenth neuromere. Its response is very similar to that of ChSIN 6 (Fig 1F; 5F) to glucose, which is inhibited by citric acid also and has a completely different and intersegmental morphology.

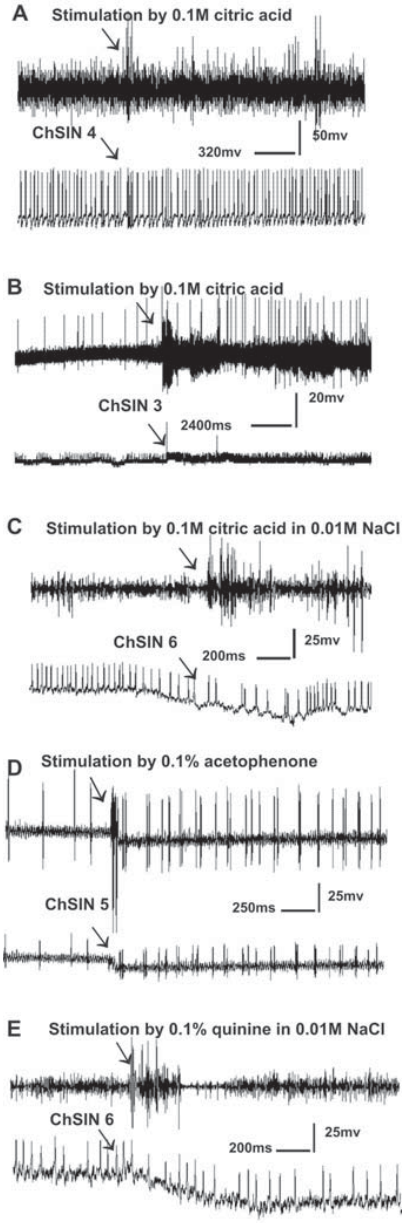

Figure 6A-6C Intracellular responses (lower traces) to ovipositor valve stimulation with 0.1M citric acid and extracellular response (upper traces) in 6A. from ChSIN 4, phasic excitation; 6B. from ChSIN 3, phasic-tonic excitation; 6C. from ChSIN 6 transient inhibition. 6D and 6E. Intracellular responses (lower traces) to ovipositor valve stimulation with 0.1M acetophenone and 0.1M quinine in water and extracellular response (upper traces) in 6D. from ChSIN 5 in response to acetophenone, phasic excitation; 6E. from ChSIN 6 in response to quinine, transient inhibition.

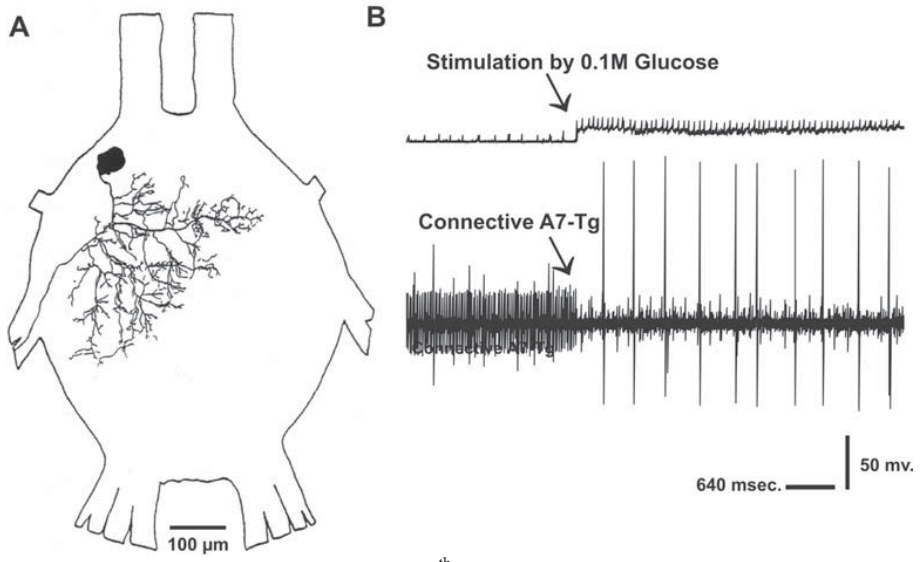

Figure 7. Response of a ventral motoneuron of the 8th neuromere A. Morphological overview; B. Phasic-tonic intracellular response (upper trace) to 0.1M glucose applied to the ventral ovipositor and corresponding activity in the ipsilateral ascending connective (lower trace).

3.4.4 Comparative motor neuron response

For comparison, one motor neuron with chemosensory response in the terminal ganglion was recorded in conjunction with units in the connective ascending from the terminal ganglion when it responded to input from ovipositor chemosensory sensillum (Fig. 7). The cell body (40µm) of this motor neuron is located laterally in the 8th abdominal neuromere and it is characterized by its ipsi- and contralateral dendritic arborisations in the 8th and 9th neuromere. The efferent axon enters nerve 8V. Stimulation with 0.1M glucose at the ovipositor excited this motor neuron tonically while simultaneously it released in ascending interneurones of the ipsilateral connective both inhibitory and excitatory responses. No response to other chemicals (salts, acids, alkaloids, phenols) could be elicited in the motor neuron.

3.5 Responses to potentially significant chemicals:

3.5.1 Aggregation pheromones

In response to the aggregation pheromones veratrole and acetophenone (0.1M) solution (Fig. 3D, 3E), only a few spikes were elicited in the basiconic sensillum after the mechanosensory unit has responded first near the contact artefact of stimulus application. They cannot be attributed clearly to specific applied chemicals, but the responses of the ascending interneurones is pronounced especially to veratrole, but less to higher concentrations of acetophenone (Fig. 4I, 4J). Acetophenone-responses were seen to excite tonically the interneuron ChSIN 5 (Fig. 6D, 1E), which is also responsive to salts and sugar.

3.5.2 Alkaloids and phenols

Responses to application of diluted alkaloids as quinine (0.1M) and the phenolic compound salicine (0.1M) to a basiconic sensillum are rather strong and specific (Fig.3F, 3G). Correspondingly, ascending interneurons clearly perceive these types of stimuli (Fig. 4K-4M) and to tomatine as well. Intracellularly, quinine-responsiveness is seen as inhibition in ChSIN 6 (Fig. 1F, 6E), which is also inhibited by citric acid**.**

4 Discussion

The locust ovipositor valves are the first to encounter fresh substrates both when probing and digging in the substrate. Their contact chemoreceptors can *record* chemical compounds of the substrate before and during egg-laying. When a chemical component of the substrate elicits responses in interneurons via contact chemoreceptors it can be considered as *perceived* by the CNS. Primary sensory responses of insect contact chemoreceptors are usually tested by stimulating and recording from the terminal pore of a gustatory hair[26] since extracellular recording directly from the afferent axons of their very small neurons is impossible. We could study both the type of chemicals recorded by the contact chemoreceptors and their perception due to integration by higher order interneurones extra- or intracellularly from the anterior connectives or the neuropile of the terminal ganglion. In this way, taste sensilla can be stimulated by just one chemical diluted in pure water (without the salts added for electrical conduction) or possibly even gaseous chemicals: smells[3, 10, 11, 32, 33].

When higher order interneurons integrate one or several taste classes their synaptic input sites must collect information from widespread presynaptic terminals of afferents in the neuromeres of the terminal ganglion. Correspondingly, interneurons integrating single classes of taste selectively from non-glomerular structures in the neuropile should have wide branching areas for chemosensory input similar to the interneurons integrating mechanosensory input [3, 4, 34]. Our intracellular staining showed this for all taste sensitive interneurons especially when they responded to just one taste class. The occurrence of several local (but inter-neuromere) interneurons responsive to tastes indicates local processing of chemical cues for bilateral and inter-neuromere comparison of information which is required before and during oviposition (but possibly also during mating).

The interganglionic projections could not be traced with Lucifer yellow to their full extent rostrally. If we had been able to pursue the long ascending axons we might have encountered the location of the most anterior CNS areas of decision making (brain or thoracic ganglia) that initiate continuation or cancellation of oviposition on the basis of chemical cues perceived on or near the ovipositor.

We have no clue to where in the CNS of locusts commands for initiation, continuation or abandoning of egg-laying originate, while it is clear that most of the motor programs for the muscles are organised in the abdominal ganglia[4, 9, 10, 25, 27, 33, 35, 36] . Therefore, this study could only indicate basal anatomical and physiological features of primary sensory integration from contact chemosensory information of the ovipositor.

4.1 Perceived stimulants

Recording from higher order neurons of the chemosensory pathway originating from taste receptors of the ovipositor has demonstrated that the typical chemical qualities sensed by the primary taste receptors are transferred and perceived separately and jointly in the higher order interneurones of the locust terminal ganglion. Also, other stimulants unknown to us might be perceived by means of isolated taste receptors which have not been included into our testing protocol. The responses seen here fall into the categories wet (water), salty, acid, sweet, bitter (alkaloid-like) and possibly phenolic, all these being typical for taste receptor sensitivity on other locations of the locust [1,3, 10, 14, 18, 20, 27]. So presently, we must assume that the gustatory basis for the locust decision to start, continue or terminate oviposition depends on combinations and concentrations of these basic tastes perceived on or in the substrate. We also are curious to know whether functionally the taste sensitive interneurons subserve local and restricted abdominal reflexes only or whether they contribute the perception of taste that underlies behavioural decisions.

4.2 Selective and cumulative pathways

How the different chemical cues arising from the receptor level are utilized remains uncertain since tendencies in two different directions of neural processing appear: interneurons responding to just one type of stimulus can transfer this information further to centres of motor or behaviour decisions while other interneurons do the same for combinations of stimuli that might serve the perception of combined repulsive or attractive chemical stimuli for egg-laying behaviour.

Reference

1. White PR, Chapman RF. Tarsal chemoreception in the polyphagous grasshopper *Schistocerca americana*. Behavioral assays, sensilla distributions and electrophysiology. Physiology Entomology 1990; 15: 105 – 121.
2. Newland PL, Burrows M. Processing of mechanosensory information from gustatory receptors on a hind leg of the locust. Journal of Comparative Physiology 1994; 174: 399-410
3. Newland PL. Avoidance reflexes mediated by contact chemoreceptors on the legs of locust. Journal of Comparative Physiology 1998; 183: 313-324.
4. Tousson E. Neural processing of chemosensory information from the locust ovipositor. Ph.D. Goettingen University, Germany, 2001.
5. Chapman RF. Contact chemoreceptors in feeding by Phytophagous insects. Annual Review Entomology 2003; 48: 455-484.
6. 24-6 Rogers SM, Newland PL. Taste processing in the insect nervous system. Advanced Insect Physiology 2003; 31: 139-204.
7. Opstad R, Rogers S, Behmer T, Simpson S. Behavioural correlates of phenotypic plasticity in mouthpart chemoreceptor numbers in locusts. Journal of insect Physiology 2004; 50: 725-736.
8. Hallem E, Dahanukar A, Carlson J. Insect odour and taste receptors. Annual Review of Entomology 2006; 51: 113-135.
9. Tousson E, Youssef Z. Innervation, Central Projections and Intersegmental Interneurons with Chemosensory Inputs from the Locust Subgenital Plate Hair Receptors. Egyptian Journal of Experimental Biology (Zoology) 2006; 2: 21-31.
10. Newland PL, Yates PI. Nitrergic modulation of an oviposition digging rhythm of locusts. Journal of Experimental Biology 2007; In Press.
11. Ômura H, Honda K, Asaoka K, Takasa I. Tolerance to fermentation products in sugar reception: gustatory adaptation of adult butterfly proboscis for feeding on rotting foods. Journal of Comparative Physiology 2008; 194:545-555.
12. Dethier VG. The hungry fly. A physiological study of the behaviour associated with feeding. Harvard Univ. Press, 1976.
13. Newland PL. Processing of gustatory information by spiking local interneurones in the locust. Journal of Neurophysiology 2000; 82: 3149-3159.
14. Gaaboub I, Schuppe H, Newland. Receptor sensitivity underlies variability of chemosensory evoked avoidance movements of the legs of locusts. Journal of Comparative Physiology 2005; 191: 281-289.
15. Ma WC, Schoonhoven LM. Tarsal contact chemosensory hairs of the large White butterfly *Pieris brassical* and their possible role in oviposition behaviour. Entomologie Experimentalis et Applicata 1973; 16: 343-357.
16. Städler E, Renwick JA, Radke CD, Sachdev-Gupta K. Tarsal contact chemoreceptor response to glucosinolates and cardenolides mediating oviposition in *Pieris rapae*. Physical Entomology 1995; 20: 105-121.
17. Dougherty MJ, Guerin PM, Ward RD. Identification of oviposition attractants for the sandfly *Lutzomyia longipalpis* (Diptera: Psychodidae) in volatiles of faces from vertebrates. Physiological Entmology 1995; 20: 23-32.
18. Gaaboub I, Hustert H. Motor response to chemical stimulation of tarsal sensills in locusts. Proceeding of the 26 th Göttingen Neurbiology conference 1998; 26 (1): p. 336.

19. Tousson E, Gaaboub I, Hustert, H. Response characteristics and specificity of contact chemoreceptors from different sites in *Locusta migratoria*. Proceeding of the 27 th Göttingen Neurbiology conference 1999; 27 (2): 348.
20. Gaaboub I, Tousson E. Ultrastructure and Electrophysiological Studies on the Sense Organs of the Cotton Leaf Worm *Spodoptera littoralis* (Boisd.). Egyptian Journal of Experimental Biology (Zoology) 2005; 1: 167 – 176.
21. Newland PL, Rogers SM, Gaaboub I, Matheson T. Parallel Somatotopic Maps of gustatory and mechanosensory neurons in the central nervous system of an insect. Journal of Comparative neurology 2000; 275: 82-96.
22. Tousson E, Hustert H. Contact chemoreceptors from different sites have different projection patterns in the locust terminal ganglion. Proceeding of the 26 th Göttingen Neurbiology conference 1998; 26 (2): 377.
23. Tousson E, Hustert H. Central projections from contact chemoreceptors of the locust ovipositor and adjacent cuticle. Cell Tissue Research 2000; 302:285-294.
24. Rogers SM, Newland. Gustatory processing in thoracic local circuits of the locust. Journal of Neuroscience 2002; 22: 8324-8332.
25. Tousson E, Gaaboub I. neuroanatomical and electrophysiological relationships between sensory afferent arborizations in the locust paraproctal sensory systems. The 3rd Pros ICBS, 2004; 3: 595 – 614.
26. Hodgson ES, Lettvin JY, Roeder KD. Physiology of a primary chemoreceptor unit. Science 1955; 122: 417-418.
27. Gaaboub I. Neural processing of chemosensory information from the locust legs. Ph.D. Goettingen University, Germany, 2000.
28. Blaney WM. Electrophysiological responses of the terminal sensilla on the maxillary palps of *Locusta migratoria* to some electrolytes and non-electrolytes. Journal of Experimental Biology 1974; 60: 275-293.
29. Blaney WM. Behavioural electrophysiological studies of taste discrimination by the maxillary palps of larvae of *Locusta migratoria*. Journal of Experimental Biology 1975; 62: 555-569.
30. Tousson E. Neuroanatomical and electrophysiological studies of identified contact chemoreceptors on the ventral ovipositor valve of 3rd instar larvae of lubber grasshoppers (*Taeniopoda eques*). Zoology 2004; 107: 65 –73.
31. Roper SD. The cell biology of vertebrate taste receptors. Annual Review of Neuroscience 1989; 12: 329-353.
32. Lefebvre L. Grooming in crickets: timing and hierarchical organization. Animal Behaviour 1981; 29: 973-984.
33. Tousson E, Hustert H. The Intersegmental Network of Afferents in the locust abdominal ganglia. Cell Tissue Research 2006; 325: 151-162.
34. Kalogianni E. Morhology and physiology of abdominal intersegmental interneurones in the locust with mechanosensory inputs from ovipositor hair receptors. Journal of Comparative Neurology 1996; 366: 656-673.
35. Belanger JH, I Orcha. The role of sensory input in maintaining output from the locust oviposition digging central pattern generator. Journal of Comparative Physiology A , 1992; 171: 495-503.
36. Thompson KJ. Oviposition digging in the grasshopper, functional anatomy and motor program Journal of Experimental Biology 1986; 122:387-411.

Analysis and Identification of Tumor Marker in Lung Cancer using Two-dimensional Gel Electrophoresis and Matrix-assisted Laser Desorption Ionization Time of Flight Mass Spectrometry

Huizhen Zhang[1*], Hongxiang Guo[2], Qingtang Fan[1] and Yiming Wu[1]

1 Department of Labor and Environmental Health,College of Public Health, Zhengzhou University, Henan 450001, PR China,2 Department of life Sciences, Henan agriculture University, Henan 450002, PR China

Received March 10, 2009

Abstract: Tumor-specific protein spots were identified, including ApolipoproteinA-I precursor (Apo-AI), Peptidyl-prolyl cis-trans isomerase A, Calgranulin B (MRP-14), Calgizzarin (S100C protein), Ras-related protein Rab-14, apolipoprotein E. Among these 6 proteins, the potential significance of the differential expressions is discussed. These findings demonstrate that differential expression analysis of proteomes may be useful for the development of new molecular markers for diagnosis and prognosis of lung cancer. [Life Science Journal. 2009; 6(3): 46 – 53] (ISSN: 1097 – 8135)

Keywords proteome; two-dimensional electrophoresis (2DE); matrix assisted laser desorption ionization time of flight mass spectrometry (MALDI-TOF-MS); lung cancer, tumor marker

1. Introduction

Lung cancer is the leading cause of cancer death worldwide, and the number of lung cancer patients has been increased with the exposure to the environmental risk factors [1–4]. Prevention of lung cancer is a serious worldwide challenge. It is clear that the successful prevention of lung cancer will depend on the reduction of risk factors along with better methods of screening and early detection. Tumor markers are widely used for screening, diagnosis, staging, prognosis, monitoring response to treatment, and detection of recurrent disease[5]. The analysis of proteins overexpressed in lung cancer, and making the proteins serve as tumor markers, has been the subject of extensive research.

Although many insights into the molecular pathology of lung tumors have been achieved, additional information is critical to our understanding of the development and progression of these tumors as well as to early diagnosis. The most commonly evaluated markers include neuron-specific enolase, carcinoembryonic antigen, cytokeratin 19 fragments (CYFRA 21-1), squamous cell carcinoma antigen, cancer antigen CA 125, and tissue polypeptide antigen [6].

It is a complex work to detect new candidate markers because of the known heterogeneity of lung cancers. Methods have been developed to identify the tumor associated antigens such as molecular cloning in system or using a biochemical strategy based on the extraction of antigenic peptides bound to major histocompatibility complex class 1 molecules from tumor cells. These methods have allowed the recognition of certain human tumor antigens[7]. However, no evidence has been obtained indicating that the detection of these markers precedes clinical diagnosis of lung cancer.

Proteome is defined as the total proteins expressed by a genome and the comparative analyses of proteomes from cancer cells or tissues promise the discovery of new biomarkers for early detection of cancers [8, 9]. In this proteomics approach, two-dimensional polyacrylamide gel electrophoresis (2D-PAGE) and mass spectrometry have been the most important technologies for the separation and identification of proteins respectively [10, 11]. 2D-PAGE is a powerful research technique, which makes it possible to simultaneously examine hundreds of polypeptides in a tissue sample. It has been widely used for the detection and identification of potential tumor markers [12].Using 2D-PAGE and matrix assisted laser desorption/ionization-time of flight-mass spectrometry (MALDI-TOF-MS), we tried to identify the biomarkers of lung cancer by the comparative proteomes analysis of human normal lung tissues and cancerous lung tissues,

*Corresponding Author Huizhen Zhang, PhD
E-mail : Huizhenzhang@zzu.edu.cn

and the study will help to elucidate the molecular mechanism of cellular events associated with cancer progression, such as cellular signaling[13,14].

1 Materials and methods

1.1Reagents

Immobiline DryStrips (pH 3–10, 17 cm), DryStrip coverfluids, immobilized pH gradient (IPG) buffer, 3-[(3-cholamidopropyl) dimethylammonio]-1-propanesulfonate(CHAPS), bromophenol blue, agarose, acrylamide, tris-base, glycine, sodium dodecyl sulfate (SDS), N,N,N',N'-tetramethylethylenediamine (TEMED), and coomassie brilliant blue R-250, dithiothreitol(DTT), iodoacetamide, acetic acid, trypsin(sequencing grade), trifluoroacetic acid were bought from Bio-Rad and Sigma. The remaining chemicals were of analytical grade. All buffers were prepared with Milli-Q water.

1.2 Tissues and extraction preparation

Lung cancer tissues and corresponding adjacent noncancerous lung tissues were obtained with informed consent from patients at the First Affiliated Hospital of Zhengzhou University. Cancer samples were obtained from the "core" part of the tumor to avoid the adjacent noncancerous tissue. For each of the normal tissues, surface epithelium was procured selectively by dissection with special care for minimal contamination of nonepithelial cells, and samples were immediately snap-frozen in liquid nitrogen. They were classified histologically according to Lauren's classification after hematoxylin and eosin staining.

Fragments of normal and malignant tissues were sharp dissected and homogenized with a homogenizer in 2 mL fresh lysis buffer [7 mol/L urea, 2 mol/L thiourea, 40 mmol/L Tris ,40 g/L 3-([3-cholamidopropyl] dimethylammonio), 1-propanesulfonate (CHAPS), 100mmol/L dithiothreilol, 0.5 mmol/L PMSF, 0.5 mmol/L EDTA, 2%(V/V)NP-40 , 2%(V/V) Bio-Lyte 3/10, 1%(V/V)TritonX-100], then placed into tubes on ice for dealing with ultrasonic for 10 min. The mixture was centrifuged at 1 000 r/min for 5 min to remove tissue and cell debris, then centrifuged in a tableletop ultracentrifuge at 12000 g for 30 min at 4°C. The supernatant was pipetted off and stored at -80°C until use. These were used as the 2DE samples for the soluble fraction. Protein concentration of 2-DE samples was estimated according to a commercial Bradford reagent. BSA was used as standard.

1.3 2D electrophoresis and image analysis

First-dimension iso-electric focusing (IEF) was carried out on a ProteanIEF cell (Bio-Rad) using precast 17 cm pH 3–10 IPG gelstrips (Bio-Rad). 300μg total protein for silver staining gels (1000μg for Coomassie Brilliant Blue staining gels) was mixed with rehydration solution (8 M urea, 2% CHAPS, 50 mM DTT,0.2% Bio-Lyte 3/10 ampholyte, and 0.001% bromophenol blue) to a total volume of 500μL. Rehydration and IEF were carried out as follows: 12 h of passive rehydration, IEF at 500 V for 30 min, 5000 V for 3 h, and 10,000 V for 8h. The current was limited to 70μA per gel strip. All IEF steps were carried out at 17°C. After IEF separation, the gel strips were immediately equilibrated using two steps in equilibrium buffer containing 50 mM Tris-HCl (pH 8.8), 6 M urea, 30% glycerol, and 2% SDS. At the first step, 2% DTT (W/V) was included in the equilibrium buffer. 2.5% iodoacetamide (W/V) was added at the second step. The second dimension separation (13% T, 2.7% C) was carried out using Tris-glycine buffer containing 1 g/L SDS on a Protean II xi 2-D cell (Bio-Rad) according to the following procedure: 5 mA/gel for the initial 0.5 h and 18 mA/gel there after and a temperature of 4 °C, until the bromophenol blue front reached the bottom of the gel.

For silver staining, gels were immersed in ethanol: acetic acid: water (35:7:58) for 1.5 h, followed by washed twice in deionized water for 20 min. Gels were pretreated for 1 min in a solution of 0.2 g/L $Na_2S_2O_3$ and followed by 3 of 1-min washes in deionized water. Proteins were stained in a solution containing 2 g/L $AgNO_3$ and 0.075% formalin (37 g/L formaldehyde in water) for 20 min, and washed twice in deionized water for 1 min. Subsequently, gels were developed in a solution of 0.6 g/L formaldehyde, 20 g/L $Na_2S_2O_3$ and 0.004 g/L $Na_2S_2O_3$. When the desired intensity was attained, the developer was discarded and reaction was stopped by 10 g/L EDTA-Na_2. For Coomassie Brilliant Blue staining of gels, gels were equilibrated in a solution containing 500 ml/L methanol, 50 ml/L acetic acid and 25 g/L Coomassie Brilliant Blue R-250. Gels were rinsed in 300 ml/L ethanol containing 70 ml/L acetic acid.

To account for experimental variation, three batches of total proteins extracted from the experimental and

control sample respectively, were subjected to 2-D electrophoresis and replicate gels were simultaneously run three times. Protein patterns in the gels after staining were recorded as digitalized images using a high-resolution scanner. Gel image matching was done with PDQuest software(version 6.2, Bio-Rad, Richmond, CA).

1.4 In-gel digestion

Protein spots on Coomassie blue stained gel were performed essentially as described. After the completion of staining, the gel slab was washed twice with water for 10 min. The spots of interest were excised with a scalpel and put into 1.5 mL micro-tubes. The particles were washed twice with water and then twice with water/acetonitrile (1:1) for 15 min. The solvent volumes were about twice that of the gel. Liquid was removed, acetonitrile was added to the gel particles and the mixture was left for 2 h. After that, liquid was removed and the particles were rehydrated in 25 mmol/L NH_4HCO_3 for 5 min. Acetonitrile was added to produce a 1:1 mixture of 25 mmol/L NH_4HCO_3 /acetonitrile and the mixture was incubated for 15 min. All liquid was removed. Gel particles were dried in a vacuum centrifuge, reswelled in 10 mmol/L dithiothreilol and 25 mmol/L NH_4HCO_3, and incubated for 30 min at 56 °C to reduce the peptides. After chillness of tubes to room temperature and removal of the liquid, 55 mmol/L iodoacetamide in 25 mmol/L NH_4HCO_3 was added. The tubes were incubated for 30 min at room temperature in the dark to S-alkylate the peptides. Then iodoacetamide solution was removed, the particles were washed with 25 mmol/L NH_4HCO_3 and acetonitrile, dried in a vacuum centrifuge, rehydrated in digestion buffer containing 50 mmol/L NH_4HCO_3 and 12.5 ng/L trypsin (TPCK-treated, proteomics grade, Sigma, USA), incubated for 8 h～12 h at 37 °C. After digestion, 25 mmol/L NH_4HCO_3 was added, and the tube was incubated for 15 min. Acetonitrile was added and the tube was incubated for another 15 min. The supernatant was recovered, and the extraction was repeated twice with 50 g/L TFA/acetonitrile (1:1). The three extracts were pooled and dried in a vacuum centrifuge.

1.5 MALDI-TOF-MS identification of peptide mixtures and database searching

The peptide mixtures solubilized with matrix solution CCA (α-cyano-4-hydroxycinnamic acid) was spotted on the target and dried. Dried spots were analyzed in an REFLEX-III (Bluker) MALDI-TOF mass spectrometer. The spectrometer was run in positive ion mode and in reflector mode with the setting: accelerating voltage, 20 kV; grid voltage, 76%; guide wire voltage, 0.01%; and a delay time of 150 ns. The low mass gate was set at 500 m/z. Protein identification was carried out by peptide mass fingerprinting with searching the protein databases of Swiss-Prot/TrEMBL (http://www.expasy.ch/tools/peptident.html) and Mascot (http://www.matrixscience.com/). The following search parameters were applied: a mass tolerance of 50 ppm and one incomplete cleavage were allowed; acetylation of the N-terminus, alkylation of lysine by carboxyamidomethylation were considered as possible modifications.

2 Results

2.1 Protein expression maps of paired samples and image analysis

In order to evaluate the reproducibility of the soluble protein preparations and to quantify the protein extracts for 2DE gel analysis, mini 2DE gels (7 cm, pH3-10) were used at first. To ensure quality and reproducibility of results, three gels per sample were processed simultaneously with the same power supply and analyzed using PDQuest 2-D software(version 7.1, Bio-Rad, Richmond, CA). Protein extracts prepared from tissues were compared in this way and found to be highly reproducible. Protein patterns were analyzed using PDQuest software. Qualitative and quantitative comparisons were made between replicate groups, comprising the three gels for each sample. Quantitation is based on the peak intensity and area of Gaussian-fitted spots, allowing more accurate quantitation than summation of pixel intensities. Any differential spots that were not present or absent in all three gels within a replicate group were excluded.

Two-dimensional gel electrophoresis maps were constructed for human normal lung tissues and cancerous lung tissues proteins in fig.1. We made separate maps for the pH range 3 ～ 10. The second-dimensional gel electrophoresis was performed with 12.5% SDS-PAGE. For each sample, over 800 protein spots were resolved in a 2-DE gel (20 cm×20

cm) with silver-stained by computer-aided image analysis, and over 500 protein spots were resolved with Coomassie Brilliant Blue-stained. Figure 1A (from cancer tissues) contains a total of 530 spots, whereas figure 1B (from normal tissues) contains a total of 560 spots. A total of 515 spots from cancer tissues could be matched to those from normal tissues. In total, we were able to identify cancer-specific spots in 2DE gels. The positions of the identified proteins are shown in figure 1A. All of the identified spots could be considered as abundant proteins because of Coomassie Blue staining.

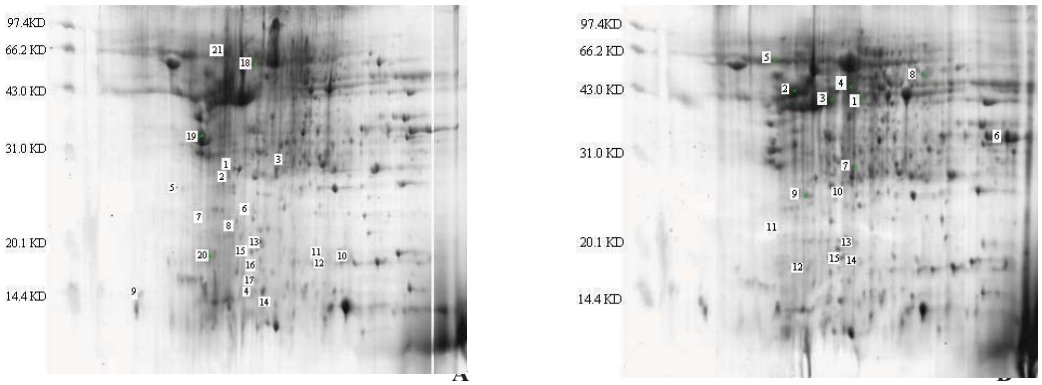

Figure 1. 2-D gel images of protein expression in lung cancer tissue and normal lung tissue

A: sample from lung cancer tissue. B: sample from normal lung tissue of the same patient.

Proteins were separated on pH 3-10 linear IPG strip in the first dimension and 125 g/L SDS-PAGE in the second dimension. All labeled spots were different expresses proteins.

To evaluate the potential for spurious differences that are not stage-specific, we also compared replicate groups in which gels were arbitrarily assigned to one of three groups, each containing one gel from each stage. No differences were detected between these groups, which suggested that the differentially represented spots are genuinely sample-specific.

2.2 Identification of overexpression proteins in cancerous lung tissues using peptide mass fingerprinting

Overexpression proteins spots were excised from the 2-D gels of cancerous lung tissues and subjected to trypsin digestion and MALDI mass spectrometry. 6 spots were identified successfully. The criteria used to accept identifications including the extent of sequence coverage, the number of peptides matched, the probability score, and whether human protein appeared as the top candidates in the first pass search where no restriction was applied to the species of origin. The data for the protein spot 1 as an example are shown in fig. 2. Fig. 2A shows the MALDI-TOF MS peptide mass fingerprint spectrum of trypsin-digested protein spot 1. Fig. 2B is the probability based mowse score. Score is -10*Log(P), where P is the probability that the observed match is a random event. Protein scores greater than 53 are significant (p<0.05). The score of two proteins is significant, we choice the protein with the highest score .Fig. 2C lists the matching peptides. Twenty peptides were matched with ApolipoproteinA-I, accession-numbered as P02647 in the protein database SWISS-PROT. These 20 peptides are indicated in the protein sequence shown in fig. 2D. The results of identification are summarized in the table 1. These identified protein spots are numbered as shown in Figure. 1.

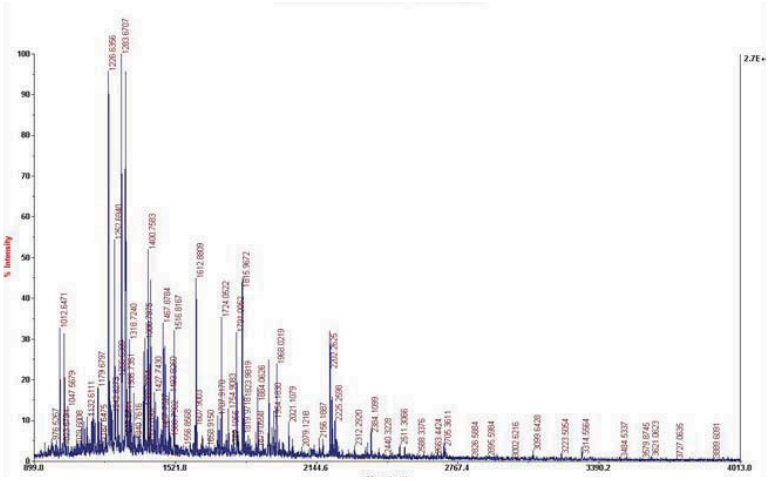

A

APA1_HUMAN;
Apolipoprotein A-I precursor (Apo-AI)
Nominal mass (Mr): 30759; Calculated pI value: 5.56
Score: 179
Sequence Coverage: 59%
Number of mass values searched: 51
Number of mass values matched: 20

Start - End	Observed	Mr(expt)	Mr(calc)	Delta	Sequence
37 - 47	1235.68	1234.67	1234.68	-0.01	DLATVYVDVLK
48 - 64	1815.97	1814.96	1814.84	0.12	DSGRDYVSQFEGSALGK
52 - 64	1400.76	1399.75	1399.66	0.09	DYVSQFEGSALGK
70 - 83	1612.89	1611.88	1611.78	0.10	LLDNWDSVTSTFSK
84 - 101	2202.26	2201.25	2201.11	0.14	LREQLGPVTQEFWDNLEK
86 - 101	1933.05	1932.04	1931.93	0.12	EQLGPVTQEFWDNLEK
121 - 130	1252.70	1251.69	1251.61	0.08	VQPYLDDFQK
121 - 131	1380.80	1379.80	1379.71	0.09	VQPYLDDFQKK
131 - 140	1427.75	1426.74	1426.66	0.08	KWQEEMELYR Oxidation (M)
132 - 140	1283.67	1282.66	1282.57	0.10	WQEEMELYR
132 - 140	1299.66	1298.65	1298.56	0.09	WQEEMELYR Oxidation (M)
143 - 155	1467.89	1466.88	1466.78	0.09	VEPLRAELQEGAR
165 - 173	1031.59	1030.59	1030.51	0.08	LSPLGEEMR
165 - 173	1047.58	1046.57	1046.51	0.07	LSPLGEEMR Oxidation (M)
165 - 175	1318.72	1317.71	1317.63	0.08	LSPLGEEMRDR Oxidation (M)
202 - 212	1157.69	1156.68	1156.62	0.06	LFALEENGGAR
220 - 230	1215.69	1214.68	1214.61	0.07	ATEHLSTLSEK
231 - 239	1012.65	1011.64	1011.57	0.07	AKPALEDLR
240 - 250	1230.78	1229.77	1229.70	0.07	QGLLPVLESFK
251 - 262	1386.80	1385.79	1385.71	0.08	VSFLSALEEYTK

B

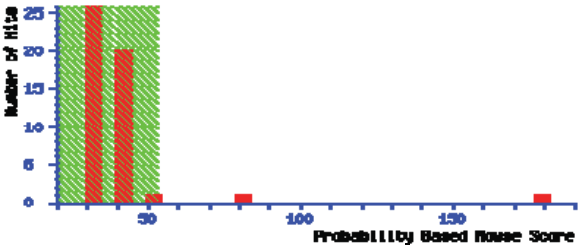

C

APA1_HUMAN;
Apolipoprotein A-I precursor (Apo-AI)
(P02647)

1 MKAAVLTLAV LFLTGSQARH FWQQDEPPQS PWDRVKDLAT VYVDVLKDSG
51 RDYVSQFEGS ALGKQLNLKL LDNWDSVTST FSKLREQLGP VTQEFWDNLE
101 KETEGLRQEM SKDLEEVKAK VQPYLDDFQK KWQEEMELYR QKVEPLRAEL
151 QEGARQKLHE QLQKLSPLGE EMRDRARAHV DALRTHLAPY SDELRQRLAA
201 RLEALKENGG ARLAEYHAKA TEHLSTLSEK AKPALEDLRQ GLLPVLESFK
251 VSFLSALEEY TKKLNTQ%

D

Figure 2. Analysis of spot NO.1 from human lung 2-DE map (pH 3–10) by MALDI-TOF MS. (A) MALDI-TOF MS peptide mass fingerprint spectrum obtained from crude peptide mixture after in-gel tryptic digest of spot NO.1. (B) Probability based mowse score (C) The list of matching peptides between the experimental and theoretical values. (D) The sequence of ApolipoproteinA-I identified. The matched peptides are shadowed in the sequenc

Table 1. MALDI-TOF-MS identification of overexpression proteins in lung cancer tissues

Spot*	AC**	Matched Peptide	Top score	Theoretic Mr	Sequence*** coverage (%)	Name and description
1	P02647	20	179	30759	42	ApolipoproteinA-I precursor (Apo-AI)
2	gi4557325	8	66	36246	34	apolipoprotein E precursor
3	P35287	9	66	23912	49	Ras-related protein Rab-14
4	P06702	6	60	13234	52	Calgranulin B (MRP-14)
5	P05092	10	62	17870	47	Peptidyl-prolyl cis-trans isomerase Cyclophilin A
6	P31949	16	110	11733	54	

* The numbering and lettering corresponding to the two-dimensional gel electrophoresis image in Fig. 1.

**Accession number in NCBInr, SWISS-PROT.

***Percentage of the protein sequence covered by the matched peptides.

3 Discussion

Proteomic study means the analysis of the entire protein complement expressed by a genome [15]. Classically, proteome analysis consists of three steps: Two-dimensional gel electrophoresis (2-DE) used for proteins profiling, mass spectrometry (MS) for critical confirmation of the molecular weights and bioinformatics for protein identification. Comparative proteome analysis is a good strategy to discover proteins that undergo changes in expression level and may underlie the differences of phenotype[16]. 2-DE with its recent developments has been seen as an ideal tool for proteome analyses. Immobilized pH-gradient (IPG) strips are used in the first-dimensional gel electrophoresis to provide a basis for reproducible separation according to proteins isoelectric points. Advanced computer graphics and image analysis systems have offered a possibility for quantitative detection of protein spots, in addition to edition and storage of the 2-DE images. Proteome comparison between tissues in the different situations can cast a light on some protein spots, which are differently expressed in quantity under different surroundings. Nowadays, mass spectrometry such as matrix-assisted laser desorption ionization-time of flight mass spectrometry (MALDI-TOF-MS)[17], can routinely identify and characterize proteins. Peptide mass fingerprinting identifies a protein based on the molecular weights of its peptides obtained by MS after digestion by trypsin[18]. The developed bioinformatics allows the identification of most proteins[19].

In this paper, we reported comparative proteome studies between normal lung tissues and cancerous lung tissues. The pH 3～10 range in the first-dimensional gel electrophoresis separates the soluble proteins in the lung tissues. All paired samples, which would be compared each other, were run together at the same conditions. This avoids any artificial differences between samples due to the different running conditions.

The 2-DE patterns of normal lung tissues and cancerous lung tissues were compared each other with the help of the software PDQest, and different expressional protein spots were found. These protein spots have a consistent increase in all 8 independent paired samples. Over-expressed protein spots were excised from the gel and digested with trypsin. Molecular weights of the tryptic peptides were determined by MALDI-TOF-MS. Obtained protein scores are significant ($P < 0.05$) in the protein database search. 19%～72% coverage of protein sequences was obtained in the analyses of MALDI-TOF MS.

Number 4 and number 6, were identified as Calgranulin B (S100A9, MRP14) and Calgizzarin (S100A11, S100C protein), two members of the S100 family. S100 proteins comprise a family of 10～14 kDa EF-hand-containing calcium binding proteins that function to transmit calcium-dependent cell regulatory

signals, which are specifically expressed in a variety of tissues and cell types. It is thought that they are primarily involved in Ca^{2+}-mediated signal transduction. Changes in intracellular calcium levels alter the structure and function of these proteins[20]. They have been frequently described in association with cell growth and differentiation, with cell cycle regulation and with several human diseases such as cancer and skin disorders. Studies suggest that these members of the S-100 protein family have a role in cytoskeletal changes seen in various skin diseases. Calgizzarin(S100A11)is a calcium-binding protein implicated in a variety of biologic functions such as proliferation and differentiation in cancer. Calgizzarin, a new tumor marker protein in nasopharyngeal carcinoma (NPC)[21],plays a significant role in tumor suppression and it is involved in prostate cancer development and progression. Calgranulin B represents a novel molecular parameters of the early events of inflammatory reactions that reveal interesting aspects for the pathomechanism of chronic inflammatory reactions[22]. Tumor specific protein markers were identified in colon tumors as calgranulin B that is also upregulated in colorectal cancer [23,24]. Calgizzarin and Calgranulin B present in lung cancer has not be documented.

Apolipoprotein A-I (apoA-I) is the major protein constituent of high density lipoproteins (HDL) and lymph hylomicrons. In human, proapoA-I is synthesized as a precursor protein, preproapoA-I, of 267 amino acids and is thought to occupy a surface position on the lipoprotein. ApoA-I activates lecithin-cholesterol acyltransferase, which is the cholesterol-esterifying enzyme of plasma involved in the production of mature circulating HDL [25]. Apolipoprotein E (apoE), a protein with three common isoforms, has a large impact on longevity and successful aging. Impairments in cognitive performance have been observed in aged apolipoprotein (apoE)-deficient mice [26]. In this study, apolipoprotein (apo)A-I and Apolipoprotein E are found to be up-regulated in lung cancer.

Cyclophilins (CyPs) are a large class of highly conserved ubiquitous peptidyl-prolyl cis-trans isomerases. CyPs have also been identified as a specific receptor for the immunosuppressive drug cyclosporin A and are involved in a variety of biological functions. Cyclophilin A (CypA) is a cytosolic protein that has many biological functions including immune modulation, cell growth, tumorigenesis, and vascular disease. The objective of this study was to determine the effect of CypA on cell proliferation and several gene expressions in human endothelial cells and vascular smooth muscle cells[27]. Cyclophilin A (CyPA) is overexpressed in non-small cell lung cancer (NSCLC), but it was not found that CyPA is of prognostic significance[28].This paper reported Cyclophilin A (CypA) overexprssed in lung cancer ,but it's function of a biomarker for lung cancer need further study to validate.

In conclusion, the differences of the proteins between normal and cancerous lung tissues are complex. To affirm proteins studying above be cancer-associated of lung cancer and to serve for the further basic and clinical investigation, we need do some other works such as enlarging sample, purifying and analyzing these differential proteins, and study the actions during the multistage process of lung cancer.

Acknowledgements

This work was finished in Henan Key Laboratory for Molecular Medicine. This work was supported by the key disciplines granted from the national "211 Project" and the National Natural Science Foundation of China (No.30371695).

References

1. Greenlee RT, Murray T, Bolden S, et al. Cancer statistics. CA Cancer J Clin, 2000, 50:27–33

2. Kamp DW, Graceffa P, Pryor WA, et al. The role of free radicals in asbestos-induced diseases. Free Radical Biol Med, 1999,12: 293–315

3. Weitzman SA, Graceffa P. Asbestos catalyzes hydroxyl and superoxide radical generation from hydrogen peroxide. Arch Biochem Biophys, 1984,228: 373–376

4. Bailey-Wilson JE, Pugh EW, Wiest JS, et al. Lung cancer: genetic epidemiology. In:Bertino JR,editor . Encyclopedia of cancer.San Diego, CA:Academic Press,995-1003

5 .Lindblom A, Liljegren A. Tumor markers in malignancies. Br Med J, 2000,320:424–427

6. Stieber P, Aronsson AC, Bialk P, et al. Tumor markers in lung cancer: EGTM recommendations. Anticancer Res, 1999,19:2817–1819

7. Lawrie LC, Fothergill JE, Murray GI. Spot the differences: proteomics in cancer research. Lancet Oncol, 2001,2:270-277

8. Simpson RJ, Dorow DS. Cancer proteomics: signaling networks to tumor markers. Trends Biotechnol, 2001,19(10 Suppl):S40–S48

9. Bichsel VE, Liotta LA, Petricoin EF 3rd. Cancer protoemics: from biomarker discovery to signal pathway profiling. Cancer J, 2001,7(1): 69–78

10. Gorg A, Obermaier C, Boguth G, et al. The current state twodimensional electrophoresis with immobilized pH gradients. Electrophoresis, 2000,21:1037–1053

11. Lahm HW, Langen H. Mass spectrometry: for the identification of proteins separated by gels. Electrophoresis, 2000,21:2105–2114

12. Okuzawa K, Franzen B, Lindholm J, et al. Characterization of gene expression in clinical lung cancer materials by two-dimensional polyacrylamide gel electrophoresis. Electrophoresis, 1994,15:382–390

13. Gygi SP, Corthals GL, Zhang Y, Rochon Y, Aebersold R. Evaluation of two-dimensional gel electrophoresis-based proteome analysis technology. Proc Natl Acad Sci U S A, 2000, 97: 9390-9395

14. Ni XG, Zhao P, Liu Y, et al. Application of proteomic approach for solid tumor marker discovery. Aizheng[Chinese journal of cancer], 2003, 22: 664-667

15. Wilkins MR, Sanchez JC, Gooley AA, et al. Progress with proteome projects: why all proteins expressed by a genome should be identified and how to do it. Biotechnol Genet Eng Rev, 1996,13:19–50

16. O'Farrel PZ. High-resolution two-dimensional electrophoresis of proteins. J Biol Chem, 1975,250: 4007–4021

17. Nordhoff E, Egelhofer V, Giavalisco P, et al. Large-gel two-dimensional electrophoresis-matrix-assisted laser desorption/ionization time of flight mass spectrometry: an analytical challenge for studying complex protein mixtures. Electrophoresis, 2001,22(14): 2844–2855

18. Mann M, Hojrup P, Roepstorff P. Use of mass spectrometric molecular weight information to identify proteins in sequence databases. Biol Mass Spectrom, 1993,22:338–345

19. Tripathi KK. Bioinformatics: the foundation of present and future biotechnology. Curr Sci, 2000,79(5):570–575

20. Ruse M, Lambert A, Robinson N, et al. S100A7, S100A10, and S100A11 are transglutaminase substrates. Biochemistry, 2001,40(10):3167-3173

21.Fung LF, Lo AK, Yuen PW, et al. Differential gene expression in nasopharyngeal carcinoma cells. Life Sci, 2000, 67(8):923-936

22. Sorg C. The calcium binding proteins MRP8 and MRP14 in acute and chronic inflammation. Behring Inst Mitt, 1992,(91):126-37

23. Chaurand P, DaGue BB, Pearsall RS, et al. Profiling proteins from azoxymethane-induced colon tumors at the molecular level by matrix-assisted laser desorption/ionization mass spectrometry. Proteomics, 2001,1(10):1320-1326

24. Jungblut PR, Zimny-Arndt U, Zeindl-Eberhart E, et al Proteomics in human disease: cancer, heart and infectious diseases. Electrophoresis, 1999,20(10):2100-2110

25. Ghiselli G, Gotto AM, Tanenbaum S, et al. Proapolipoprotein A-I conversion kinetics in vivo in human and in rat. Proc Natl Acad Sci U S A, 1985,82:874-878

26. Law A, Gauthier S, Quirion R. Alteration of nitric oxide synthase activity in young and aged apolipoprotein E-deficient mice. Neurobiol Aging, 2003,24 (1):187–190

27. Huang LL, Zhao XM, Huang CQ, et al. Structure of recombinant human cyclophilin J, a novel member of the cyclophilin family. Acta Crystallogr D Biol Crystallogr, 2005,61(Pt 3):316-321

28. Howard BA, Zheng Z, Campa MJ, et al.Translating biomarkers into clinical practice: prognostic implications of cyclophilin A and macrophage migratory inhibitory factor identified from protein expression profiles in non-small cell lung cancer. Lung Cancer, 2004,46(3):313-323

Detection of genomic *Toxoplasma gondii* DNA and anti-*Toxoplasma* antibodies

Nahed H. Ghoneim[1]; S. I. Shalaby[2]; Nawal A. Hassanain[3*]; G.S.G. Zeedan[4]; Y.A. Soliman[5] and Abeer M. Abdalhamed [4]

[1]Dept. Zoonotic Dis., Faculty of Vet. Med., Cairo Univ., Giza, Egypt.; [2]Dept. Compl. Med., Med. Res. Div., National Research Centre, Giza, Egypt; [3]Dept. Zoonotic Dis., Vet. Res. Div., National Research Centre, Post Box: 12622, El-Tahrir Street, Dokki, Giza, Egypt; [4]Dept. Parasitol. and Anim. Dis., Vet. Res. Div., National Research Centre, Giza, Egypt; [5]Central Lab. for Evaluation of Vet. Biologics, Abbassia, Cairo, Egypt

Received July 30, 2009

Abstract Toxoplasmosis is a disease of zoonotic nature; being reported to be widespread in animals and humans. Serological diagnosis represents the first and the most widely used approach to define the stage of toxoplasmosis and diagnosis of primary and late infection in pregnancy can be improved by determination of Toxoplasma DNA. Eighty-eight and 88 coagulated and non coagulated blood samples were collected from high risk women {68 pregnant that had bad obstetric history and 20 non pregnant that aborted in different times (1st or 2nd trimester)} with an average age (17 -45 years)} and their contact animals (62 sheep and 24 goats) in three centers at El-Fayoum Governorate in Egypt. Results showed that the prevalence of anti -Toxoplasma IgM and IgG among pregnant women (30.5 and 20.45 %, respectively) was higher than non pregnant women (13.6 and 7.95 %, respectively). The positive percents of PCR in the examined positive ELISA (IgG and IgM) pregnant and non pregnant women were (21.5 % and 9 %, respectively) suggesting a recent or late infection. The high risk pregnant and non pregnant women aged 35-45 years old showed the highest percent of IgG (66.7 % and 62.5%), IgM (50 and 50%) and positive PCR (50% and 37.5%), respectively. Sheep and goats showed high seroprevalence of Toxoplasma IgG (98.4 % and 41.7 %) and positive PCR (67.7 and 25%), respectively and those animals may constitute a potential source of infection to the investigated women at El-Fayoum Governorate. The relationship between positivity and some risk factors was assessed by ELISA and data collected by questionnaire. The strongest risk factors associated with acquiring toxoplasmosis were eating undercooked sheep or goat meat, drinking unpasteurized sheep or goat milk and handling raw sheep or goat meat. [Life Science Journal. 2009; 6(3): 54 – 60] (ISSN: 1097 – 8135)

Key words: Toxoplasmosis; ELISA IgG; ELISA IgM

1 Introduction

Toxoplasmosis is a zoonotic disease caused by a protozoan parasite called Toxoplasma gondii which can infect all mammals and birds species throughout the world. Approximately one-third of humanity has been exposed to the parasite world wide[1, 2]. Except feline species which acts as a definitive host, all animal species act as intermediate hosts[3, 4].

T. gondii infection in humans may occur vertically by tachyzoites that are passed to the fetus via the placenta, or horizontal transmission which may involve three life –cycle stages i.e. ingesting sporulated oocysts from cats or ingesting tissue cysts in raw or under cooked meat or tachyzoites in blood products or primary offal (viscera) of many different animals, tissue transplants, and unpasteurized milk[5].

While infection of healthy adult humans is usually mild, serious disease can result in utero or when the host is immunocompromised[6,7]. The fetus is only at risk of congenital disease when acute infection occurs in pregnancy. Congenital infection has also been reported from a chronically infected immunocompromised mother with a reactivation of toxoplasmosis.

Economical losses of toxoplasmosis are of medical and veterinary importance, in humans are due to abortion, fetal abnormalities[8], morbidity and mortality in congenitally infected and immunocompromised individuals[9, 10]. In small ruminants (sheep and goat),

economical losses occur due to prenatal death and abortion[8].

Avelino et al[11] mentioned that pregnant women living under unfavorable environmental conditions had an approximately two times increased risk of being infected for each risk factor (contact with host animals and presence of vehicles of oocysts transmission). Previous pregnancy was the risk factor that had the strongest influence on acquiring toxoplasmosis. Han et al[12] stated that T. gondii infection in Korea is positively correlated with eating raw meat, but is not associated with the consumption of unwashed vegetables, drinking untreated water, a history of raising a cat, or blood transfusion. Fallah et al[13] reported that age, consumption of fresh undercooked meat and frequent consumption of raw vegetables were statistically significantly associated with higher infection rates.

Therefore, the present work aimed to detect Toxoplasma infection among high risk women {pregnant women that had bad obstetric history and non pregnant women that aborted in different times (1st or 2nd trimester)} in relation to some risk factors e.g. age, contact animals, eating raw meat) in El fayoum, Tamyia and Senoris centers at El-fayoum Governorate (Egypt) using ELISA and PCR.

2 Materials and Methods

Blood samples were collected from 88 women (68 pregnant and 20 non pregnant women with an average age (17 -45 years) in three centers (El fayoum, Tamyia and Senoris centers) at El fayoum Governorate during the period from October 2005 to December 2006. Blood samples were also collected from their contact animals (62 sheep and 24 goats). Serum was separated and blood samples with EDTA were stored at -20oC until used. A questionnaire was carried out with the investigated women to detect the relationship between positivity and some risk factors (eating undercooked meat, drinking raw sheep or goat milk, preparation of raw sheep or goat meat, own or exposures to cats or Feline species).

ELISA Assay

ELISA in women: The collected serum samples from pregnant and non pregnant women were tested for the presence of the specific IgM and IgG antibodies by using Clinotech Toxo ELISA IgM and IgG kits (Clinotech Diagnostics & Pharmaceuticals, Canada). Clinotech Toxo IgM and IgG ELISA kits are microwell ELISA test designed for the qualitative detection of IgM or IgG antibodies to T. gondii in human serum.

ELISA in small ruminants: ELISA was carried out according to Voller et al[14]. Whole soluble tachyzoite antigens were prepared as described by Waltman et al[15]. The optimal antigen (soluble tachyzoites antigen preparation) concentration, antibody and conjugate dilutions were chosen after preliminary checker board titration. In the present study, the optimum conditions were 10 µg/ml coating buffer antigen concentration, 1:100 sheep and goat serum dilutions. 1:1000 Horse radish peroxidase- labeled anti-sheep-IgG and anti-goat-IgG (Sigma Co.) as conjugate and 1 mg p-nitrophenyl phosphatase dissolved in one ml substrate buffer as substrate. The absorbance of the colored reaction was read within 30 min at 405 nm using a titertek multiskan ELISA reader. All incubation steps were carried out at 37°C in a moist chamber. The positive threshold value was determined to be two-fold the mean cut-off value of negative sera. PCR

DNA extraction

Extraction of genomic DNA from the RH T. gondii strain: It was carried out according to Sambrook et al[16]. The DNA pellet was dissolved in 50µl of TE (pH 8) and stored at -20°C till used as positive control.

Extraction of genomic DNA of T. gondii from the collected blood samples: The genomic DNA from blood samples collected from women (88) and animal (86) was extracted with the Biospin Blood Genomic DNA Mini-Prep Kit (BioFlux Cat # BSJ040100001S80) as manufacture instructions. DNA concentration and purity was measured according to Sambrook et al[17].

PCR amplification of B1 gene: B1 gene was amplified16 using primers 1 (5′-TCG GAG AGA GAA GTT CGT CGC AT -3′ and 2 (5′-AGC CTC TCT CTT CAA GCA GCG TA-3′) [18]. The following reaction mixture was added in a 0.2 ml PCR tubes: DNA tamplet (100 ng/µl), 10 µl; Taq polymerase (5u/µl), 1 µl; 10x enzyme buffer, 2 µl; dNTPs, 0.8 µl; each Primer, 1 µl and Bidist. water to 20 µl. The mixture was briefly spined and placed in the thermal cycler (T gradiant, Biometra, Germany), which was programmed as follow: initial denaturing (95^{o}C/2 minute) and 40 cycles

consisting of denaturing (95°C/1 minute), annealing (55°C/30 seconds), extension (72°C/45 seconds) and final extension (72oC/10 minutes). PCR product was electrophoresed at 80 v/15 minutes[16] and finally examined using UV transilluminator. 100 bp DNA ladder (Finzyme) was used as a marker. 3 Results

Table (1 & 3) show that high risk women of the age group 35-45 years gave the highest total percent of anti-Toxoplasma IgG (66 and 62.5%) and positive PCR (50 and 37.5%), respectively. Also, they showed the highest and equal total percents of anti-Toxoplasma IgM (50 %) (Table 2). Sheep showed higher percent of anti-Toxoplasma IgG and positive PCR (98.4 and 67.7% %) than goats (41.7 and 25%), respectively (Table 4). Table (5) shows that consumption of raw or undercooked sheep or goat meat, drinking raw sheep or goat milk and handling raw sheep or goat meat are the strongest risk factors of acquiring T. gondii infection by high risk women at El-Fayoum Governorate. The PCR product (300 bp) was detected in positive blood samples in women (Figure 1) and small ruminants (Figure 2).

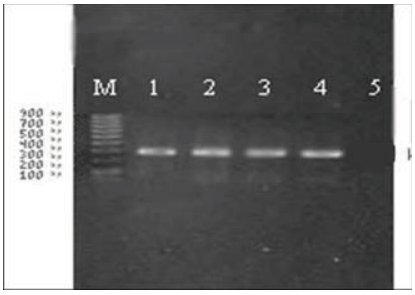

Figure 1. Electrophoretic pattern of the PCR products (300 bp) from human samples. Lane 1: positive control; lane 2, 3 and 4: positive women samples; lane 5: negative blood samples; M: DNA marker (100 bp).

4 Discussion

Routine serologic diagnosis of toxoplasmosis provides high sensitivity, but specificity varies depending on the test used[19]. Pelloux et al[20] stated that diagnosis of primary and late infection with *T.gondii* in pregnancy can be improved by determination of *Toxoplasma* DNA.

In the present study, the seroprevalence of *T .gondii* IgG among pregnant (47, 42.5 and 47.8 %) was higher than non pregnant women (37.5, 40 and 45.5 %) at El-Fayoum Governorate (El Fayoum, Senoris and Tamyia centers, respectively). This higher seroprevalence may be due to alterations in the immune mechanisms in pregnancy leading to increase of the invasion of this parasite[21,22]. Hussein et al[23] determined the seroprevalence of *Toxoplasma* IgG by ELISA in 31 full term parturient (57.9%), 38 aborted (58.1%) and prematurely delivered women (44.7%). El- Fakahany et al[24] reported that seropositivity to specific IgG antibodies was 36.4 %, 59.2% and 57.9 % in complicated gestation, uncomplicated gestation and randomly population, respectively. On the other hand, Kurnatowska and Tomczewska[25] found that the incidence of *T.gondii* specific IgG was significantly higher in non pregnant women than pregnant women.

The total seroprevalences of *T .gondii* IgG and IgM among pregnant (66.6 and 50%, respectively) and non pregnant women (62.5 and 50%, respectively) of the age group 35-45 years at El-Fayoum Governorate were the highest. These high risk group women showed also the highest positive PCR results (62.550 for pregnant and 37.5% for non pregnant). Valcavi et al[26] determined the prevalence of IgG antibodies to *T. gondii* in Italy by ELISA; being 48.5% with correlation of infection with age, showed a significant increase of positivity until 30-40 approximately years. Remington et al[27] mentioned that the prevalence of the infection with *T.gondii* increases with age and there are considerable geographic differences in prevalence rates. Hung et al[28] mentioned that older age group of ≥ 35 years had a significantly higher seroprevalence than that of the younger age group of 15-25 years. This may be due to decrease the immunity with advanced in age. Also, Fallah et al[13] reported that age was statistically significantly associated with higher infection rates.

Sheep and goats showed high positive percent of *Toxoplasma* IgG and genomic DNA (98.4 and 67.7 and 41.7and 25%, respectively) at El-Fayoum Governorate. This finding is in agreement with Tenter et al[5] who reported that sheep showed high seroprevalences in many areas of the world up to 92%. On the other hand, Dodriguez et al[29] detected higher seroprevalence rate of *Toxoplasma* IgG in goats (63.3 %) in the island of Grand Canary. Clementino et al[30] reported lower seroprevalence rate of anti-*T. gondii* specific IgG in sheep (29.41%) in Brazil.

The high prevalence of *T.gondii* infection in sheep

and goats may be due to sheep free range livestock associated with *T.gondii* infection. They are kept on pastures with an increased pressure of infection due to contamination of environment with oocysts. The frequency of stray cats in a humid rainy climate favoring the survival of oocysts has contributed to the high *Toxoplasma* prevalence in Central America[27]. In Egypt, stray cats are widely spread as in El-Fayoum governorate which is in favor of a higher prevalence of oocysts in humid environment and farming animal rearing are also common. Avelino et al[11] mentioned that pregnant women living with host animals or vehicles of oocysts transmission had an approximately two times increased risk of being infected for each risk factor.

The data collected by questionnaire and ELISA positivity showed that eating undercooked sheep or goat meat, drinking raw sheep or goat milk, and preparation of raw sheep or goat meat were the risk factor that had the strongest influence on acquiring toxoplasmosis by the investigated women at El-Fayoum Governorate. While, any raw meat exposure or drinking any raw milk of different animals (cow or buffalo milk) had less influence followed by own or exposure to cats or Feline species. Han et al[12]and Fallah et al[13] stated that *T. gondii* infection is positively correlated with eating raw meat. Laila Nimri et al[31] found that the increase of infection with *Toxoplasma*, in Jordan, is due to consumption of lamb greater than that of beef, and these animals are reared outdoors which put them at greater risk of environmental exposure than animals reared indoors. Han et al[12] reported that *T. gondii* infection is not associated with a history of raising a cat.

We can conclude that the high prevalence of toxoplasmosis among the investigated high risk women at El-Fayoum Governorate is due to many risk factors including age, contact with host animals (small ruminants), eating undercooked meat, drinking raw sheep or goat milk, preparation of raw sheep or goat meat and own or exposure to cats or Feline species). It is recommended to consider routine serological testing in pregnancy due to high prevalence of toxoplasmosis in the investigated pregnant women. Women are advised to avoid the numerous risk factors, making compliance difficult.

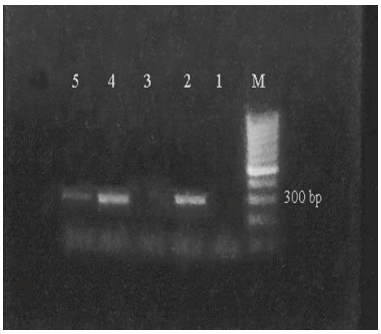

Figure 2. Electrophoretic pattern of the PCR products (300 bp) from small ruminants. Lane 1: negative control; lane 2: positive control; lane 3: negative sheep blood samples; lane 4 and 5: positive sheep and goat blood samples. M: DNA marker (100 bp).

References

1. Evengard B, Lilja G, Capraru T, *et al.* A Retrospective study of seroconversion against *Toxoplasma. gondii* during 3,000 pregnancies in Stockholm. Scand J Infect Dis., 1999; 31:127-129.
2. Sukthana Y. Toxoplasmosis beyond animals to humans. Trends Parasitol 2006 ; 3:173-142.
3. Innes EA. Toxoplasmosis: Comparative species susceptibility and host immune response. Comp Immunol. Microbiol Infect Dis., 1997; 20: 131-138.
4. Jenum PA, Stray-Pedersen B. Development of specific immunoglobulins G, M, and A following primary *Toxoplasma gondii* infection in pregnant women. J Clin Microbiol., 1998; 36: 2907-2913.
5. Tenter AM, Heckeroth AR, Weiss LM. *Toxoplasma gondii*: from animals to humans. Int J Parasitol, 2000; 30:1217-1258.
6. Al-Qurashi AR, Ghandour AM, Obeid OE, *et al.* Seroepidemiological study of *Toxoplasma. gondii* infection in the human population in the Eastern Region. Saudi Med.J, 2001; 22:13.

7. Marcinek P, Nowakowska D, Szaflik K, *et al*. Analysis of complications during pregnancy in women with serological features of acute toxoplasmosis or acute parvovirosis. Ginekol Pol, 2008; 79: 1886-1891.
8. Buxton D. Epidemiology and economic impact of toxoplasmosis in animal production: In Proceedings of the Cost-820 Annual Workshop, Vaccines Against Animal Coccidioses.Tecni Publication España, SL, Madrid, 1998; 52–53.
9. Dunn D, Wallon M, Peyron F, *et al*. Mother-to-child transmission of toxoplasmosis: risk estimates for clinical counselling or risk estimates for clinical decision-making. Lancet, 1999; 53:1829-1833.
10. Petersen E, Pollak A, Reiter-Owona I. Recent trends in research on congenital toxoplasmosis. Int J Parasitol, 2001; 31: 115-144.
11. Avelino MM, Campos DJ, Parada JB. Risk factors for *Toxoplasma.gondii* infection in women of childbearing age. Braz J Infect Dis 2004; 8:164-174.
12. Han K, Shin DW, Lee TY, *et al*. Seroprevalence of *Toxoplasma gondii* infection and risk factors associated with seropositivity of pregnant women in Korea. J Parasitol, 2008; 94:963-965.
13. Fallah M, Rabiee S, Matini M, *et al.* Seroepidemiology of toxoplasmosis in primigravida women in Hamadan, Islamic Republic of Iran, 2004. East Mediterr Health J, 2008; 14:163-71.
14. Voller A, Bidwell DE, Bartlett A, et al, A microplate enzyme-immunoassay for *toxoplasma* antibody. J Clin Pathol, 1976; 29: 150-153.
15. Waltman WD, Dreesen DW, Prickett DM, *et al*. Blue JL, Enzyme-linked immunosorbent assay for the detection of toxoplasmosis in swine interpreting assay results and comparing with other serological tests. Egypt soc parasitol 1984; 30: 27-42.
16. Sambrook J, Russell D, Gola J. Molecular Cloning 3rd A laboratory manual. 2001;1: 32–34.
17. Sambrook J, Fritsch EF, Maniatis T, Molecular Cloning: A Laboratory Manual Cold Spring Harbor Laboratory, Cold Spring Harbor, N Y. 1989.
18. Burg JL, Grover CM, Pouletty P, et al, Direct and sensitive detection of a pathogenic protozoan, *Toxoplasma gondii*, by polymerase chain reaction. J Clin Microbiol, 1989; 27: 1787–1792.
19. Liesenfeld O, Press R, Flander R, et al, Study of Abbott Toxo Imx system for detection of immunoglobulin G and immunoglobulin M toxoplasma antibodies: value of confirmatory testing for diagnosis of acute toxoplasmosis. J clin Microbio, 1996; 34:2526–2530.
20. Pelloux H, Brun E, Vernet G, *et al*. Determination of anti-*Toxoplasma gondii* immuno-globulin G avidity: adaptation to the Vidas system(BioMerieux).Diagn Microbiol Infect Dis., 1998; 32: 69–73.
21. Crouch SP, Crocker IP, Fletcher J. The effect of pregnancy on polymorphonuclear leukocyte function. J Immunol, 1995; 155:5436–43.
22. Boyer KM, Remington JS, MacLeod RL. Toxoplasmosis. In: Feigin RD, Cherry JD (editors),Textbook of Pediatric Infectious Diseases.4thed.Philadelphia:WB Saunders Company 1998; 4:73–90.
23. Hussein AH, Ali AE, Saleh MH, *et al*. Prevalence of *toxoplasma* infection in Qualyobia governorate, Egypt. J Egypt Soc Parasitol, 2001; 31 :355-363.
24. El- Fakahany A,F, Abdel-Maboud AI, El-Garhy MF, *et al*. Comparative study between ELISA IgG, IgM and PCR in diagnosing and studying toxoplasmosis in Qualyobia Governorate,Egypt. J Egypt Soc Parasitol, 2002; 32:475-486.
25. Kurnatowska A, Tomczewska I. Prevalence of *Toxoplasma gondii* and analysis of specific immunoglobulins concentration in serum of women during the reproductive period in a sample of Wloclawek population. Wiad Parazytol, 2001; 47 77-82.
26. Valcavi PP, Natali A, Soliani L, et al, Prevalence of anti-*Toxoplasm*a *gondii* antibodies in the population of the area of Parma (Italy). Eur J Epidemiol, 1995; 11: 333-337.
27. Remington JS, McLeod R, Thulliez P, et al, Toxoplasmosis, Infectious diseases of the fetus and newborn infant; in Remington JS, Klein J (5thed.). W. B. Saunders, Philadelphia, Pa 2001; pp 205.
28. Hung CC, Fan CK, Su KE, et al, da Conceicao dos Reis Ferreira M, de Carvalho JM, Cruz, C, Lin YK, Tseng LF, Sao KY, Chang WC, Lan HS, Chou SH. Serological screening and toxoplasmosis exposure factors among pregnant women in the

Democratic Republic of Sao Tome and Principe**.** 2Trans R Soc Trop Med Hyg, 2007; 101:134- 139.

29. Dodriguez-Ponce E, Molina JM, Hernandez S. Seroprevalence of goat Toxoplasmosis on grand Canary island 9Spain). Preventive Vet Med,1995; 24 :229-231.
30. Clementino MM, Souza MF, Andrade Neto VF. Seroprevalence and *Toxoplasma. gondii*-IgG avidity in sheep from Lajes , Brazil. Vet Parasitol, 2007; 146:199-203.
31. Laila N, Herve P, layla EL. Detection of *Toxoplasma gondii* and specific antibodies in high-risk pregnant women. Am.J.Trop Med.Hyg, 2004; 71: 831–835.

Table 1. Percentage of anti-*Toxoplasma* IgG antibodies by ELISA in high risk women with different ages at El-Fayoum Governorate.

locality	17-25y		25-35y		35-45y		Total positive	
	Pr	Non pr	Pr	Non pr	Pr	Non pr	Pr	Non pr
El-Fayoum	40	33.3	37.5	33.3	75	50	47	37.5
Senoris	44.4	25	42.8	33.3	33.3	66.6	42.5	40
Tamyia	25	33.3	42.8	40	80	66.6	47.8	45.5
Total*	38.8	30	41.3	36 .3	66.6	62.5	45.8	41.4
Total samples in pr and non pr women at El-Fayoum Governorate							30.7	13.6

* = Total samples in prgnant or non pregnant women at El-Fayoum Governorate;
-Pr = pregnant women; -Non pr = non pregnant women.

Table 2. Percentaceof anti-*Toxoplasma IgM* antibodies by ELISA in high risk women with different ages at El-Fayoum Governorate.

locality	17-25y		25-35y		35-45y		Total positive	
	Pr	Non pr	Pr	Non pr	Pr	Non pr	Pr	Non pr
El-Fayoum	20	0	25	0	50	100	29.4	25
Senoris	22.2	0	14.2	0	33.3	33.3	21	10
Tamyia	50	33.3	28.5	40	60	33.3	39.1	36.4
Total*	27.7	10	24.13	18.1	50	50	30.5	24.2
Total samples in pr and non pr women at El-Fayoum Governorate							20.45	7.95

***** = Total samples in prgnant or non pregnant women at El-Fayoum Governorate;
-Pr = pregnant women, - Non pr = non pregnant women.

Table 3. Detection of *Toxoplasma gondii* DNA by PCR in high risk women with different ages at El-Fayoum Governorate.

locality	17-25y		25-35y		35-45y		Total positive	
	Pr	Non pr	Pr	Non pr	Pr	Non pr	Pr	Non pr
El-Fayoum	20%	33.3%	37.5%	33.3%	50%	50%	35.3%	37.5%
Senoris	11%	0%	28.5%	33.3%	66.6%	33.3%	26.3%	20%
Tamyia	50%	33.3%	28.5%	20%	40%	33.3%	34.7%	27.3%
Total*	22.2%	20%	31.3%	27.3%	50%	37.5%	32.2%	27.5%
Total samples in pr and non pr women at El-Fayoum Governorate							21.5%	9%

* = Total samples in prgnant or non pregnant women at El-Fayoum Governorate;
-Pr = pregnant women ; - Non pr = non pregnant women.

Table 4. Detection of *Toxoplasma gondii* IgG and DNA in small ruminants in different localities at El-Fayoum Governorate.

locality	ELISA IgG		PCR	
	sheep	goat	sheep	goat
EL-Fayoumcenter	95%	37.5%	90%	37.5%
Senoris center	100%	33.33%	60%	16.7%
Tamyia center	100%%	50%	54.5%	20%
Total*	98.4	41.7%	67.7%	25%

Table 5. Risk factors for the investigated women at El-Fayoum Governorate

Non pregnant women	Pregnant women	Risk factors
-Eating undercooked sheep or goat meat	+++	+++
-Drinking raw sheep or goat milk	+++	+++
-Preparation of raw sheep or goat meat	+++	+++
-Any raw meat exposure or drinking any raw milk of different animals (Cow's milk or buffaloes)	++	++
-Own or exposures to Cats or Feline species	+	+

The Novel Biomaterial of Visible Photoluminescence by Saving Energy Technology of Rapid Thermal Annealing

Jen-Hwan Tsai[1], Chih-Hsiung Liao[2] and Shen Cherng[3]

[1]Department of Mathematics and Physics, Air Force Academy, Kangshan, Kaohsiung, 820, Taiwan ROC; [2]Department of Physics, Chinese Military Academy, Fengshan, Kaohsiung, 830, Taiwan ROC; [3]Department of Computer Science and Information Engineering, Chengshiu University, Niaosong, Kaohsiung, 833 Taiwan, ROC

Received March 20, 2009

Abstract

In this article, the novel biomaterial of visible photoluminescence by saving energy technology of rapid thermal annealing is presented. A shift in the photoluminescence (PL) peak from blue to near-infrared region was observed in the Si^+-implanted 400-nm-thick SiO_2 film with the rapid thermal annealing (RTA) method only. As the Si^+-fluence was $1x10^{16}$ ions/cm^2, a blue band was observed in the films after RTA at 1050^{o}C for 5 seconds in dry-N_2 atmosphere; then, the band shifted from blue to orange upon increasing the holding temperature of RTA to 1250 ^{o}C in the films after the isochronal RTA in dry N_2. Furthermore, while the fluence was increased to $3x10^{16}$ ions/cm^2 and the holding temperature was at the same range between 1050^{o}C and 1250 ^{o}C, the PL peak occurred between red and near-infrared regions. Although the RTA and conventional thermal annealing (CTA) methods produce the similar mechanism, the CTA method needs a much longer annealing-time and a higher Si^+-implanted dose than the RTA method to observe the same range and intensity of PL peak from the as-implanted sample. Therefore, the RTA method can produce the mechanism in the Si^+-implanted sample with the energy of PL peak between blue and near-infrared band in palce of the CTA method. [Life Science Journal. 2009; 6(3):61–67] (ISSN: 1097 – 8135)

Keywords: rapid thermal annealing (RTA), Si^+ implantation, photoluminescence, SiO_2 films, FTIR spectra

1 Introduction

With the advancement of Si technology for electronic integrated circuits and in view of the potential applications in optoelectronics and photonics, there has been a significant interest in the structures consisting of silicon nanocrystals embedded in SiO_2[1]. Room temperature visible luminescence had been firstly observed from porous silicon (P-Si), however, several problems have been encountered in practical application [2, 3]. The plasma deposition technologies by using silane, gas evaporation, and termination of glass-melt reaction was used to produce visible light emission and silicon nanocrystals, but still none of them were appropriate for the manufacturing process of integrated device products. In addition to above methods, silicon-implantation into SiO_2 film on crystal Si with subsequent conventional thermal annealing (CTA) was another alternative method to fabricate Si-based luminescence structures. Broad emission bands between ~1.5 and ~2.5 eV had been observed by several research groups by implanting Si^+ into the SiO_2 films and following CTA at a temperature higher than 1000°C in vacuum, in Ar, or in N_2[4-9]. The $1x\ 10^{17}$ cm^{-2} Si^+-implanted films after the CTA in dry-N_2 at about 1000^{o}C emits visible blue-light and the PL peaks were shifted from the blue ~2.5 eV to yellow ~2.2 eV upon increasing the annealing temperature from 1000^{o}C to 1250^{o}C[5]. The other light emission between red and near-infrared band was presented at the flux between $1x\ 10^{17}$ cm^{-2} and $3x\ 10^{17}$ cm^{-2} and were attributed to the quantum confinement effect in silicon nanocrystals that was confirmed by transmission electron microscopy [5-6,8]. In those reports[4-9], the flux of implanted silicon was relatively high and the whole annealing process required several hours. Although ion implantation of III-V compounds was routinely used in the production of optoelectronic integrated circuits, the methods using silicon implantation seem not suitable for applications in optoelectronics.

Recently, we successfully used the rapid thermal annealing (RTA) method only to observe the photoluminescence (PL) peak between blue and near-infrared regions in the Si^+-implanted 400-nm-thick SiO_2 films. At the Si^+-fluence of $1x10^{16}$ ions/cm^2, the light shifted from blue to orange band when the holding temperature of RTA was increased from 1050^{o}C to 1250 ^{o}C in the films after RTA for 5 seconds in dry N_2. Furthermore, while the fluence was increasing to $3x10^{16}$ ions/cm^2 and the holding temperature was at the same range between 1050^{o}C and 1250 ^{o}C, the ranges of PL peak were observed between red and near-infrared regions in the films after the RTA for 20 seconds. On the other hand, by means of RTA and CTA method, the PL

*Corresponding Author Chih-Hsiung Liao, Ph.D.
liao550226@yahoo.com.tw

peaks from the Si^+-implant SiO_2 films were both shifted with the increase of the Si^+ concentration in the oxide matrices and of the thermal annealing duration. However, the shifting affect using RTA method was much better than that using CTA method. In additional, the mechanisms achieved by RTA and CTA are both not dependent on hydrogen-related bonds and have similar existent ratio after isothermal and isochronal RTA test. The results show that the mechanisms in the Si^+-implanted SiO_2 films after the RTA and CTA methods are similar. However, for the same range and intensity of PL peak from the as-implanted sample, the CTA method needs a much longer annealing-time and a higher dose of Si^+-implantation than the RTA method. Therefore, using RTA method to produce the mechanisms in the Si^+-implanted samples with the energy of PL peak between blue to near-infrared band is better than using CTA method.

2 Experimental Procedure

Samples were prepared by implantation of Si^+ into a 400-nm-thick wet SiO_2 film which was thermally grown on (100)-oriented p-doped Si substrates. The respective fluences of the Si^+-implantation are $1x10^{15}$, $4x10^{15}$, $1x10^{16}$, $2x10^{16}$, and $3x10^{16}$ ions/cm^2. The temperature of the samples during ion implantation was kept at liquid nitrogen temperature. The acceleration energy of ~ 160 keV was selected so that the maximum concentration was at a depth of ~250 nm below the surface and the standard deviation of the implanted region was ± 60 nm. These samples were subjected to RTA treatments at substrate temperature of 1050^{o}C, 1150^{o}C, and 1250^{o}C, respectively, under dry and wet N_2. The introduction of wet N_2 into the furnace was performed by heating liquid H_2O at 100 ^{o}C in a cylinder, which was connected to the furnace through a guiding tube, and by mixing up with dry N_2 in the guiding tube. Furthermore, the atmospheric pressure of 50 mbar was provided into the furnace and a heating rate of 100^{o}C/s and the cooling rate of about 100^{o}C /min was used. On the other hand, in order to display the advantage of RTA system, we also annealed the samples at temperatures between 1050^{o}C and 1250^{o}C by using a conventional electric oven. The atmospheric pressure of 50 mbar was provided but a maximum heating rate of 10^{o}C /min and the cooling rate of 50^{o}C /min were used in the CTA system. It shall be noted that the two thermal annealing treatments both include three procedures as heating, holding, and cooling. On the other hand, to detect the PL spectra, a He-Cd laser (3.8 eV) was used as the excitation and a lock-in amplifier was employed to improve the signal-to-noise ratio, in conjunction with a monochromator and cooled photomultiplier tube. The excitation was operated at a small and fixed power of 5 mW to not detect any PL sign in the $3x10^{16}$ cm^{-2} Si^+-implanted 400-nm-thick wet SiO_2 films without RTA. Finally, the FTIR measurements were performed to examine the presence or absence of hydrogen-related species in samples of oxide film. With the reference being the same silicon plate as the sample, the spectra were measured at room temperature in N_2 atmosphere at a 2 cm^{-1} resolution with 200 scan accumulations.

3 Results and Discussion

In order to demonstrate that the RTA method is better than the CTA method for producing the mechanism in Si^+-implanted SiO_2 films with the energy of PL peak between the blue and near-infrared band, the fluence of the silicon implantation in the films was kept at $1x10^{16}$ and $3x10^{16}$ ions/cm^2 and the experimental results are shown in Figs.1 and 2, respectively. From Fig. 1, when the holding temperature of RTA increases from 1050^{o}C to 1250^{o}C in the $1x10^{16}$ cm^{-2} Si^+-implanted 400-nm-thick films after the dry-N_2 RTA for 5 seconds, the PL peak shifted from the blue band of ~2.5 eV to the orange band around 2.1 eV. Furthermore, at the same range of holding temperature as in Fig.1, Fig. 2 shows that the PL peak shifted from the near-infrared band of ~1.85 eV to ~1.5 eV in the $3x10^{16}$ cm^{-2} Si^+-implanted 400-nm-thick films after the dry-N_2 RTA for 20 seconds. Keeping the holding temperature in the range between 1000 ^{o}C and 1250 ^{o}C, a similar shift of PL peak (~2.5 eV to ~2.3 eV) as shown in Fig. 1 was observed in the 160 Kev Si^+-implanted 430 nm-thick SiO_2 films after CTA by the group of Mutti. et al.[5]. However, the silicon fluence was 1 x 10^{17} ions/cm^2 and the duration at those high temperatures was 1 hr. On the other hand, a similar band of PL peak (~1.5 eV) as the result in Fig. 2 were observed in the 150 Kev Si^+-implanted 800 nm-thick SiO_2 films after CTA at 1100 ^{o}C by Garrido et al[8]; but, the silicon fluence must be increased to ~3 x 10^{17} ions/cm^2 and the duration at the high temperatures was 8 hr. Besides, At the silicon fluece of 3 x 10^{17} cm^{-2}, Mutti. et al. can only produce the PL peak of ~1.65 eV in the 160 Kev Si^+-implanted 430 nm-thick SiO_2 film after CTA at 1000 ^{o}C for 5 hrs[5].

Figure 3 shows that the PL peak is shifted from ~2.1 eV to ~1.7 eV when the 3 x 10^{16} cm^{-2} as-implanted films are treated by the dry-N_2 RTA at 1150^{o}C and the RTA duration is increased from 5 to 20 seconds,. At the same time, Fig. 4 shows that the PL peak is shifted from ~1.75 eV to ~1.7 eV in the 3 x 10^{16} cm^{-2} as-implanted films after CTA at 1150^{o}C for the duration from 4 to 12 hrs. Referring to Fig.3, the results indicate that the band

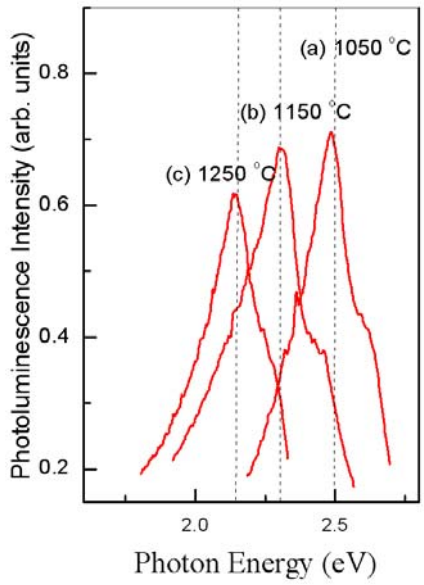

Figure 1. PL spectra of the Si^+-implanted 400-nm-thick SiO_2 film grown on crystal Si at a fluence of $1x10^{16}$ ions/cm^2 after dry-N_2 RTA for 5 seconds at (a) 1050°C, (b) 1150°C, and (c) 1250°C.

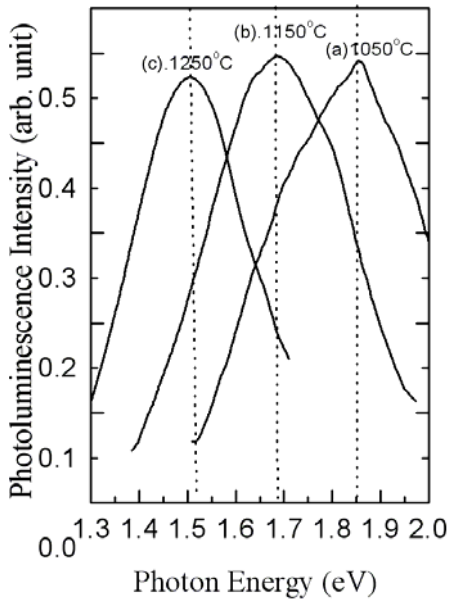

Figure 2. PL spectra of the Si^+-implanted 400-nm-thick SiO_2 film grown on crystal Si at a fluence of $3x10^{16}$ ions/cm^2 after dry-N_2 RTA for 20 seconds at (a) 1050°C, (b) 1150°C, and (c) 1250°C.

of PL peak can be decreased by increasing the RTA duration. However, the results in Fig. 4 indicate that the PL peak is weakly affected by the CTA duration although the intensity of PL spectra become large due to the increase in CTA duration,. The result agrees with that of the study by Shimizu-Iwayama et al.[6], in which the peak energy of the PL is found to be weakly dependent on annealing time, while the intensity of the luminescence increase as the annealing time increases. In addition, comparing Figs. 3 with 4, under the same Si^+-flux of $3x10^{16}$ ions/cm^{-2} and holding temperature of 1150 °C, the intensity of PL-peak in the as-implanted film after the RTA method for the holding duration between 5 and 20 seconds as shown in Fig. 3 is always bigger than that after the CTA method for the duration between 4 and 12 hrs as shown in Fig.4.

Figure5 shows the effect of Si^+ fluence on the luminescence in the RTA-treated film, where the PL spectrum of the Si^+-implanted 400-nm-thick SiO_2 films grown on silicon crystal at three different fluences after RTA in dry N_2 at 1150°C for 20 seconds. As the Si^+ fluence into the as-implanted film was $1x10^{16}$ ions/cm^2, the PL spectrum has a peak at ~1.95 eV shown in Fig.5(a); as those films have the fluence of $2x10^{16}$ and $3x10^{16}$ ions/cm^2, the PL spectra have the peaks at ~1.8 eV and ~1.7 eV, shown in Figs. 5(b) and 5(c), respectively. The results indicate that the PL peak can be red-shifted with the increase of fluences. The peak energy of the PL spectra is obviously decided by the fluence of the Si^+-implantation. Thus, the Si^+ concentration plays the important role during the production of the respective mechanisms in the RTA-treated films. On the other hand, Fig.6 shows the effect of Si^+ fluence on the luminescence

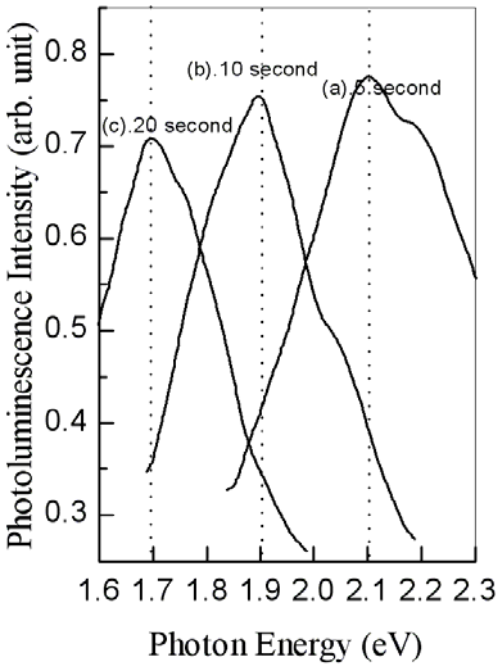

Figure 3. The PL spectra of the Si^+-implanted 400-nm -thick SiO_2 film grown on crystal Si at a fluence of $3x10^{16}$ ions/cm^2 after dry-N_2 RTA at 1150 °C for (a) 5 seconds, (b) 10 seconds, and (c) 20 seconds.

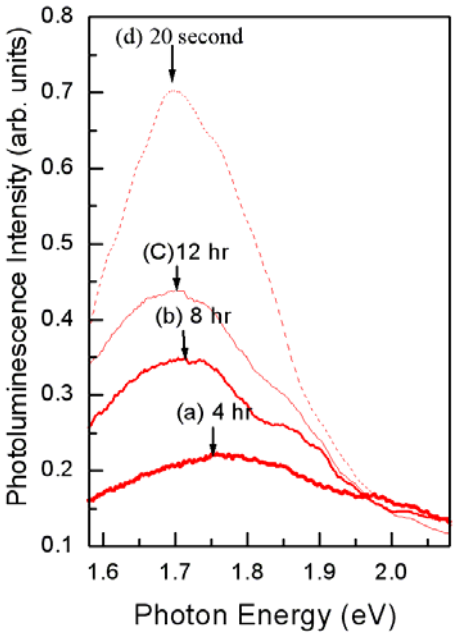

Figure 4. The PL spectra of the Si^+-implanted 400-nm -thick SiO_2 film grown on crystal Si at a fluence of $3x10^{16}$ ions/cm^2 after dry-N_2 CTA at 1150 °C for (a) 4 hours, (b) 8 hours, and (c) 12 hours and (d) after isothermal dry-N_2 RTA for 20 seconds.

in the CTA-treated film, where is also the PL spectrum of the Si^+-implanted 400-nm-thick SiO_2 films grown on silicon crystal at three fluences as above but after CTA in dry N_2 at 1150°C for 12 hrs. Referring to Figs.5 and 6, under the same holding temperature of 1150°C and the Si^+-fluence between $1x10^{16}$ and $3x10^{16}$ ions/cm^2, the PL intensity of the as-implanted film by CTA has obvious increase upon increasing with the dose of implanted Si^+ but the respective PL Peak shifts only from ~1.75 eV to~1.70 eV as shown in Fig.6, which are always weaker than that by RTA as shown in Fig.5. The results show that the intensity of the PL spectrum is obviously affected

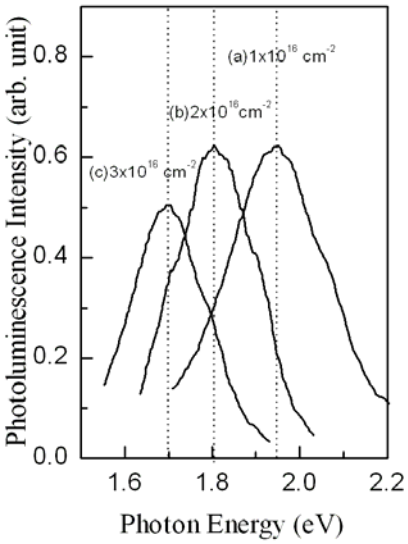

Figure 5. PL spectra of the Si^+-implanted 400-nm-thick SiO_2 film grown on crystal Si at a fluence of (a) $1x10^{16}$ ions/cm^2, (b) $2x10^{16}$ ions/cm^2, and (c) $3x10^{16}$ ions/cm^2 after dry-N_2 RTA treatment for 20 seconds at 1150°C.

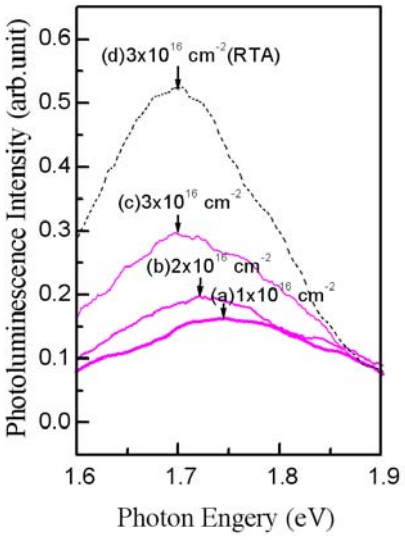

Figure 6. PL spectra of the Si^+-implanted 400-nm-thick SiO_2 film grown on crystal Si at a fluence of (a) $1x10^{16}$ ions/cm^2, (b) $2x10^{16}$ ions/cm^2, and (c) $3x10^{16}$ ions/cm^2 after dry-N_2 CTA for 12 hours at 1150°C and at a fluence of (d) $3x10^{16}$ ions/cm^2 after dry-N_2 isothermal RTA for 20 seconds.

by the concentration of implanted Si^+, but the peak energy is weakly affected by the concentration of implanted Si^+ in the CTA-treated film. Otherwise, the result shown in Fig.6 is consistent with the observation of several other research groups[6, 8, 14-15]. According to the observation of Shimizu-Iwayama et al.[6], although the intensity of PL is strongly affected by the dose of implanted Si^+, the peak energy of the PL that is weakly

affected by the Si^+-dose shifted from 1.75 eV to 1.7 eV as the Si^+ -fluence implanted into the 600 nm-thick SiO_2 film with the energy of 180 KeV increases from $1x10^{16}$ to $2x10^{17}$ ions/cm^{-2} and the thermal annealing was carried out by the CTA at 1050 ^oC for 4 hrs. Furthermore, the shift of PL peak from 1.7 eV to 1.5 eV was obsedved by Fernandez et al.while the Si^+ -fluence implanted into the 800 nm-thick SiO_2 film with the energy of 150 KeV increases from $1x10^{17}$ to $3x10^{17}$ ions/cm^2 and the thermal annealing was treated by the CTA at 1100 ^oC for 8 hrs [8]. Anyway, the red-shifting phenomena of PL can be observed by RTA, which can decrease the fluence of the Si^+- implantation and shorten the thermal annealing time as compared with CTA. Moreover, although the growth of PL mechanism in the as-implanted SiO_2 film treated by CTA is much slower than that treated by isothermal RTA, the mechanism in the film treated by the RTA or CTA method is dependent of Si^+ concentration in the oxide matrices and of the thermal annealing temperature and duration.

Remarkably, besides of the enhanced diffusion and aggregation of Si^+ implanted in oxide matrix during RTA [21], we believe that the procedure of Si^+-nanocrystals formation all be enhanced by using the RTA method but the effect is very sensitive to the heating rate of RTA. According to our initial observation, the PL intensity from the as-implanted film by RTA with the heating rate of 100 $^oC/s$ was much stronger than that by RTA with the heating rate of 50 $^oC/s$ and no significant intensity could be found after the heating rate of 25 $^oC/s$. At the same time, the shift of PL peak from the as-implanted film by RTA with the heating rate of 100 $^oC/s$ could occur at the holding duration less than 20 seconds. However, after the heating rate decreasing to 50 $^oC/s$, the shifting phenomena could occur only at the holding duration less than 5 seconds. The results conform to the observation by Shimizu-Iwayama et al.. They found that, under the Si^+ fluence of $\geq 5x10^{16}$ ions/cm^{-2}, the PL intensity of sample only after RTA at $\geq$ 1050 ^oC for 5 min with the heating rate of 30 $^oC/s$ was much weaker than that treated by the same RTA at first and achieved finally by CTA at $\geq$ 1050 ^oC for $\geq$ 1 hr [21].

On the other hand, Fig. 7 shows the FTIR spectra of the films with the different treated process. Figure 7(a) shows the FTIR spectrum in the 3750 cm^{-1} range of original 400-nm-thick SiO_2 film grown on the Si crystal without RTA. Besides, for the Si^+-implanted 400-nm-thick SiO_2 films with the same fluence of $3x10^{16}$ ions/cm^2, but proceeding the RTA in dry N_2 at 1150^oC for 20 seconds and the CTA at 1150^oC for 12 hours, the FTIR spectra in the 3750 cm^{-1} range are show in Figs. 7(b) and 7(c), respectively**.** Moreover, in order to confirm the absence of Si-O-H structures in the as-implanted samples by the RTA and CTA**,** the spectra in the 3750 cm^{-1} range of the Si^+-implanted 400-nm-thick SiO_2 films with the respective fluences of $1x10^{15}$ and $4x10^{15}$ ions/cm^2 after the RTA but in wet N_2 are displayed in Figs. 7(d) and 7(e). According to these FTIR spectra in Figs.7(b) and 7(c), the absorption valleys of Si-O-H structures in the dry-N_2-annealed films after above RTA and CTA, which are indicated by the signature at ~ 3750 cm^{-1} in the FTIR spectra[16-20], are both shallow as the sample of original wet SiO_2 films without RTA treatment shown as Fig. 7(a) and seem un-change with the increase of silicon implantation fluence. However, from Figs. 7(d) and 7(e), we observed that the absorption valleys of Si-O-H structures in the respective $1x10^{15}$ cm^{-2} and $4x10^{15}$ cm^{-2} Si^+-implanted SiO_2 films after RTA in a wet N_2 are deepened with the increase of Si^+-implantation fluence and so their respective mechanism in the films, that lead to the luminescence, are related closely to the Si-O-H structures[11, 12]. In addition, no samples with the above mechanisms in this study display an FTIR signature at ~2100 cm^{-1} and~1450 cm^{-1} (or ~2300 cm^{-1}), related to the absorption of SiH_x (x=1,3) and CH_x structures, respectively[13, 16]. Hence, the above mechanisms in the $3x10^{16}cm^{-2}$ Si^+-implanted SiO_2 films after the above dry-N_2 RTA and CTA are all independent of the Si-O-H related bonds and the SiH_x or CH_x structures according to the FTIR spectra.

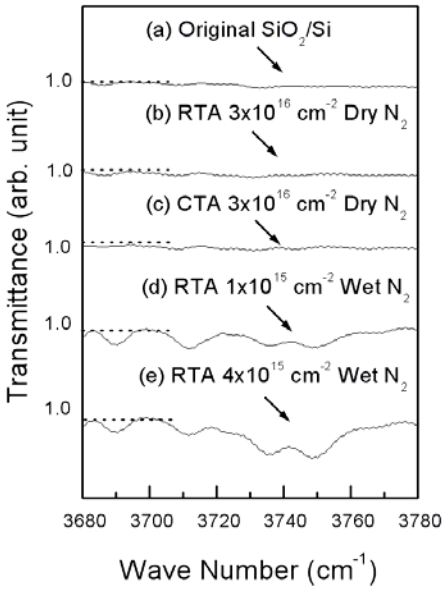

Figure 7. FTIR spectra in the 3750 cm^{-1} range of (a) original 400-nm-thick SiO_2 film grown on Si crystal without RTA, the Si^+-implanted 400-nm-thick SiO_2 film grown on crystal Si at a fluence of $3x10^{16}$ ions/cm^2 (b) after Dry-N_2 RTA at 1150^oC for 20 seconds and (c) after Dry-N_2 CTA at 1150^oC for 12 hours, and that at a fluence of (d) $1x10^{15}$ ions/cm^2 and (e) $4x10^{15}$ ions/cm^2 with RTA as in (b) but in wet N_2.

Otherwise, Fig. 8 shows the peak-intensity of the PL spectra as a function of the re-annealing temperature by RTA for 5 min in nitrogen. The PL peaks from the respective $1x10^{16}$ cm^{-2} as-implanted films achieved by the CTA (shown as Fig. 8(a)) and RTA (shown as Fig. 8(b)) both decay nearly one-half intensities after isochronal re-annealing at the temperature of 1000 ^oC

and both disappear since the temperature of 1100 °C. Furthermore, when the fluence is increased to $3x10^{16}$ ions/cm^2, the PL mechanism in the as-implant films achieved by the CTA (shown as Fig. 8(c)) and RTA (shown as Fig. 8(d)) can persist even after re-annealing at the temperature of >1100°C and both disappear at 1200 °C. The results of the above PL mechanism imply that the ratio of remainder number after the above re-annealing is ambiguously dependent of productive method (RTA or CTA) but depends on the Si^+ dose implanted into the SiO_2 film. Hence, under the same dose of implanted Si^+, the PL mechanism in the film achieved by RTA and CTA have similar existent ratio after isothermal and isochronal RTA test.

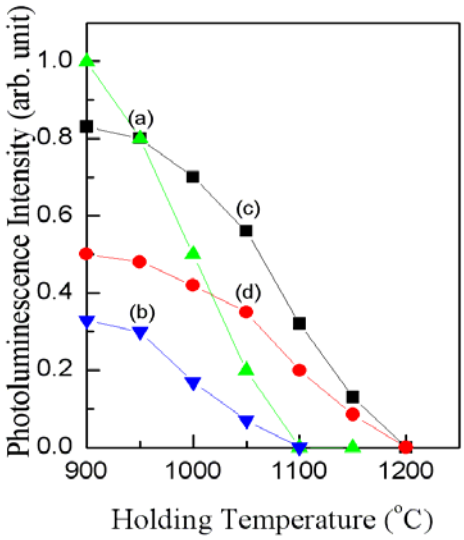

Figure 8. Changes in the PL intensity from the $1x10^{16}$ cm^{-2} Si^+-implanted 400-nm-thick SiO_2 film grown on crystal Si (a) after RTA at 1150°C for 20 seconds and (b) after CTA at 1150°C for 12 hrs and from the $3x10^{16}$ cm^{-2} as-implanted sample (c) after RTA at 1150°C for 20 seconds and (d) after CTA at 1150°C for 12 hrs as a function of the re-annealing temperature, respectively. Re-annealing of the these groups of specimens was achieved by RTA for 5 min with heating rate of 30 °C/s .

Finally, both the RTA and CTA methods can produce the mechanisms in the Si^+-implant SiO_2 film with the energy of PL peak between blue and near-infrared band. In addition, their respective PL peaks are both shifted with the increase of Si^+ concentration in the oxide matrices and of the thermal annealing temperature and duration. The two mechanisms are both independent of hydrogen-related bonds and have the similar existent ratio after the test of RTA at high temperature. Therefore, the respective mechanism in the Si^+-implanted SiO_2 films after RTA and CTA are similar. It is well known that Si ion implanted into SiO_2 and subsequent high-temperature CTA induce the formation of embedded luminescence Si nanocrystals[4-9, 21]. Hence, the mechanism in the as-implanted film,produced by RTA,was also attributed to silicon nanocrystals embedded in SiO_2.

4 Conclusion

The PL peak between ~2.5 eV and ~1.5 eV can be observed in the Si^+-implanted 400 nm-thick SiO_2 film after dry-N_2 RTA only. The studies indicate that light emission in the lower dose Si^+-implanted film with the ~30 minutes RTA has the similar shifting phenomena like that in the higher dose as-implanted film with the several-hours CTA method. Under the implanted Si^+ dose between $1x10^{16}$ cm^{-2} and $3x10^{16}$ cm^{-2} and the holding temperature of 1150 °C, the intensity of PL spectrum from the as-implanted film treated by the RTA method is always stronger than that treated by the CTA method. Furthermore, light emission from the as-implanted film by the two methods, in which the peak positions are both shifted with the variation of Si^+ concentration in oxide matrices and the thermal annealing temperature and duration. The PL mechanisms in the film achieved by RTA and CTA are both independent of hydrogen-related bonds and have similar existent ratio after isothermal and isochronal RTA test. The phenomena imply that the two methods produce the similar PL mechanism in the oxide matrix, that were both attributed to silicon nanocrystals embedded in SiO_2. Therefore, using RTA method to produce the mechanisms in the Si^+-implanted films with the energy of PL peak between blue and near-infrared band is better than using the CTA method.

References

1. Brus L, Semiconductors and Semimetals, edited by D. Lockwood (Academic, New York, 1998), Vol. 490, p. 303.
2. Sabet-Dariani R, McAlpine NS and Haneman D, J. Appl. Phys. **75** (1994) 8008.
3. Qin G G, Li AP, Zhang BR and Li B, J. Appl. Phys. **78** (1995) 2006.
4. Shimizu-Iwayama T, Nakao S and Saitoh K, Appl. Phys. Lett. **65** (1994) 1814.
5. Mutti P, Ghislotti G, Bertoni S, Bonoldi L, Cerfolini GF, Meda L, Grilli E and Guzzi M, Appl. Phys. Lett. **66** (1995) 851.
6. Shimizu-Iwayama T, Kurumado N, J. Appl. Phys. **83** (1998) 6018.
7. Kenyon AJ, Chryssou CE, Pitt CW, Shimizu-Iwayama T, Hole DE, Sharma N and Humphreys CJ, J. Appl. Phys. **91** (2002) 367.
8. Fernandez BG, Lopez M, Garcia C, Perez-Rodriguez A, Morante JR, Bonafos C, Carrada M and Claverie A, J. Appl. Phys. **91** (2002) 798.
9. Chen T P, Lin Y, Tse M S, Fung S and Dong G, J. Appl. Phys. **95** (2004) 8481.
10. Chou ST, Tsai JH, and Sheu BC, J. Appl. Phys. **83** (1998) 5394.
11. Tsai JH, Yu AT, and Sheu BC, Jpn. J. Appl.

Phys. **39** (2000) L107.
12. Tsai JH, Yu AT, Jpn. J. Appl. Phys. **44** (2005) 1389.
13. Allian G, Delerue C, and Lannoo M, J. Lumin. **57** (1993) 239.
14. Bonafos C, Garrido B, Lopez M, Perez-Rodriguez A, Morante JR, Kihn Y, Ben Assayag G, and Claverie A, Mater. Sci. Eng. **69** (1999) 379.
15. Agarwal M and Dunham ST, J. Appl. Phys. **78** (1995) 5313.
16. Shim HW, Kim KCand Seo YH, Nahm K S, Suh E. K, Lee HJ, and Hwang YG, Appl. Phys. Lett. **70** (1997) 1757.
17. Zvznut ME, Chen TL, Stahlbush RE, Steigerwalt ES, and Brown GA: J. Appl. Phys. **77** (1995) 4329.
18. Zvznut ME, Chen T L, Appl. Phys. Lett. **69** (1996) 28.
19. Weng YM, Fan ZN and Zong XF, Appl. Phys. Lett. **63** (1993) 168.
20. Lin GR and Lin C J, J. Appl. Phys. **95** (2004) 8484.
21. Iwayama TS, Hama T, Hole DE, Boyd IW, Vacuum , **81**(2006) 179.

Study of Biomaterial Based on Saving Energy Technology of Rapid Thermal Annealing for Si^+-implanted SiO_2 Thin Film

Jen-Hwan Tsai[1], Chih-Hsiung Liao[2*] and Hsien-Chiao Teng[3]

[1]Department of Mathematics and Physics, Air Force Academy, Kangshan, Kaohsiung, 820, Taiwan, R.O.C.; [2]Department of Physics, Chinese Military Academy, Fengshan, Kaohsiung, 830, Taiwan, R.O.C.; [3]Department of Electrical Engineering, Chinese Military Academy, Fengshan, Kaohsiung, 830, Taiwan, R.O.C.

Received March 20, 2009

Abstract

Varying with the heating rate of rapid thermal annealing (RTA), room-temperature photoluminescence (PL) could be observed in the 3×10^{16} cm^{-2} Si^+-implanted 400-nm-thick SiO_2 films after RTA at 1150 °C in dry nitrogen and the respective PL peak was located in the range between blue band to near-infrared band. At the heating rate of 100 °C/s, the PL peaks was shifted from 2.6 eV to 1.7 eV for the isothermal RTA durations from 5 seconds to 20 seconds and no obvious shift was further found since the RTA duration of 20 seconds. However, after the heating rate was decreasing to 25 °C/s, no significant shift of PL peak could be seen in the films after the isothermal RTA for the durations ≥1 second. Like the shift of PL peak, the average rate of the FTIR peak change at ~1100 cm^{-1}, reflecting the repaired condition of SiO_2 structure, from the as-implanted films after RTA for the durations ≤ 20 seconds were quicker than those for the durations ≥ 20 seconds at the heating rate of 100 °C/s, and near a constant for the RTA durations ≥ 1 second at that of 25 °C/s. The above PL and FTIR phenomena should be attributed to the Si^+ re-crystals and the improvement of the broken structure in the RTA-treated as-implanted SiO_2 films In comparison with the isothermal conventional thermal annealing method, the RTA method saves vast dosages of Si^+-implantation, thermal budget and the respective electrical energy under obtaining the same results. [Life Science Journal. 2009; 6(3): 68 – 73] (ISSN: 1097 – 8135)

Keywords: photoluminescence, Si^+-implanted SiO_2 films, rapid thermal annealing**,** FTIR spectra, conventional thermal annealing

1 Introduction

Thermal annealing is a treatment that can recombine sample's broken structure and let the structure be stable. For a Si^+-implanted SiO_2 film, the stable structure after annealing treatment is that these implanted ions are re-crystallized and embedded in the groups of SiO_2 bonds. Hence, the method of silicon-implantation into SiO_2 films on Si substrate with subsequent thermal annealing treatment produces silicon crystals in a SiO_2 film and has the effect of luminescence emission. The emission bands between 1.5 and 2.6 eV have been observed by several research groups from Si^+-implanted SiO_2 films after ≥ 1000 °C conventional thermal annealing (CTA) in vacuum, Ar or N_2.[1-9] However, in those reports[4-9], the flux of implanted silicon was relatively high (≥1x 10^{17} cm^{-2}) and the whole annealing process required several hours. The enormous consumption of electric and thermal energy for these CTA tests seriously goes against the tacit understanding of saving energy and environmental protection. Recently, single-wafer rapid thermal annealing (RTA), which has become indispensable in the present-day manufacture of integrated circuits, has replaced CTA (batch furnace) to satisfy device and production requirements for low manufacturing cost and low energy consumption. We have demonstrated that the light emission can be red-shifted by RTA method with the dose of Si^+ implantation ≤$3x10^{16}$ cm^{-2} and the shorter whole annealing-time ≤30 minutes.[10~12] By controlling the flux of the Si^+-implantation between $4x10^{15}$ and $3x10^{16}$ cm^{-2}, the emission bands between 1.7 and 2.2 eV have been observed by us from the Si^+-implanted 400 nm-thick SiO_2 film after RTA at the range between 950 and 1150 °C for the durations between 5 and 20 seconds in N_2. The PL peak position from the above as-implanted SiO_2 films could shift with the varying of the Si^+ concentration in oxide matrices and the thermal annealing temperature and duration, and is independent of hydrogen-related bonds. Because only the PL band due to the silicon nanocrystals in oxide matrix (nc-Si) has above properties, these emissions should be attributed to the Si^+ re-crystal after RTA[4-9]. Otherwise, the above 1.7 eV PL peak (near-infrared band) can also be produced by us from the $3x10^{16}$ cm^{-2} Si^+-implanted 400 nm SiO_2 film after CTA in N_2 for ~12 hours and the main difference between RTA and CTA method is the heating rate in additional to the thermal annealing duration. Thus, the correlation of Si^+ re-crystal in Si^+-implanted SiO_2 films with the heating rate of the

*Corresponding Author Chih-Hsiung Liao, Ph.D.
liao550226@yahoo.com.tw

annealing treatments is necessary to study.

In this study, the Si^+-implanted 400-nm-thick SiO_2 films with the fixed flux of $3x10^{16}$ cm^{-2} after RTA at 1150 ^oC in 50 mbar dry nitrogen were continuously used as samples. As the RTA heating rate increasing from 25 to 100 $^oC/s$, the PL peaks shifted from blue-light of 2.6 eV to original light of 2.0 eV were observed from the film after RTA for the duration of 1 seconds and from 2.0 eV to near-infrared light of 1.7 eV after keeping the RTA duration at 20 seconds. In addition, when the heating rate was less than 10 $^oC/s$ and the laser power was kept at ~5 mW, no PL sign could be seen in the $3x10^{16}$ cm^{-2} Si^+-implanted 400-nm-thick SiO_2 films after the isothermal RTA. On the other hand, fixing the heating rate at 100 $^oC/s$ and varying the isothermal RTA duration from 1 to 20 seconds, the PL peaks shifted from ~2.6 eV to ~1.7 eV and no obvious shift of PL peak was found for the RTA duration greater than 20 seconds in the above as-implanted Si^+-implanted films. Similar, the respective FTIR-peak positions around 1100 cm^{-1} from the as-implanted RTA-treated samples shifted to higher wave-numbers with the increase of the duration and their rates for the RTA durations from 1 second to 20 seconds were faster than those for the durations ≥ 20 seconds. Furthermore, after the heating rate decreasing to 25 $^oC/s$, no obvious shift of PL peak from 2.0 eV was found and, in the respective FTIR spectra, the rates of the peak position shifting to higher wave-number were not obviously vary since the RTA durations ≥1 second. These implies that the shift of PL and FTIR peaks related closely to the varying of silicon cluster's size after RTA was determined by the RTA heating rate for a given RTA temperature and duration. The heating rate shall make decision of the active-time of the Si^+ re-crystal in the as-implanted films and so the Si^+ re-crystal plays an important role for the repairing of the Si-O bonds in the films[13, 14], In final**,** isothermal RTA and CTA have the same effect of PL mechanism production and Si-O bonds repair in a Si^+-implanted oxide matrix. But if the saves of Si^+-implanted dosage, thermal annealing budget and its respective electrical energy are also compared, the RTA method is much superior to the CTA method.

2 Experimental Procedure

Samples were prepared by implantation of $^{28}Si^+$ onto a 400-nm-thick SiO_2 layer which was thermally grown on (100)-oriented p-doped Si substrates. The fluences of the Si^+-implantation was $3x10^{16}$ cm^{-2}. The temperature of the samples during ion implantation was kept at liquid nitrogen temperature. The acceleration energy of ~ 160 keV was selected so that the maximum concentration was at a depth of ~250 nm below the surface and the standard deviation of the implanted region was ±60 nm. In order to clarify the PL mechanism in the as-implanted films, the respective layers of 100 nm, 200 nm, and 250 nm were etched off from the top of the rapid-thermal-annealed films. The layer thickness removed by HF(10%) was monitored by ellipsometer. These samples were subjected to RTA system at substrate temperature of 1150 ^oC under dry N_2. Furthermore, the heating rates were 25, 50 and 100 ^oC /s, respectively and cooling rate of about 100 ^oC /min were used for the RTA system. To detect the PL spectra, a He-Cd laser (3.8 eV) was used as the excitation and the lock-in technique were employed to improve the signal-to-noise ratio, in conjunction with a monochromator and cooled photomultiplier tube. Moreover, FTIR measurements were performed to examine the Si-O-Si bonding quality of the SiO_2 films in the samples according to the absorption peak position at ~1100 cm^{-1} in the spectra. The absorption peak position was assigned to the anti-symmetric stretching mode (TO_3 mode) of Si-O-Si units[14]. With the reference being the same silicon plate as the sample, the spectra were measured at room temperature in N_2 atmosphere at a 1 cm^{-1} resolution with 100 scan accumulations.

3 Results and Discussion

When a He-Cd laser (3.8 eV) was used as the excitation source to detect the PL spectra and operate at a power of ~5 mW, no PL sign could be found in the $3x10^{16}$ cm^{-2} Si^+-implanted 400-nm-thick SiO_2 films without RTA. Like a conventional thermal annealing (CTA), RTA includes three procedures as heating, holding, and cooling and the holding time in RTA calls RTA duration. The effect of heating rate on luminescence is presented in Fig.1 where three PL spectra of the $3x10^{16}$ cm^{-2} Si^+-implanted 400-nm-thick SiO_2 films after RTA at 1150 ^oC for 1 second are shown. The PL spectrum with a peak at ~2.0 eV from the as-implanted films has the heating rate of 25 $^oC/s$ and those with peaks at ~2.3 eV and ~2.6 eV from the films have the heating rate of 50 $^oC/s$ and 100 $^oC/s$, respectively. The results shown in the figure imply that no PL sign could be seen in the films at the heating rate of RTA <10 $^oC/s$, then, a significant original light of 2.0 eV was not observed until the heating rate at 25 $^oC/s$ and, finally, the PL peak shifted progressively from 2.3 eV to blue-light of 2.6 eV as the heating rate increased from 50 $^oC/s$ to 100 $^oC/s$.

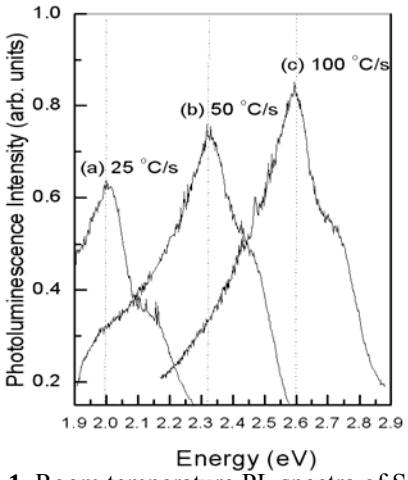

Figure 1. Room temperature PL spectra of Si^+-implanted SiO_2 films after 1150 ^oC RTA for 1 seconds at the

heating rate of (a) 25 °C/s, (b) 50 °C/s, and(c) 100 °C/s. Furthermore, Figure 2 shows three PL spectra of the as-implanted 400-nm-thick SiO_2 films after the same RTA as above but for the duration of 20 seconds. As shown in this figure, when the RTA duration was increasing and kept at 20 seconds, a red shift of the PL peak from 2.0 eV to 1.7 eV would be found in the films as the heating rate of RTA was increasing from 25 °C/s to 100 °C/s. Hence, the two figures both imply that, for a given RTA duration and temperature, the bands of PL-peak in the as-implanted films were adjusted by the heating rate of RTA.

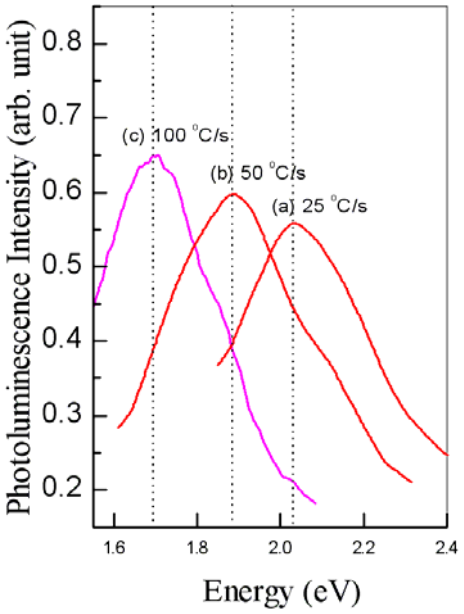

Figure 2. Room temperature PL spectra of Si^+-implanted SiO_2 films after 1150 °C RTA for 20 seconds at the heating rate of (a) 25 °C/s, (b) 50 °C/s, and(c) 100 °C/s.

Moreover, Figs. 3-5 all show the PL spectra of the $3x10^{16}$ cm^{-2} Si-implanted 400-nm-thick SiO_2 film after RTA for the duration of 20 seconds at 1150°C and subsequently etching-off the 100-nm-thick and 200-nm-thick layer from the as-implanted films. But, the respective heating rate of RTA was the value of 100 °C/s in Fig.3, 50 °C/s in Fig.4 and 25 °C/s in Fig.5. With the decreasing of the thickness of the films from 400 nm to 200 nm, Fig. 3 clearly shows that the PL spectrum declines and the peak position is shifted from ~1.7 eV to ~1.6 eV; Fig.4 shows that PL spectrum declines, too, but the peak position is shifted from ~1.9 eV to ~1.8 eV. Lastly, Fig.5 shows that the peak position of the declining PL spectrum is shifted from ~2.0 eV to ~1.88 eV. The PL phenomena in the three figures shall all be related closely to the Si^+ concentration implanted in the films because the deeper layer of the as-implanted 400nm-thick films has the larger Si^+ concentration before 150-nm-thick layer and led to the smaller PL band after the RTA treatment. Hence, the mechanisms in the RTA-treated Si^+-implanted SiO_2 films are not related to the defects that has been investigated in the as-implanted films, such as an NBOHC, oxygen-deficient center (ODC) (~2.7 eV), [15] a weak oxygen bond (~3.0 eV)[16], neutral oxygen vacancies (NOVs) (~2.8 eV) [16] and so forth, but is similar to the nc-Si in an oxide matrix (1.5 eV~2.0 eV). Among these defects, only the nc-Si in the films can vary as the ion concentration in oxide matrices, at a fixed heating rate and thermal annealing duration and under the independent of hydrogen-related bonds[4-9]. To sum up above points, we believe that the ion concentration shall be proportional to the average-size of nc-Si in the respective layer of the as-implanted film for a given RTA duration and temperature and heating rate. On the other hand, figure 6 shows that the band of PL peaks from the Si^+-implanted SiO_2 films after the isothermal RTA was changed as a function of the RTA duration when the heating rate were 25 °C/s, 50 °C/s, and 100 °C/s, respectively. As shown in the figure, when the heating rate of RTA was kept at 100 °C/s, a red shift of the PL peak from 2.6 eV to 1.7 eV was observed from the films after the isothermal RTA at 1150 °C for the duration from 1 seconds to 20 seconds and no obvious shift of the PL peak position was continuously found from the isothermal RTA-treated as-implanted films for the duration of >20 seconds.

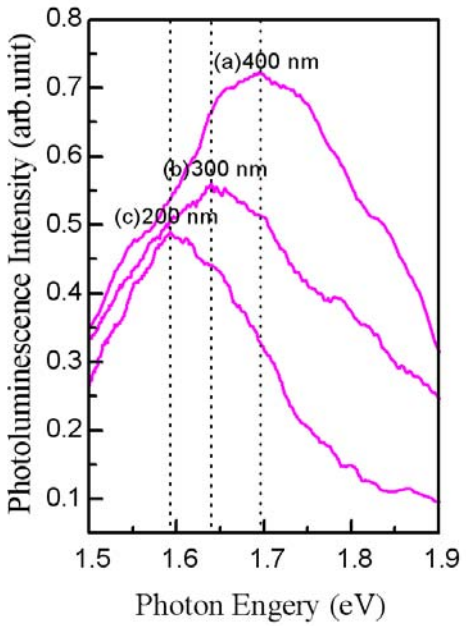

Figure 3. Room temperature PL spectra of the Si^+-implanted 400-nm-thick SiO_2 film after RTA for the heating rate of 100 °C/s and RTA duration of 20 seconds at 1150°C (a) without HF etching, (b) with etched 100-nm-thick layer, and (c) with etched 200-nm-thick layer. The HF-etching procedure was performed after RTA.

Moreover, Figure 6 also shows a smaller shift of the

PL peak from 2.3 eV to 1.9 eV was observed from the as-implanted films after the above isothermal RTA for the duration from 1 seconds to 5 seconds and no obvious shift of the PL peak position was continuously found from the films for the duration of >5 seconds at the heating rate of 50 °C/s. Then, after the heating rate was decreasing and assigned to 25 °C/s, no significant shift of the PL peak could be seen in the films after the isothermal RTA since the durations of 1 seconds and the PL peak position seems to be fixed at 2.0 eV. These results imply, for a given RTA temperature of 1150°C, the maximum active-time about the PL mechanism's production was

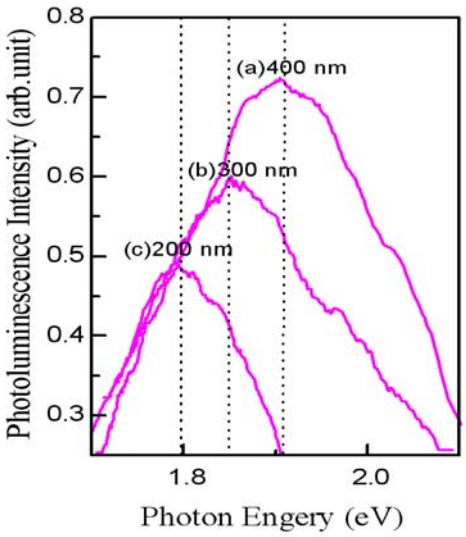

Figure 4. Room temperature PL spectra of the Si^+-implanted 400-nm-thick SiO_2 film after RTA for the heating rate of 50 °C/s and RTA duration of 20 seconds at 1150°C (a) without HF etching, (b) with etched 100-nm-thick layer, and (c) with etched 200-nm-thick layer. The HF-etching procedure was performed after RTA.

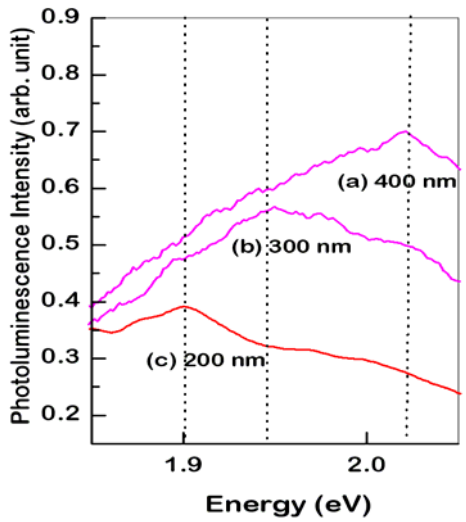

Figure 5. Room temperature PL spectra of the Si^+-implanted 400-nm-thick SiO_2 film after RTA for the heating rate of 25 °C/s and RTA duration of 20 seconds at 1150°C (a) without HF etching, (b) with etched 100-nm-thick layer, and (c) with etched 200-nm-thick layer. The HF-etching procedure was performed after RTA.

about 20 seconds for the heating rate of 100 °C/s, about 5 seconds for the heating rate of 50 °C/s, and less than 1 seconds for 25 °C/s. The maximum active-time was increasing with the increasing of heating rate of RTA. Anyway, for a given RTA duration, although the RTA temperature determining the average speed of Si^+ re-diffusion plays an important role of Si^+ re-crystal in the as-implanted film, the RTA heating rate determining the active-time plays the main role.

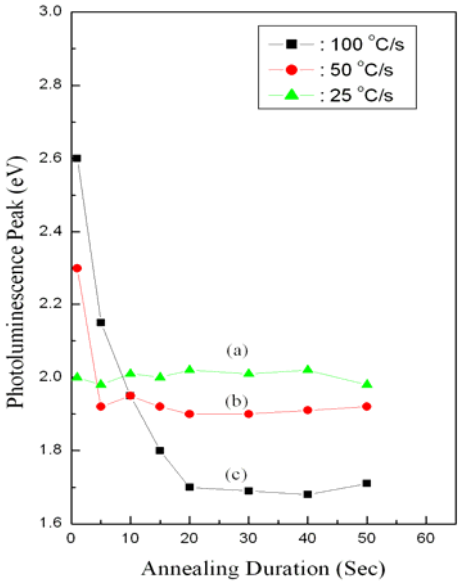

Figure 6. The change in the band of PL peaks from Si^+-implanted SiO_2 films after 1150 °C RTA at the heating rate of (a) 25 °C/s, (b) 50 °C/s, and(c) 100 °C/s, as a function of the RTA duration.

Finally, the position of FTIR peak in the ~ 1100 cm^{-1} range shows the anti-asymmetric stretching vibration of Si-O-Si unit in a SiO_2 film, which can reflects the repairing condition of Si-O bonds in the film. The shift of the FTIR peak to high wave-number, observed from the as-implanted SiO_2 films after RTA, represents the improvement of the broken SiO_2 structure and causes the relaxation of the Si-O bonding network in the films.[14, 17] Fig. 7 shows that the FTIR absorption peak in the 1100 cm^{-1} range from the Si^+-implanted SiO_2 films after RTA at the heating rate of 25 °C/s, 50 °C/s, and 100 °C/s for the duration of 1 second, respectively, changed as a function of the holding temperature in RTA.

As shown in Fig. 7, under this short duration of RTA, the changes in the FTIR peak of the three heating rates were all slow until the holding temperature in RTA was above the dissociation temperature (~1000 ^{o}C) of a-SiO_2 phase variance[18] and the lower heating rate has the bigger change in the positions of FTIR peak. It implies that the lower RTA heating rate wasting more time from 1000 ^{o}C to the holding temperature of 1150 ^{o}C than the bigger heating rate has the better repairing effect for a damaged and substoichiometric oxide matrix where were due to the outcome of Si^{+}-implantation.

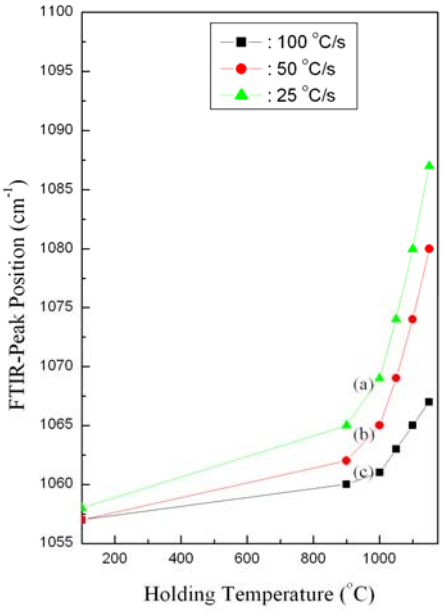

Figure 7. The changes in the FTIR peak positions around 1100 cm^{-1} from the Si^{+}-implanted SiO_2 films after RTA for the duration of 1 second for the heating rate of (b) 25 ^{o}C/s, (c) 50 ^{o}C/s, and(d) 100 ^{o}C/s, as a function of the holding temperature in RTA.

Moreover, the FTIR absorption peak's position at ~ 1100 cm^{-1}, observed from the original 400-nm-thick SiO_2 film without RTA and the $3x10^{16}$ cm^{-2} Si^{+}-implanted 400-nm-thick SiO_2 films after the 1150 ^{o}C RTA but at the different heating rate, change as a function of RTA duration and are shown in Fig. 8. In the figure, at the RTA heating rate of 100 ^{o}C/s, the wave-number of the Si-O-Si stretching mode from the as-implanted SiO_2 films was quickly increasing from 1067 cm^{-1} to 1083 cm^{-1} as the RTA duration changed from 1 second to 20 seconds, the average changed rate is about 0.83 cm^{-1}/s in this period of 19 seconds; then, the wave-number from the films progressively increased to only 1087 cm^{-1} as the duration had increased up to 60 seconds, the average changed rate is decreasing to the value of 0.1 cm^{-1}/s in this period of 40 seconds. At the RTA heating rate of 50 ^{o}C/s, the wave-number of the Si-O-Si stretching mode from the as-implanted SiO_2 films increased from 1080 cm^{-1} to 1085 cm^{-1} as the RTA duration changed only from 1 seconds to 5 seconds, the average changed rate is about 1.25 cm^{-1}/s in this period of 4 seconds; then, the wave number from the films progressively increased to 1092 cm^{-1} after the duration increasing up to 60 seconds, the average changed rate is decreasing to the value of 0.18 cm^{-1}/s in this period of 40 seconds. After decreasing the RTA heating rate to 25 ^{o}C/s, the wave-number of the Si-O-Si stretching mode from the films smoothly increased from 1087 cm^{-1} to 1095 cm^{-1} as the RTA durations changed from 1 second to 60 seconds. Clearly, the peak's positions of ~ 1100 cm^{-1}, where were measured from the films treated at different RTA heating rate, all shift to higher wave-number as the RTA duration varying from 1 seconds to 1 min; besides, for a given RTA duration and temperature, the wave-number of FTIR peak from the as-implanted films was increasing with the decreasing of heating rate of RTA and never bigger than that from the original 400-nm-thick SiO_2 films without RTA. These imply that, for the RTA durations $\leq$ 20 seconds at the heating rate of 100 ^{o}C, $\leq$ 5 seconds at the heating rate of 50 ^{o}C/s, and $\leq$ 1 second at that of 25 ^{o}C/s, the respective average rate of the FTIR-peak change from the RTA-treated as-implanted film was quicker than that for the other durations and so was the repairing rate of the Si-O bonds in the films. Certainly, the final repairing situation of the RTA-treated as-implanted SiO_2 film can not recover to the original situation of the SiO_2 film before implantation. Therefore, the heating rate of RTA determining the active-time of PL-mechanism production has an important contribution for the improvement of the broken structure in the RTA-treated as-implanted SiO_2 film.

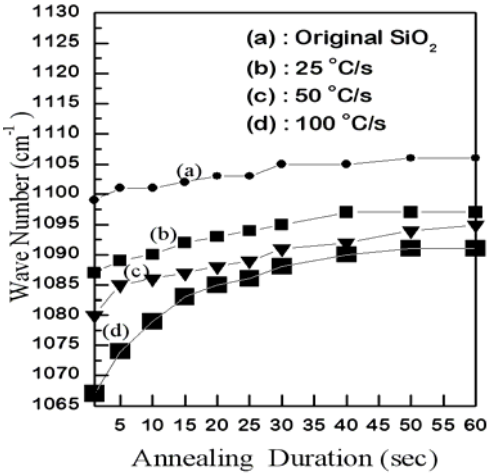

Figure 8. The changes in the FTIR peak positions around 1100 cm^{-1} from the (a) original and Si^{+}-implanted SiO_2 films after RTA at 1150 ^{o}C and at the heating rate of (b) 25 ^{o}C/s, (c) 50 ^{o}C/s, and(d) 100 ^{o}C/s, as a function of the RTA duration.

4 Conclusion

Room-temperature visible photoluminescence (PL) was observed in $3x10^{16}$ cm^{-2} Si^{+}-implanted 400-nm-thick SiO_2 films after RTA at 1150 ^{o}C in dry nitrogen. For the RTA duration of 1 seconds, the PL peak at ~2.6 eV from the as-implanted films has the heating rate of 100 ^{o}C/s and those with peaks at ~2.3 eV and ~2.0 eV from the films have the heating rate of 50 ^{o}C/s and 100 ^{o}C/s, respectively. Moreover, when the RTA duration was increasing from 1 s to 20 seconds, a broader shift of the PL peak from 2.6 eV to 1.7 eV would be found in the films as the RTA heating rate of 100 ^{o}C/s. However, after the heating rate was decreasing to 25 ^{o}C/s, no significant shift of the PL peak could be seen in the films after the isothermal RTA for the duration > 1 seconds. Similarly, the average rate of the FTIR-peak change at ~ 1100 cm^{-1} from the as-implanted films after the isothermal RTA was quick for the RTA duration ≤ 20 seconds at the heating rate of 100 ^{o}C, ≤ 5 seconds at the heating rate of 50 ^{o}C/s, and not obviously vary for the RTA duration >1 s at that of 25 ^{o}C/s. For these PL and FTIR phenomena should be related closely to the formation of nc-Si crystal and the improvement of the broken structure in the RTA-treated as-implanted SiO_2 films, the RTA heating rate really plays the main role of Si^{+} re-crystal and the repair of broken Si-O bonds in the as-implanted SiO_2 film for a given RTA temperature and duration.

References

1. Brus L, *Semiconductors and Semimetals, edited by D. Lockwood* (Academic, New York), Vol. 490 (1998) 303.
2. Qin GG, Li AP, Zhang BR and Li B, *J. Appl. Phys.* 78 (1995) 2006.
3. Lin GR and Lin CJ, *J. Appl. Phys.* 95(12) (2004) 8484.
4. Shimizu-Iwayama T, Nakao S and Saitoh K, *Appl. Phys. Lett.* 65 (1994) 1814.
5. Mutti P, Ghislotti G, Bertoni S, Bonoldi L., Cerfolini GF, Meda L, Grilli E and Guzzi M, *Appl. Phys. Lett.* 66 (1995) 851.
6. Zhu JG, White CW, Budai J D, Withrow P and Chen Y, *J. Appl. Phys.* 78 (1995) 4386.
7. Ghislotti G, Nielsen B, Asoka-Kumar P, Lynn KG, Gambhir A, DiMauro LF and Bottani CE, *J. Appl. Phys.* 79 (1996) 8660.
8. Min KS, Shcheglov KV, Yang CM and Atwater HA, *Appl. Phys. Lett.* 69 (1996) 2033.
9. Aidong Lan, Baixin Liu and Xinde Bai, *Jpn. J. Appl. Phys.* 36 (1997) L1019.
10. Chou ST, Tsai JH, and Sheu BC, *J. Appl. Phys.* 83(10) (1998) 5394.
11. Tsai JH, Yu AT, and Sheu BC, *Jpn. J. Appl. Phys.* 39 (2000) L107.
12. Tsai JH and Yu AT,, *Jpn. J. Appl. Phys.* 44(3) (2005) 1389.
13. Nakamura M, Kanzawa R, and Sakai K, *Journal of Electrochemical Society* 133(6), (1986) 1167.
14. Sano N, Sekiya M, Hara M, and Kohno A, *Appl. Phys. Lett.* 66(16) (1995) 798.
15. Trukhin AN, Jansons J, Fitting HJ, Barfels T, and Schmidt B: J. Non-Cryst. Solid 331 (2003) 91.
16. Lin GR and Lin CJ: J. Appl. Phys. 95 (2004) 8484.
17. Garrido Fernanedz B, Lopez M, Garcia C, Perez-Rodriguez A, and Morante JR, *Jpn. J. Appl. Phys.* 91(2) (2002) 798.
18. Sosman RB, *Trans. Br. Ceram. Soc.* 54, (1995) 655.

Somatic Embryogenesis and *In Vitro* Regeneration of an Endangered Medicinal Plant Sarpgandha (*Rauvolfia serpentina. L*)

Prabhat Singh, Anand Singh, Arvind K. Shukla, Lalit Singh, Veena Pande and Tapan K. Nailwal
Department of Biotechnology, Kumaun UniversityNainital,Uttarakhand- 263001,India

Received March 7, 2009

Abstract

An efficient protocol for *in vitro* regeneration of endangered medicinal plant *Rauvolfia serpentina* has been developed. The juvenile leaf explants were transferred to MS medium containing different combinations of PGRs. Among the various combinations of BAP (1.0-3.0) and IAA (0.1-0.5) the intensity of callus induction was highest in BAP (2.5) + IAA (2.0) mg/l and BAP (1.0) + IAA (0.5) mg/l. The frequency of callus induction was highest 77.77% in BAP (1.0) + IAA (0.5) mg/l. During organogenic callus formation, different types of calli with variation in colour and texture were noticed and among them, the light green, fragile calli responded well for the induction of shoots. Among the various combinations of BAP and IAA used the frequency of shoot regeneration was highest 75% in BAP (2.5) +IAA (0.4) mg/l. For elongation of shoot 1ppm GA_3 was also used, this provides a better result. The shoot was transferred to M.S. Media for root regeneration containing PGRs BAP (2.5) + IAA (0.3-0.5) + NAA (0.3-0.5) mg/l. The frequency of root regeneration was 100% in MS Medium containing BAP (2.5) + IAA (0.5) + NAA (0.5) mg/l. After rooting on shoots the plantlets were shifted to sterile soil field pots for acclimatization.The survival percentage of plants after hardening was 67%. The protocol was optimized by manipulations of different PGRs for enhanced multiplication. Protocol explained in this research paper provides a rapid plant regeneration system which could be used for the somaclonal variation; shoot induction and producing transgenic plants in *Rauvolfia* through *Agrobacterium* and biolistic methods. [Life Science Journal. 2009; 6(3): 74 – 79] (ISSN: 1097 – 8135)

Key words: Somatic Embrygenesis

1 Introduction

Medicinal plants have been the subjects of man's curiosity since time immemorial[1]. Almost every civilization has a history of medicinal plant use[2]. Approximately 80% of the people in the world's developing countries rely on traditional medicine for their primary health care needs, and about 85% of traditional medicine involves the use of plant extracts [3]. *In vitro* cell and tissue culture methodology is envisaged as a mean for germplasm conservation to ensure the survival of endangered plant species, rapid mass propagation for large-scale revegetation, and for genetic manipulation studies. Combinations of in vitro propagation techniques [4] and cryopreservation may help in conservation of biodiversity of locally used medicinal plants.

Rauvolfia serpentina. L commonly known as sarphgandha is an important medicinal shrub of family Apocynaceae. The snake-weed genus includes about 50 species, this has fairly wide area of distribution, including the tropical part of the Himalayas, the Indian peninsula, Sri Lanka, Burma, and Indonesia. The plant is indigenous to India, Bangladesh and other regions of Asia and found to grow in the wild in many places around the country[5]. Its roots contain 0.15% resperine-rescinnamine group of alkaloids[6]. It also contains a number of bioactive chemicals, including ajmaline, deserpidine, rescinnamine and yohimbine. This herbal plant is used as medicine for high blood pressure, insomnia, anxiety and other disorders of the central epilepsy[5].

Rauvolfia is threatened in India due to indiscriminate collection and over exploitation of natural resources for commercial purposes to meet the requirements of pharmaceutical industry, coupled with limited cultivation [7]. IUCN has kept this plant under endangered status. The chemical resperine is an alkaloid first isolated from roots of *Rauvolfia serpentina* and is used to treat hypertension[8,9]. Although, for centuries they have been used empirically in India for a variety of conditions that they were effective in relief of hypertension was first commented on by[10] subsequently, other clinical investigators working in India confirmed the effectiveness of *Rauvolfia serpentina* for that purposes [11,12]. In a short term study, a significant decrease in systolic as wall as diastolic blood pressure of patients to whom the drug was given was observed [13]. Insanity, Snakebite and Cholera can also be treated by use of this alkaloid. The pectic polysaccharide named rauvolfian RS was obtained from the dried callus of *Rauvolfia serpentina* L. by extraction with 0.7 % aqueous ammonium oxalate and it was found to posses some anti-inflammatory effect [14].

In approximately 60% of medicinal plants used in traditional medicines, roots are the principal source of drug preparation. The development of fast growing culture

system can offer an opportunity for producing drugs from the roots in the laboratory with out having to depend solely on field cultivation.

In vitro regeneration of sarphgandha has been done from several genotypes. Micropropagation has been achieved from explant of *Rauvolfia micrantha* Hook F cultures. Micropropagation can be considered as an important tool for the production of higher quality plant based medicines**.** In view of this, there is an urgent need to apply in vitro culture methods for the micropropagation and conservation of this valuable endangered plant. Here efforts have been made to define efficient protocol for the recovery of plants through organogenesis of *Rauvolfia serpentina. In vitro* regeneration of *Rauvolfia* has been reported by many authors[15-19]. The present study was undertaken to develop a more efficient protocol for rapid *in vitro* multiplication of *Rauvolfia serpentina* using leaf explant as an initial plant material.

2. Materials and Methods

2.1 Plant material

Plantlets of *Rauvolfia serpentina* were obtained from Corbett jadibuti Udhyan Kaladhungi, Nainital, Uttarakhand and grown in sterile vermiculite at 25-30 ^{0}C in light. All the explants were taken from these donor plants for present investigation. Leaf explants from 2 month old donor plant was kept for 2 hrs in systemic fungicide Bavistin (VIMCO pesticides, Gujarat) and Tween-80 an antimicrobial agent, prior to surface sterilization. For surface sterilization, chemicals such as $HgCl_2$ (0.1%), NaOCl (1%), H_2O_2 (1%) and ethanol (70%) was used. Juvenile leaves were washed thoroughly in running tap water for 30 min. and then with distilled water three times. Leaves were treated with bavistin solution for 4-5 min., and then rinsed thoroughly with sterile distilled water. The leaves were subjected to 0.1% $HgCl_2$ for 30 sec., washed with distilled water and then placed in 70% ethanol for 1 min. and again washed with distilled water, followed by addition of three drops of antibiotic solution (Cefotaxime) in laminar airflow cabinet. In the antibiotic solution, all leaves were dissected into small pieces and treamed so that maximum part can be exposed to media. All the chemicals used were purchased from Hi-media unless stated otherwise.

2.2 Culture media and growth condition

The medium comprised of macro and micro elements according to[20] with Mesoinosotol (100 mg/l), Thiamine-HCL (0.5mg/l), pyridoxine-HCL (1mg/l), Nicotinic acid (0.5mg/l) and sucrose (30g/l), solidified with (0.6%) agar. The Plant growth regulators used were 6- Benzyl-aminopurine (BAP), α- naphthalene acetic acid (NAA) and indole acetic acid (IAA). All experiments were carried out in culture tubes (150 × 25 mm) containing 30 ml of culture medium. The pH of media were adjusted to 5.8 prior to autoclaving at 121^{0}C at 15 lbs pressure for 20 min. Culture were incubated under 16 h /8h light/ dark cycles (artificial light , 80 µM per m^2/s).

2.3 Callus induction and shoot regeneration:

For callus induction juvenile leaf section (3-5 mm in length) with cut end surface in contact with culture medium were placed on MS medium supplemented with various concentrations of PGRs BAP and IAA. After 20 days of culture, the leaves cultured on MS basal medium supplemented with 3% (w/v) sucrose, BAP (1.0 ppm) and IAA (0.5ppm) were found to give profuse callusing and when callusing was observed in entire explant, the callus was cut into small pieces transferred to MS media having BAP and IAA in same concentration as for callus induction. Subculturing was done after every 1-2 week. After 3-4 weeks of subculturing first shooting is observed in callus.

2.4 Regeneration of roots and development of complete plantlets:

For initiation of roots the 6-8 weeks old shoots (2.5-4.0 cm. in length) were cultured on half strength MS basal medium supplemented with 2% (w/v) sucrose and different concentration of PGR were tested BAP(2.5ppm) **:** IAA(0.3ppm): NAA(0.3ppm),BAP(2.5ppm) **:** IAA(0.4ppm) **:** NAA(0.4ppm), BAP (2.5ppm) **:**IAA(0.5ppm) **:** NAA(0.5ppm), for 2-3weeks. The shoots were also tested on hormone free full and half strength MS basal medium with 3% sucrose ((w/v) for root initiation.

The complete rooted plantlets (6-10 weeks old) were washed free of agar and dipped in 0.2% bavistin fungicide for 5-10 min., and potted in small plastic pots containing sterilized soilrite. The plantlets were covered with polythene bags to maintain high humidity**.** These were acclimatized at 25±3^{0}C under 16h photoperiod and watered regularly. After 3-4weeks, the polythene bags were removed and established plantlets were transplanted to earthen pots in a greenhouse.

3. RESULTS AND DISCUSSION

The smaller size of explants were chosen due to fact that smaller size of explants provide less chance of contamination, as well as longer leaves showed total loss of morphogenic potential.[21]. Initiation of calluses from leaf explants did not pose a major problem. During initiation the explants did not show any leaching or browning of tissues. MS basal medium was the most effective for callusing of leaf explants. The explant cultured on MS basal medium supplemented with different combinations of BAP and IAA show varied response for callusing (Table 1). Leaf explants culture on MS basal medium without any PGR supplementation show only swelling of explants that were not significant for callusing. This was possibly due to significant role of PGR over callusing. In the media supplemented with BAP and IAA, the leaf segments remain green for long period with very slow process of callus induction (Fig .1). Further transfer into media containing BAP and IAA rapidly shows callus induction because the excretion of phenolic compounds from explants to the medium was strictly avoided by regular sub-culturing of callus. (Fig. 2)

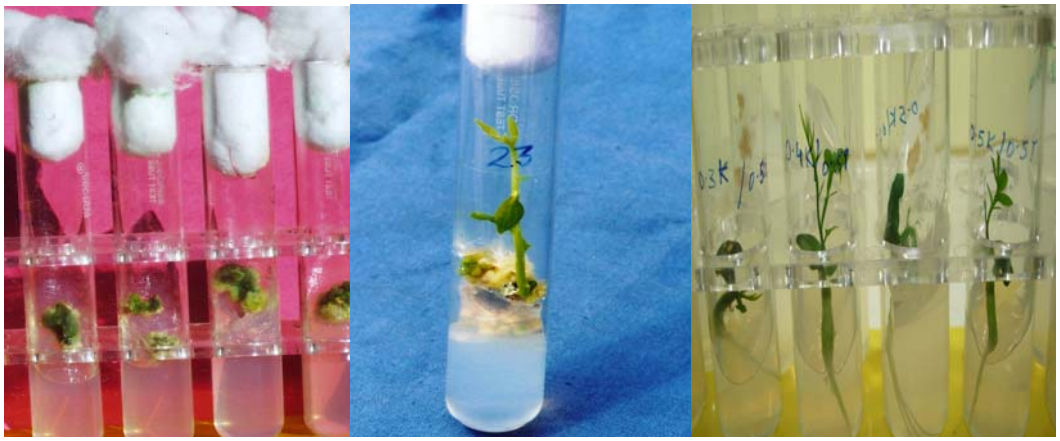

Figure 1. Callus induction in R. sepentina from leaf explants in MS media containing BAP(1.0) and IAA(0.5)mg/l ;
Figure 2. Shoot regeneration from callus on BAP (2.5) + IAA (0.4) mg/l MS media;
Figure 3. Rooting regeneration on BAP (2.5) + IAA (0.5) + NAA (0.5) mg/l MS media.

Table 1. Effect of different concentrations of PGR added to MS medium on induction of callus from leaf in *R. serpentina*. Observation after 27 Days:

PGR(mg/l)		Intensity of callus induction	Nature of callus
IAA	BAP		
0.1	-	-	No callus formation
0.1	1.0	++	White coloured, fragile
0.1	1.5	+	Green coloured ,fragile
0.2	0.0	-	No callus formation
0.2	1.0	++	Light green coloured ,fragile
0.2	1.5	+	Light green coloured ,fragile
-	2.0	-	No callus formation
-	2.5	-	No callus formation
-	3.0	-	No callus formation
0.1	2.0	+	White coloured, fragile
0.1	2.5	-	No callus formation
0.1	3.0	-	No callus formation
0.2	2.0	-	No callus formation
0.2	2.5	+++	White coloured, fragile
0.2	3.0	-	No callus formation
0.3	-	-	No callus formation
0.3	1.0	++	Green coloured ,fragile
0.3	1.5	+	Light green coloured ,fragile
0.3	2.0	-	No callus formation
0.3	2.5	++	Light green coloured ,fragile
0.3	3.0	-	No callus formation
0.4	-	-	No callus formation
0.4	1.0	++	Light green coloured ,fragile
0.4	1.5	+	Light green coloured ,fragile
0.4	2.0	-	No callus formation
0.4	2.5	++	Light green coloured ,fragile
0.4	3.0	-	No callus formation
0.5	-	-	No callus formation
0.5	1.0	+++	Light green coloured ,fragile
0.5	1.5	+	Green coloured ,fragile
0.5	2.0	++	Light green coloured ,fragile
0.5	2.5	-	No callus formation
0.5	3.0	-	No callus formation
-	-	-	Swelling of the explant observed.

Table 2: Effect of different concentration of PGRs added to MS medium on induction of callus and regeneration of shoots from leaf of *R. serpentina*.

PGR (mg/l) BAP	PGR (mg/l) IAA	Days for Callus formation	Days of shoot Regeneration after callusing	Frequency of Callusing	Frequency of Shoot Regeneration (%)
2.5	0.4	24	18	72.00	75
2.5	0.3	24	36	40.00	45.03
1.0	0.5	24	37	77.77	52
2.0	0.5	24	38	70.00	39.45

Table 3: Effect of different concentration of PGR added to MS medium for root regeneration from shooted callus of *R. serpentina*.

PGR (mg/l) BAP	PGR (mg/l) IAA	PGR (mg/l) NAA	Days of Rooting	Frequency of Rooting (%)
2.5	0.3	0.3	12	85
2.5	0.4	0.4	15	96
2.5	0.5	0.5	10	100

Table 4: Estimated survival of plants after hardening.

Number of pots containing Plants	Number of plants survived	Percentage of survival (%)
5	3	60
3	2	67
4	2	50

Figure 4. In vitro regeneration of complete plantlets of R. serpentina from leaf explant.
Figure 5. Hardening of plantlet to mixture of sterile soil, sand and vermicompost.

Callus is an unorganized mass of plant cells and its formation is controlled by growth regulating substances present in the medium (auxins and cytokinins) [22]. The specific concentration of plant regulators needed to induce callus, varies from species to species and even depends on the source of explant [23]. It has been demonstrated in many cases that 2,4-D is usually the choice of auxin for callus induction and subculture of grasses[24,25]. Lately more and more experimental results indicate that the addition of a low concentration of cytokinin in callus culture medium often enhances callus regeneration [25-28]. Minimal cytokinins and auxins in culture media would avoid somaclonal variation and efficiently produce true to type plantlets[29].

The success of micropropagation largely relies on the selection of suitable plant part, which is to be used as the starting material for the experiment. In the present experiment leaf explants was best fit for purposes. The best callusing was observed in media having BAP: IAA in concentration ratio of (1.0: 0.5ppm). In the media supplemented with only BAP and IAA the callus induction was very significant (Fig. 2). This remains in accordance with previous reported work of (Mathur et.al., 1987). Different types of calli with variation in colour and texture were noticed (Table 1) and among them, the light green, fragile calli responded well for the induction of shoots.

This study further demonstrates that shoot regeneration from callus was very earlier in media supplemented with BAP and IAA in concentration ratio of (2.5: 0.4 ppm), in comparison to 2.5:0.3, 1.0:0.5 or 2.0:0.5 (Table 2; Fig. 3). Thus, the PGR concentrations have significant impact on shoot regeneration. This is basically due to endogenous level of growth regulators. For elongation of shoot 1ppm GA_3 was also used, this provides a better result (Fig. 4).

No root could be induced in either basal medium of full or half strength MS media. However, when 2.5-4.0 cm. elongated shoots were placed on half strength MS basal medium supplemented with BAP ,IAA and NAA in concentration ratio of (2.5: 0.5: 0.5 ppm)roots were induced in nearly 100% of shoots within 2 weeks. (Fig. 5,6,7) Other concentration BAP, IAA and NAA (2.5:0.4:0.4 and 2.5:0.3:0.3) induce rooting in slightly lower percentage (Table 3). Basal media supplemented with NAA was found to be better for root regeneration this was in accordance with previous reported work of [30].

Taking care of root regeneration data it can be concluded that the standard protocol developed for regeneration of *Rauvolfia* was nearly 100% efficient but in accordance with hardening data (Table 4) there is a need for further standardization and work to increase the efficiency, during hardening so that this medicinally important plant could be propagate at larger scale and its medicinal importance properties could be utilized for well being of human population. This further become important due to advancement in commercialization of plant tissue cultured plantlets by commercial sectors have led to continued exponential growth within the industry in terms of numbers of new units as well as numbers of plants produced by the units[31]. The development of a reliable *in vitro* protocol are of great importance for producing plant material and for conservation of rare plant species, and offset the pressure on the natural populations as well as plant medicinal purposes.

The present study describes a well documented and reliable protocol of *R. serpentina* from leaf explants with much higher rate of multiplication. This protocol can be used as a basic tool for commercial cultivation of sarphgandha plant.

References:

1. Constable F, Medicinal plant biotechnology. *Planta Med*. 1990;56: 421-425.
2. Ensminger AH.,Ensminger ME, Konlande JE *et al*. *Food & Nutrition Encyclopedia*. Pegus Press, Clovis, California, U.S.A. 1983;2:1427-1441.
3. Vieira RF, Skorupa LA. Brazilian medicinal plants gene bank. *Acta Hort*. 1993;330: 51-58.
4. Fay, M.F. Conservation of rare and endangered plants using in vitro methods. *In Vitro Cell. Dev. Biol.-Plant*. 1992;28: 1-4.
5. Ghani, A.Medicinal plants of Bangladesh. Chemical constituents and uses. Asiatic Society of Bangladesh, Ed. 1998;2:36.
6. Anonymous. In the wealth of India, Raw materials, Publication and information Directorate, CSIR, New Delhi, India 1969;3.
7. Gupta R. *Indian J Plant Genet Resources* 1989;1:98-102.
8. Ford RV, Moyer JH. Extract of *Rauvolfia serpentina* in hypertension. *Genl. Practice*. 1953;8:51.
9. Vida F. Behandlung der Hypertonie mit der indischen *Rauvolfia serpentina. Die Med*. 1953;37:1157.
10. Bhatia BB. On the use of *Rauvolfia serpentina* in high blood pressure, *J.Ind. Med.Assn*. 1942;11:262.
11. Chakraverti NK, Raichudjuri MN Chaudjuri RN. *Rauvolfia serpentina* in essential hypertension. *Ind. Med. Gazette*. 1951;86:348.
12. Gupta JC. Alkaloids of *Rauvolfia serpentina*. Rep. Adv. School Bd., Ind. Res.Fund Assn. 1942;70.
13. Vakil RJ. A clinical trial of *Rauvolfia serpentina* in essential hypertension. *Brit. Heart J*. 1949;11:350.
14. Popov SV, Vinter VG, Patova OA *et al.* Chemical characterization and anti-inflammatory effect of rauvolfin, a pectic polysaccharide of *Rauvolfia* callus. *Biochemistry (Mosc*). 2007;72(7): 778-784
15. Butenka RG. Isolated tissue culture and physiology of plant morphogenesis. Nauka, Moscow. 1964
16. Mitra GC, Kaul KN. In vitro culture of root and stem callus of *Rauwolfia serpentina* Benth. for reserpine. *Indian J. Exp Biol* 1964;2: 49-51.
17. Vollosovich AG, Butenka RG. Tissue culture of *Rauwolfia serpentina* as a resource of alkaloids. In: Culture of isolated organs, tissues and cells of plant.. Butenka, R.G. (Ed) Nauka, Moscow 1970;. 253-257

18. Kukreja AK, Mathur AK, Ahuja PS *et al.* Tissue Culture and Biotechnology of Medicinal and Aromatic Plants. ICSIR, Lucknow, India. 1989
19. Roy SK, Hossain MZ, Islam MS. Mass Propagation of *Rauvolfia serpentina* by *in vitro* Shoot Tip Culture. *Plant Tissue Cult.* 1994; 4 (2): 69-75
20. Murashige T, Skoogs F. *Physiol Plant.* 1962;15:473-479.
21. Mujib A., Das S, Dey S. Free cell culture, organization and plant regeneration in *Santalum album* L.. *Plant tissue culture* . 1997;7:63-69.
22. Shah MI, Jabeen M, llahi l. *In vitro* callus induction, its proliferation and regeneration in seed explants of Wheat (*Triticum aestivum* L.) var. Lu-26S. *Pak. J. Bot*. 2003;35(2):209-217
23. Charriere F, Sotta B, Miginiac E *et al.* Induction of adventitious shoots or somatic embryos on invitro culture.*Plant Physiol.Biochem*. 1999;37(10):752-757.
24. Bhaskaran S, Smith RH. Regeneration in cereal tissue culture: A review . *Crop Sci*. 1990;30: 1328-1336.
25. Chaudhury A, Qu R. Somatic embryogenesis and plant regeneration of truf-type bermudagrass:effect of 6-Benzaldehyde in callus induction medium. *Plant cell tiss. Org.Cult* 2000; 60:113-120.
26. Alpeter F, Posselt UK. Improved regeneration from cell suspensions of commercial cultivars, breeding and in bred lines of perennial ryegrass (*Lolium perenne L.). J. Plant Physiol*. 2000;156:790-796.
27. Bai Y, Qu R. Factors influencing tissue culture responces of mature seeds and immature embryos in turf-type tall fescue (*Festuca arundinacea schreb*.)*Plant Breeding*. 2001; 120: 239-242.
28. Bradley DE, Bruneau AH, Qu R. Effect of cultivar, explant treatment and medium supplements on callus induction and plantlet regeneration in perennial ryegrass. *Int. Turfgrass Soc. Res. J*. 2001; 9: 152-156.
29. Edson JL, Leege-Brusven AD, Everett RL *et al.* Minimizing growth regulators in shoot culture of an endangered plant, *Hackelia ventusa* (Boraginaceae).*In vitro cell Dev.Biol.Plant.* 1996;32 :267-271.
30. Kumar KP, Soniya EV, Lawrence B *et al.* Micropropagation of *Clitoria terntea* L. (Paplionaceae) through callus regeneration and shoot tip multiplication. *Journal of species and aromatic crops*. 1993;2:41- 46.
31. Govil S, Gupta SC.Commercialization of Plant tissue culture in India. *Plant cell ,Tissue and Organ Culture*. 1997;51:65-73.

Synergistic effect of N-terminal pyroglutamyl amyloid ß protein in Alzheimer's disease and in normal aging

Ying-Chuan Wang[1], Ren-Jing Huang [2,3] ,Shieh-Ding Wu [2,3,*]

[1]Department of Nursing, Shu Zen College of Medicine and Management ,Hwan-Chio Rd., Luju Kaohsiung 452, Taiwan ROC. [2]School of Medical Imaging and Radiological Sciences, Chung Shan Medical University TaiChung 402, Taiwan ROC. [3]Department of Medical Image, Chung Shan Medical University Hospital TaiChung 402, Taiwan ROC

Received March 4, 2009

Abstract

Amyloid ß protein (Aß) has been considered as the main pathogenetic basis of Alzheimer's disease (AD). Substantial evidence indicates that the soluble Aß aggregates containing N-terminally truncated Aß starting with pyroglutamate at position 3 ($Aß_{PE3}$) and position 11($Aß_{PE11}$) account for the major neuronal toxicity of AD. In addition to the heterogeneity in soluble Aß aggregate, the composition ratio of Aß variants in the brain from AD and in normal aging possess a significant role for the development of AD. For this reason, we postulate that Aß variants with different composition ratio may cause aggregation behavior entirely different. In this study, two mixtures, AD and NA, composed of three Aß variants ($Aß_{1-40}$, $Aß_{PE3-40}$, $Aß_{PE11-40}$) with different composition ratio were investigated. Thioflavine T fluorimetric assay revealed that AD mixture with a high $Aß_{PE3-40}/Aß_{PE11-40}$ composition ratio has highly increased ß-sheet structure compared with the three individual Aß variants. By contrast, NA mixture with a low $Aß_{PE3-40}/Aß_{PE11-40}$ composition ratio leads to an unobvious increase. This suggests that $Aß_{PE3-40}$ may have synergistic effect to regulate the aggregation propensities of the Aß mixtures. Surface plasmon resonance kinetics assay demonstrated that the aggregation rates of the three soluble Aß variants interacting both AD and NA mixtures have a consistent of order as follows, $Aß_{PE3-40} > Aß_{PE11-40} > Aß_{1-40}$. Both $Aß_{PE3-40}$ and $Aß_{PE11-40}$ have a higher aggregation rate than $Aß_{1-40}$ to form aggregates. Therefore, the investigated N-terminal pyroglutamyl Aß variants and their composition ratio in mixtures may play an important role to regulate aggregation behaviors and to influence the development of AD. [Life Science Journal. 2009; 6(3): 80– 85] (ISSN: 1097 – 8135).

Key words: Alzheimer's disease, amyloid, surface plasma resonance, synergistic effect, amyloid ß protein (Aß), amyloid ß precursor protein (AßPP), Alzheimer's disease (AD), normal aging (NA), surface plasmon resonance (SPR), thioflavine T (ThT)

1 Introduction

Alzheimer's disease (AD), a neurodegenerative disease, is the most common cause of dementia in the elderly population. This widespread progressive neurodegeneration characterized by the presence of proteinaceous deposits in the brain is described as amyloid. The extracellular deposition of amyloid ß protein (Aß) and the intracellular generation of neurofbrillary tangles are the main histopathological features of AD (1,2).

Aß is a 39- to 43-amino acid polypeptide, and is a normal metabolic product which can be found in cerebrospinal fluid and plasma (3). Aß is derived from the proteolytic product of amyloid ß precursor protein (AßPP) through the cleavage of ß-secretase and ?-secretase (4,5). Authentic evidence indicates that several factors can lead to the formation of amyloid plaques in AD (2) including (i) genetic mutations of APP resulting in early-onset familial AD (FAD), and the over expression of APP resulting from elevated gene dosage in trisomy 21 (Down's syndrome), (ii) FAD-causing mutations on chromosome 14 and 1 in genes encoding the homologous presenilin proteins PS1 and PS2, which affect APP processing, (iii) apolipoprotein E4 allele which lower the average age of AD. These factors can result in two predominant aggregates of Aß including $Aß_{1-40}$ and $Aß_{1-42}$ which are the primary component in senile plaques (6,7).

Although previous studies demonstrate fibrillar form of Aß is inferred as a key role leading to the pathogenesis of AD. Recent data show that the more neurotoxic forms of Aß are small, still water-soluble oligomers, amyloid-derived diffusible lignds (8) and protofibrils (9) which correspond better than fibrils with neurodegeneration. In addition to $Aß_{1-40}$ and $Aß_{1-42}$, N-terminal truncated forms of water soluble Aß were also seen in Aß plaques of the brain of AD and Dome syndrome patients. The most common forms of N-terminally truncated Aß is post-translationally modified N-terminal pyroglutamyl Aß variants, termed $Aß_{PE3-40/42}$, $Aß_{PE11-40/42}$ and p3 ($Aß_{17-40/42}$) (10,11). The C-terminal heterogeneity of Aß and its role in the pathogenesis of AD have been well characterized (2,12). Several studies demonstrated that N-terminal pyroglutamyl Aß variants, $Aß_{PE3-40/42}$ and $Aß_{PE11-40/42}$, can stabilize the peptides against degradation and they appear very early in the disease progress to show an enhanced cytotoxicity (13,14).

Most recent investigation show that the molecular composition ratio of water-soluble Aß variants in the

* corresponding author: Shieh-Ding Wu
Email: htwu@csmu.edu.tw

soluble Aß aggregates between AD patients and normal aging (NA) individuals is unlike; the major differentiation is the molecular composition ratio of N-terminal pyroglutamyl Aß variants in aggregates which can make different depositability and cytotoxicity for the development of AD (15). In this study, the mixtures of three Aß variants, including two pyroglutamyl Aß variants ($Aß_{PE3-40}$ and $Aß_{PE11-40}$) and a full-length $Aß_{1-40}$ at different molecular composition ratios, were investigated to study the variations of aggregation propensities induced by composition change

2. Materials and Methods

All solvents and chemical used were either of analytical grade or chemically pure. Aß peptides, including $Aß_{1-40}$, $Aß_{PE3-40}$ and $Aß_{PE11-40}$, were purchased from AnaSpec (San Jose, CA). Thioflavine T (ThT), dimethyl sulfoxide (DMSO) and phosphate-buffered saline (PBS) were obtained from Sigma Chemical (St. Louis, MO). All of the surface plasmon resonance (SPR) experiments used in kinetics assay of Aß variants aggregation were performed on a Biacore X apparatus, at 25 °C. The instrument, sensor chips (type CM5), and coupling reagents, including (N-ethyl-N'- (3-dimethylaminopropyl) carbodiimide hydrochloride (EDC), N-hydroxysuccinimide (NHS), and ethanolamine HCl), were from Biacore AB (Uppsala, Sweden).

Preparation of soluble Aß Solutions.

Prior to analysis, the lyophilized amyloid peptides were subjected to a disaggregation procedure described by Dahlgren et al. (16). Afterward, stock solutions of $Aß_{1-40}$, $Aß_{PE3-40}$ and $Aß_{PE11-40}$ in a concentration of 1 mM were prepared in pure DMSO. Aß solutions treated in this way have been described to be free of oligomeric species (17,18).

Two soluble Aß variants mixtures at the molecular composition ratios referring to the investigation on AD and NA individuals described by Piccini et al. (15) with little modifications, AD ($Aß_{1-40}$, 36%; $Aß_{PE3-40}$, 48%; $Aß_{PE11-40}$, 16%) and NA ($Aß_{1-40}$, 40%; $Aß_{PE3-40}$, 29%; $Aß_{PE11-40}$, 31%), and three soluble Aß variants were suspended in PBS and kept for 24h at room temperature, at a final concentration of 1µM, PH 7.2, for subsequent analyses.

SPR Kinetics Binding Assay

SPR biosensing technology has been chosen as analytical tool to study ligand-ligate binding kinetics, which is capable of the ability to detect specific binding events between target biomolecules in liquid phase (ligate) and a specific binding partner immobilized on chip surface (ligand) without the use of labeling molecules on the target molecules and tedious processing procedures keeping peptides in native state.

In this study, SPR biosensor was adopted to investigate the real-time aggregation kinetics of the two Aß mixtures and the three Aß variants in detail. The three Aß variants kept for 24h at room temperature were separately immobilized onto chip surface as ligand by using standard amine coupling method (19). Sensor chips were first activated with an injection of a 1:1 ratio of 0.4M EDC and 0.1M NHS at a flow rate of 20µL/min for 7min. The three Aß variants, at 10µM in 10 mM sodium acetate, pH 4.0, were injected over the activated surface for 7 min. The remaining activated surface groups were blocked with a 7-min injection of 1M ethanolamine, pH 8.0. The SPR signals from each of the Aß variants result in 500-800 Biacore response units (RU).

These three immobilized Aß variants were then used to interact with the incubated soluble Aß variants and the two incubated soluble Aß mixtures. The binding data were analyzed using the BIA evaluation program.

Thioflavine T Binding Assay

The three Aß peptides and two mixtures, AD and NA, were aggregated in 100 µl of RPMI buffers, at a concentration of 100nM, for 24h at room temperature. Ten µl of each reaction mixture were mixed with 990µl of ThT (3 µM in 50 mM sodium phosphate, pH 6.0), and the fluorescence was subsequently measured at Ex/Em of 450/482 nm by a fluorescence spectrophotometer (Hitachi F-4500). The relative fluorescence intensity was defined by taking fluorescence of 100 nM $Aß_{1-40}$ aggregated for 24 h as 100 %.

3. Results

Thioflavine T binding to amyloid is a specific interaction for anti-parallel ß-pleated sheet secondary structure which produces a change in the emission spectrum of ThT (20). Thereby, the emission intensity of ThT is proportional to the total quantity of ß-pleated sheet amyloid. Fig. 1 shows that after a 24h of incubation time, $Aß_{PE11-40}$ revealed a highest amount of ß-pleated sheet amyloid among the three tested Aß variants and AD mixture displayed a much higher amount of ß-pleated sheet amyloid than does NA mixture. In our experiments, both two mixtures have a close composition ratio of $Aß_{1-40}$, but AD mixture having a high $Aß_{PE3-40}/Aß_{PE11-40}$ (48:16) composition ratio revealed a much higher increase in the amount of ß-pleated sheet amyloid than the three tested Aß variants under the same test condition of peptide concentration. By contrast, the NA mixture, which has a low $Aß_{PE3-40}/Aß_{PE11-40}$ (29:31) composition ratio, leads to a less amount of ß-pleated sheet amyloid than does AD mixture. The amount of ß-pleated sheet amyloid of NA mixture is only a little higher than does $Aß_{1-40}$.

To measure the aggregation propensities of the three individual Aß variants, SPR biosensing technique was used to directly detect specific biomolecular interactions in real time through a molecular recognition mechanism (21) which is a noninvasive optical method better than the traditional approaches for measuring aggregation kinetics (22). In Fig. 2, the sensogram, showing real-time aggregation kinetics of the three individual soluble Aß variants, revealed that the order of aggregation rates was as follows, $Aß_{PE11-40} > Aß_{PE3-40} > Aß_{1-40}$. The time response of the two pyroglutamyl Aß variants showed that $Aß_{PE3-40}$ and $Aß_{PE11-40}$ are capable of much higher aggregation rate than does $Aß_{1-40}$.

Meanwhile, the aggregation propensities of both AD and NA mixtures with the three individual Aß variants were measured. In Fig. 3a, the three immobilized Aß variants interacting with AD mixture shows that $Aß_{PE3-40}$ has a highest aggregation rate and $Aß_{PE11-40}$ has a

relatively lower aggregation rate. In Fig. 3b, the three immobilized Aß variants interacting with NA mixture show that $Aß_{PE3-40}$ has a highest aggregation rate, but this time response just a little higher than does $Aß_{PE11-40}$. Both two mixtures, AD and NA, revealed a lowest aggregation rate with $Aß_{1-40}$.

4. Discussion

In ThT binding assay, the three studied Aß variants show that the more charges the N-terminal pyroglutamyl-containing Aß peptides lose in the N terminus, the peptides have a higher amount of ß-pleated sheet secondary structure. Thereby, $Aß_{PE11-40}$ has a highest quantity of ß-pleated sheet structure and $Aß_{1-40}$ has a least quantity of this specified structure. Since the lose of three charges for $Aß_{PE3}$ and six charge for $Aß_{PE11}$ could alter their conformational properties and make them more hydrophobic to forward amyloid formation. In addition, The N-terminal glutamic acid residues of Aß peptides develop pyroglutamyl species after post-translational modification making these peptides less susceptible to further proteolysis (23). The resistance to proteolysis of pyroglutamyl Aß peptides, $Aß_{PE3}$ and $Aß_{PE11}$, probably results in a varying degree of accumulation relative to other N-terminally truncated pyroglutamyl Aß showing in neuritic plaques and in diffuse plaques. However, AD mixture in ThT binding assay containing a high $Aß_{PE3-40}/Aß_{PE11-40}$ composition ratio revealed a much higher quantity of ß-pleated sheet structure. This is even higher than does $Aß_{PE11-40}$ alone. The enhanced aggregation mechanism is not clear; one possible interpretation is that $Aß_{PE3-40}$ in AD mixture may be capable of a positive synergistic effect in promoting turnover of conformational change. By contrast, NA mixture containing a low $Aß_{PE3-40}/Aß_{PE11-40}$ composition ratio shows a low quantity of ß-pleated sheet secondary structure by comparing with the three tested Aß variants. This is even less than does $Aß_{PE3-40}$ alone. In contrast to AD mixture, the role of $Aß_{PE3-40}$ in NA mixture could be a negative synergistic effect to prohibit the formation of amyloid. The aggregation propensity of pyroglutamyl-containing Aß peptides is mainly due to a stabilized formation of ß-pleated sheet secondary structure (13), however, the composition ratio should be taken into account. In this study, the ThT fluorescence binding assay demonstrated that the two pyroglutamyl-containing Aß variants have relatively higher amount of ß-pleated sheet amyloid than $Aß_{1-40}$. In addition, by varying the composition ratio of pyroglutamyl Aß variants in the tested mixtures can produce different synergistic effects to change the depositability of Aß mixtures.

Previous ThT binding assay is used to differentiate the quantity of ß-pleated sheet secondary structure of the three Aß variants. It can be used to interpret the enhancement in conformational transition by the composition ratio of the composed three Aß variants in the tested mixtures. In order to provide the binding kinetics of AD and NA mixtures with the three studied Aß variants, SPR kinetics assay was analyzed which can illustrate the differentiation in aggregation behaviors of the three Aß variants with AD and NA mixtures.

SPR kinetics assay displayed that the order of aggregation rates of the three Aß variants is correspond to the quantity of ß-pleated sheet structure of the Aß variants. This suggests that intra- and intermolecular interactions between hydrophobic parts of the Aß sequence leads to the formation of Aß aggregates. The peptide by lose of charge repulsion and stabilized ß sheet structure can obviously enhance aggregation rate (24). However, this aggregation behavior cannot be applied directly to the tested mixtures. Among the three tested Aß variants, both AD and NA mixtures have a highest aggregation rate with $Aß_{PE3-40}$, not the more hydrophobic $Aß_{PE11-40}$. In addition, AD mixture has a much higher aggregation rate with $Aß_{PE3-40}$ than with $Aß_{PE11-40}$. This may explain that AD mixture has a high $Aß_{PE3-40}/Aß_{PE11-40}$ composition ratio. By contrast, NA mixture shows a similar aggregation rate with both $Aß_{PE3-40}$ and $Aß_{PE11-40}$. This may explain that NA mixture has a low $Aß_{PE3-40}/Aß_{PE11-40}$ composition ratio.

In this study, we found that the elevated $Aß_{PE3-40}/Aß_{PE11-40}$ composition ratio can provide positive synergistic effect for the formation of ß–pleated sheet secondary structure and both two mixtures have highest aggregation rate with A $_{PE3-40}$. These results suggest that higher composition of $Aß_{PE3-40}$ can form more amyloidogenic structure and higher affinity to aggregate with pathogenic Aß mixture. $Aß_{1-40}$ has less two hydrophobic C-terminal alanine and isoleucine residues than full-length $Aß_{1-42}$ resulting in a lower aggregation propensity. A pronounced elevation of only $Aß_{1-40}$ does not lead to plaque formation but can actually really retard the deposition of $Aß_{1-42}$ in the brain (25). If $Aß_{1-40}$ is mixed with a high $Aß_{PE3-40}/Aß_{PE11-40}$ composition ratio, that can result in larger pathogenic plaques. Therefore, an adequate control on the pyroglutamyl-containing Aß variants and the composition ratio can be used to define therapeutic strategy of AD.

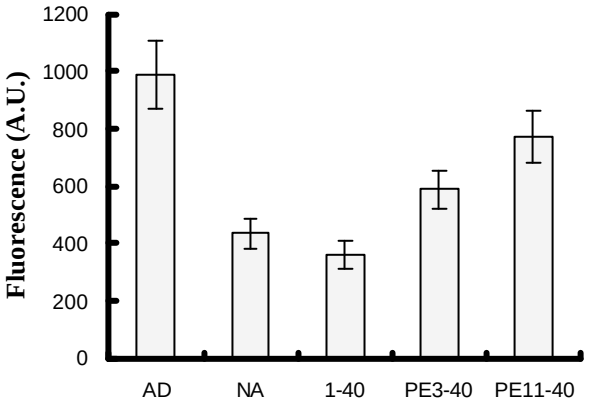

Fig. 1. Thioflavine T binding assay of $Aß_{1-40}$, $Aß_{PE3-40}$, $Aß_{PE11-40}$, and two mixtures, MD and MA. Data are expressed as fluorescence intensity in arbitrary unit as mean values ± S.D. measured from three experiments.

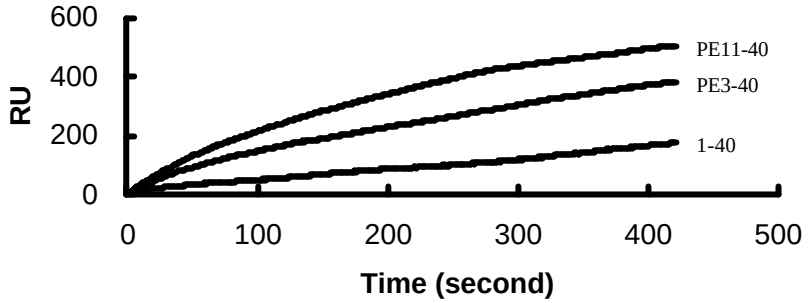

Fig.2. SPR analysis of the aggregational kinetics of $A\beta_{1-40}$, $A\beta_{PE3-40}$, and $A\beta_{PE11-40}$. After 7mins of polymerization, $A\beta_{PE11-40}$ revealed the highest aggregation rate, $A\beta_{PE3-40}$ is next, and $A\beta_{1-40}$ is lowest.

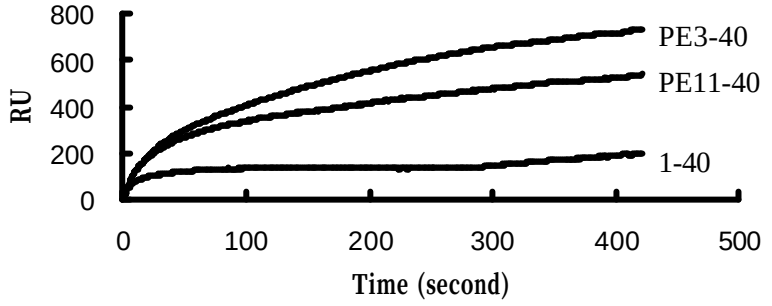

(a)

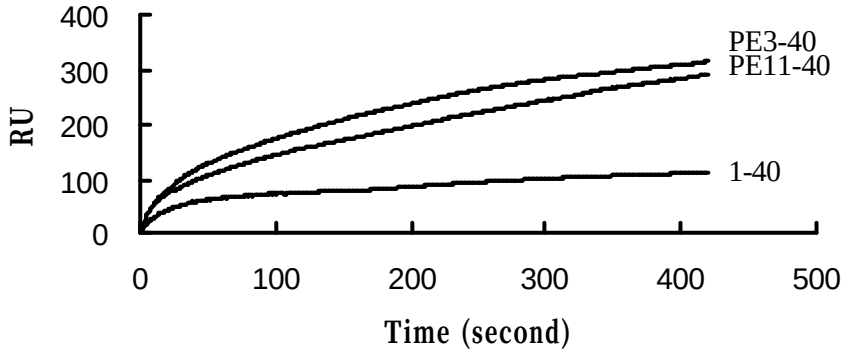

(b)

Fig.3 SPR analyses of the aggregational kinetics of mixtures (a) AD, (b) NA interact with $A\beta_{1-40}$, $A\beta_{PE3-40}$, and $A\beta_{PE11-40}$, respectively. $A\beta_{PE3-40}$ displayed a highest aggregation rate with both AD and NA mixtures. To compare with $A\beta_{PE3-40}$, $A\beta_{PE11-40}$ displayed a similar aggregation rate with NA mixture.

References

1. Selkoe, D. J. (1996) Amyloid ß-protein and the genetics of Alzheimer' s disease, *J. Biol. Chem.* 271, 18295–18298.
2. Selkoe, D. J. (2001) Alzheimer' s disease: genes, proteins, and therapy, *Physiol. Rev.* 81, 741-766.
3. Wisniewski, T., Ghiso, J., Rogers, J. (1994) Alzheimer' s disease and soluble Aß, *Neurobiol. Aging* 15, 143-152.
4. Haass, C., Lemere, C. A., Capell, A., Citron, M., Seubert, P., Schenk, D., Lannfelt, L., Selkoe, D. J. (1995) The Swedish mutation causes early-onset Alzheimer's disease by -secretase cleavage within the secretory pathway, *Nature Med* 1, 1291-1296.
5. Esler, W. P., Wolfe, M.S. (2001) A portrait of Alzheimer secreases- new features and familiar faces, *Science* 293, 1449-1454.
6. Rogers, J., Cooper, N. R., Websters, N. R., Schultz, J., McGeer, P. L., Styren, S. D., Civin, W. H., Brachova, L., Bradt, B., Ward, P. (1992) Complement activation by beta-amyloid in Alzheimer disease, *Proc. Natl. Acad. Sci. U.S.A.* 89, 10016-10020.
7. Turner, R. S., N. Suzuki, A. S. C. Chyung, S. G. Younkin, Lee, V. M.-Y. (1996) Amyloids beta(40) and beta(42) are generated intracellularly in cultured human neurons and their secretion increases with maturation, *J. Biol. Chem.* 271, 8966-8970.
8. Walsh, D. M., Klyubin, I.,, Fadeeva, J. V., Cullen, W. K., Anwyl, R., Wolfe, M. S., Rowan, M. J., Selkoe, D. J. (2002) Naturally secreted oligomers of amyloid beta protein potently inhibit hippocampal longterm potentiation in vivo, *Nature* 416(6880), 535-539.
9. Walsh, D. M., Hartley, D. M., Kusumoto, Y., Fezoui, Y., Condron, M. M., Lomakin, A., Benedek, G. B., Selkoe, D. J., Teplow, D. B. (1999) Amyloid ß-Protein Fibrillogenesis, *J. Biol. Chem.* 274, 25945-24952.
10. Saido, T. C., Yamao-Harigaya, W., Iwatsubo, T., Kawashima, S. (1996) Amino- and carboxyl-terminal heterogeneity of beta-amyloid peptides deposited in human brain, *Neurosci Lett* 215, 173-176.
11. Saido, T. C., Iwatsubo, T., Mann, D. M., Shimada, H., Ihara, Y., Kawashima, S. (1995) Dominant and differential deposition of distinct beta-amyloid peptide species, A beta N3(pE), in senile plaques. *Neuron* 14, 457-466.
12. Iwatsubo, T., Odaka, A., Suzuki, N., Mizusawa, H., Nukina, N., and Ihara, Y. (1994) Visualization of A beta 42(43) and A beta 40 in senile plaques with end-specific A beta monoclonals: evidence that an initially deposited species is A beta 42(43). *Neuron* 13, 45–53.
13. He, W., Barrow, C. J. (1999) The Aß 3-pyroglutamyl and 11-pyroglutamyl peptides found in senile plaque have greater beta-sheet forming and aggregation propensities in vitro than full-length Aß. Biochemistry 38, 10871-10877.
14. Russo, C., Violani, E., Salis, S., Venezia, V., Dolcini, V., Damonte, G., Benatti, U., D'Arrigo, C., Patrone, E., Carlo, P., Schettini, G. (2002) Pyroglutamate -modified amyloid ß-peptides- AßN3(pE)-strongly affect cultured neuron and astrocyte survival. *J. Neurochem.* 82, 1480-1489.
15. Piccini, A., Russo, C., Gliozzi, A., Relini, A., Vitali, A., Borghi, R., Giliberto, L., Armirotti,

A., D' Arrigo, C., Bachi, A., Cattaneo, A., Canale, C., Torrassa, S., Saido, T. C., Markesbery, W., Gambetti, P., Tabaton, M. (2005) ß-Amyloid is different in normal aging and in Alzheimer disease. *J. Biol. Chem.* 280, 34186–34192.

16. Dahlgren, K. N., Manelli, A. M., Stine, W. B., Jr., Baker, L. K., Krafft, G. A., LaDu, M. J. (2002) Oligomeric and fibrillar species of amyloid-ß peptides differentially affect neuronal viability. *J. Biol. Chem.* 277, 32046-32053.
17. Hardy, J., Selkoe, D. J. (2002) The amyloid hypothesis of Alzheimer' s disease: progress and problems on the road to therapeutics. *Science* 297, 353–356.
18. Stine, W. B., Jr., Dahlgren, K. N., Krafft, G. A., and LaDu, M. J. (2003) In vitro characterization of conditions for amyloid-ß, peptide oligomerization and fibrillogenesis. *J. Biol. Chem. 278*, 11612-11622.
19. Johnsson, B., Lofas, S., Lindquist, G. (1991) Immobilization of proteins to a carboxymethyldextran-modified gold surface for biospecific interaction analysis in surface plasmon resonance sensors. *Anal. Biochem.* 198, 268–277.
20. LeVine, H. (1993) Thioflavine T interaction with synthetic Alzheimer's disease ß-amyloid peptides: Detection of ß amyloid aggregation in solution. *Protein Sci* 2, 404-410.
21. McDonnell, J. M. (2001) Surface plasmon resonance: towards an understanding of the mechanisms of biological molecular recognition. *Curr. Opin. Chem. Biol.* 5,572-577.
22. Harper, J., Lansbury, P. J. (1997) Models of amyloid seeding in Alzheimer's disease and scrapie: mechanistic truths and physiological consequences of the time-dependent solubility of amyloid proteins. *Annu Rev Biochem.* 66, 385-407.
23. Sahasrabudhe, S. R., Brown, A. M., Hulmes, J. D., Jacobsen, J. S, Vitek, M. P., Blume, A. J., Sonnenberg, J. L. (1993) Enzymatic generation of the amino terminus of the ß-amyloid peptide. *J. Biol. Chem.* 269, 16699–16705.
24. Schlenzig, D., Manhart, S., Cinar Y., Kleinschmidt, M., Hause, G., Willbold, D., Funke, S. A., Schilling, S., Demuth, H.-U. (2009) Pyroglutamate formation influences solubility and amyloidogenicity of amyloid peptides. Biochemistry 48 , 7072–7078.
25. McGowan, E., Pickford, F., Kim, J., Onstead, L., Eriksen, J., Yu, C., Skipper, L., Murphy, M. P., Beard, J., Das, P., Jansen, K., DeLucia, M., Lin, W.-L., Dolios, G., Wang, R., Eckman, C. B., Dickson, D. W., Hutton, M., Hardy, J., Golde, T. (2005) Aß42 Is Essential for Parenchymal and Vascular Amyloid Deposition in Mice. *Neuron* 47, 191-199.

Doctor's Mission

Nie Wei*
Hospital Management Institute, Zhengzhou University, Zhengzhou 450052

Received April 1, 2009

Abstract
Doctor's Mission is an important concept of medicine, and an important management concept. Mission is defined as the first modern management task. This author, through serious thinking for years, held that, Doctor's Mission is to cure the sickness to save the patient, specifically speaking, cure the sickness to save the patient, conduct clinical medicine education and medical science research, in total three aspects and three levels. According to mission's concept, doctors are divided into four kinds, namely, clinical, teaching, scientific research and omnipotent. This discussion intended to promote researches on mission by all types of doctors, hospital departments and hospitals and make it more operational sense of mission. [Life Science Journal. 2009; 6(3): 86 – 88] (ISSN: 1097 – 8135)

Key words: mission; doctor; hospital management

What is the Doctor's Mission? This is an issue worth seriously considering and studying. Doctor's Mission refers to the fundamental reason for the existence of doctors, also means major responsibilities the doctors assume. For thousands of years, in terms of Doctor's Mission there were a lot of descriptions, such as "health guard", "angel in white", "heal the wounded and rescue the dying, practice medicine in order to help the people" and so on, but we have not yet found an accurate definition. Through careful and long-term thinking, this author held: Doctor's Mission is to cure the sickness to save the patient. This is a summary of Doctor's Mission, which consists of three aspects and three levels, namely, medical science research, medical education and diagnosis and treatment of patient. In accordance with the definition of Doctor's Mission, doctors can be divided into four types, namely: clinical, teaching, scientific research and omnipotent.

Doctor's Mission and significance

Modern Chinese Dictionary reads: "[Doctors] have knowledge of medicine, and take treating patients as career." [Mission] means order, and important responsibility". According to definitions of doctor and mission, together with this author's thinking, Doctor's Mission should be defined as "cure the sickness to save the patient". The so-called curing the sickness to save the patient means diagnosis and treatment of patients' diseases, saving the patients. The existence of the value of each doctor, the purpose of each patient to see a doctor in a hospital, the objective of each medical college to train doctors, aim at diagnosis and treatment of diseases and save patients. Doctor's Mission does not lie in protection of human health, or provision of disease prevention. This is because health of people is affected by social, psychological, genetic quality, living habits and cultural quality. It is just a goal. Nobody can guarantee health. Health is a long-term practice and the result of many factors. Prevention of disease is another school, namely, within research scope of prevention medicine, instead of that of doctors. Doctors can provide some knowledge of disease prevention, but do not have such a mission.

The definition of Doctor's Mission is of medical, social, economic, legal and ethical significance. In term of medical significance, it plays an important role in medical education, doctor training and medical practices and hospital management. Doctor's Mission is the highest standard for medical education. Correct grasping the doctor's sacred mission, using Doctor's Mission to guide medical education and medical students, making it a guide for medical education and medical students, will surely improve medical education purposes and diagnosis and treatment of diseases. Therefore, Doctor's Mission is of great significance for doctors' improvement in capacities. In order to become good doctors, young doctors must first improve their capacity "to cure the sickness to save the patient", which is the direction and guide to actions. Doctor's Mission has the following significance in medical behaviors and hospital management: to begin with, Doctor's Mission plays a role of standardizing medical behaviors and measuring medical quality standards. Doctors' behavior and performance appraisal must focus on "curing the sickness to save the patient", to which, all other standards, whether political, economic or religious, must be subordinated to. On the other hand, Doctor's Mission determines the mission of hospitals and other medical institutions. In fact, Doctor's Mission lies in that the mission of medical institutions are to be achieved and completed by doctors instead of their managers and supporting personnel. Last but not the least, Doctor's Mission specifies the direction for medical institutions to strengthen management and improve the medical standard. Management activities of medical institutions must focus on Doctor's Mission. The improvement of capacities of doctors to cure the sickness to save the patient will surely improve the medical standard. Therefore, hospitals must have their management focus on curing the sickness to

* corresponding: E-mail: Niewei@zzu.edu.cn

save the patient.

In terms of its social significance, Doctor's Mission theory formation can guide the people to have a correct understanding of doctor-patient relationship, reduce doctor-patient conflicts, and promote doctor-patient relationship with doctors' dedication to mission and broad masses of the people respecting doctors. Doctor's Mission determines the right doctor-patient relationship, namely, doctors carefully cure the sickness to save the patient, patients and their families respect doctors for their hard work to complete their mission. Doctor-patient relationship is an important social relation, the right doctor-patient relationship must be conducive to the promotion of a harmonious society. Especially at present, correct understanding of Doctor's Mission is of practical significance to correctly handle the more complicated doctor-patient contradictions and doctor-patient relationship and form a harmonious and stable doctor-patient relationship.

In terms of its economic significance, since it is a cause to cure the sickness to save the patient, it can effectively protect human resources, play the role of protecting productivity, promoting and safeguarding national economic sustainable development. With the economic development and the arrival of aging, it is more important and urgent to improve the capacity to cure the sickness to save the patient and to protect the important factors of production of human development and adequate quality of human resources.

In terms of its legal significance, it should be an important yardstick to judge whether legislative principles and medical behaviors to formulate health-related laws are correct. Whether doctors cure the sickness to save the patient should be the basic standard to judge whether they are legal, correct or wrong. If doctors' behaviors are to fulfill their sacred mission, they should be protected by law, and otherwise they should not be protected by law. Behaviors no to cure the sickness to save the patient and cause any losses to the patient should be severely punished by law.

In terms of its ethical connotations, Doctor's Mission should be taken as the highest standard for doctors' ethics and the supreme goal for medical ethic assessment. The doctor's ethical and moral standard mean the highest ethical standard, aiming at curing the sickness to save the patient and should be taken as the most sacred ethics in human history since doctors assume the sacred mission to cure the sickness to save the patient.

Doctor's Mission has three connotations

Doctor's Mission consists of three connotations. The first is diagnosis and treatment of patients, referring to the medical behaviors doctors must have, namely, diagnosis and treatment activities for each patient. Through the diagnosis and treatment of each patient to realize their sacred mission of "cure the sickness to save the patient", which is the basic capacity that every doctor must possess. Without such capacity, a doctor could not be called doctor, and cannot become a legal practitioner. This is the first connotation of Doctor's Mission.

The second refers to that the doctors are engaged in treatment, and clinical medicine education. They complete the diagnosis and treatment mission and training of new doctors to conduct diagnosis and treatment, increase in the number of doctors and improvement of the quality and heritage from generation to generation. The clinical medicine education includes clinical medicine education with record of formal schooling, nurturing and training of younger doctors and in-service doctors. This is the second connotation of Doctor's Mission.

The third refers to that doctors are engaged in diagnosis and treatment and at the same time engaged in medical science research. This is a medical science and technology innovation activity, with its new theory, new technology, new discovery and new product benefiting a number of patients or a category of patients, and numerous patients in the world. This is the third connotation of Doctor's Mission.

Doctor's Mission has three levels

Doctor's Mission can be divided into three levels. The first level is the diagnosis and treatment, and clinical work, which are the doctor's basic mission. Every doctor needs to complete legal practice procedures in order to be engaged in lawful medical activities. If a doctor is unable to conduct diagnosis and treatment, he/she will not be regarded as a doctor. A doctor is surely to be able to conduct diagnosis and treatment, and achieve the capacity to implement the basic mission. However, in terms of different professions and different levels, doctors have different missions. The missions of department of cardiovasology and cardiovascular surgery are different because they conduct different diagnosis and treatment of different diseases, rescue different patients. It is necessary to carefully define each Doctor's Mission, which is very important and not easy. In fact, it is important for any institution to define the mission of each and every member, which is a very critical basis for management.

The second level is clinical medicine teaching. In addition to diagnosis and treatment, doctors take advantage of their medical expertise and professional skills to cultivate more and better new doctors through clinical medicine teaching, so as to provide more diagnosis and treatment, make more doctors cure the sickness to save the patient, fulfill the sacred mission. This should be a higher level mission.

The third level is the medical science research, which is the highest level of Doctor's Mission, since the results of medical research institutes make more patients, even one or several categories of patients receive diagnosis and treatment. Such medical scientific research activities often solve serious problems or complex diseases. The consequent cutting-edge theory, technology, methods and products make the greatest contributions to diagnosis and treatment. Therefore, it is the highest level of mission.

Categories of doctors according to Doctor's Mission

According to Doctor's Mission, doctors can be divided into four categories, namely, clinical, teaching, scientific research and omnipotent.

Clinical doctor

The clinical doctor is mainly engaged in diagnosis and treatment, working in the first line. In China, the majority of doctors working at hospitals at city level or below belong to this category. They work hard in the first line, playing a major role in people's basic medical insurance. What we call "general doctor", "community doctor", "barefooted doctor" are mostly clinical doctors. Clinical doctors occupy the largest portion of doctors, and are the main forces of diagnosis and treatment. Increase in the number of clinical doctors and improvement of their diagnosis and treatment capacities are an essential solution to the current prevalence of difficulties and high cost in medical treatment.

Teaching doctor

Teaching doctor, in addition to his clinical work, completes medical education tasks. To "cure the sickness to save the patient" and fulfill a higher level of mission, it is necessary to train more and better new doctors so as to meet the demands of more patients for diagnosis and treatment, and make the medical cause develop from generation to generation. Such doctors should be engaged in clinical and teaching work, they should study and work for the completion of these two missions. The teaching doctors train more and better new doctors, offering an essential solution to the current prevalence of difficulties and high cost in medical treatment.

Scientific research doctor

Scientific research doctors, in addition to clinical work, complete medical scientific research tasks, and undertake medical scientific research missions. As is known to everyone, medical scientific researches are very hard, very dangerous and sometimes life-threatening innovation activities. To "cure the sickness to save the patient", they keep inventing, discovering and creating, with their medical scientific research results benefiting more patients. Such doctors often have opportunities to become medical masters and celebrities. At all times and in all over the world, medical masters and celebrities are almost entirely famous scientific research doctors.

Omnipotent doctor

Omnipotent doctors undertake the tasks of above-mentioned three categories of doctors, namely, clinical, teaching and research. Omnipotent doctors are the best talents and model doctors, making the greatest contributions to the medical cause and the greatest achievements. Most of such doctors work at universities and research institutions. They have the most opportunities to become celebrities. Academicians of the medical profession in our country are mostly of this category.

Discussions on categories of doctors

In accordance with Doctor's Mission, doctors are divided into four categories, which is a man-made classification with the purpose of clearer expression of Doctor's Mission. The four categories are equal. A qualified doctor, no matter which categories he/she belongs to, works hard to "cure the sickness to save the patient" and completes the sacred mission. They are worthy of respect and admiration. At the same time, we must admit that, different people have different aspirations and different people have different abilities. We respect each and every doctor for his hard work, especially those who accomplish more "curing the sickness to save the patient" mission. On the basis of their contributions and dedication, they will receive better treatment and higher honors, which is in line with the requirements and social allocation principles. Most doctors would like to make greater contributions and become omnipotent doctors with teaching and research capacities. However, it is impossible for all doctors to become omnipotent doctors, neither in terms of conditions nor in terms of opportunities. Therefore, we should develop such a consensus: as long as they can complete the basic mission of diagnosis and treatment, they are angels in white worthy of respect and reputation as good doctors.

References

1. Institute of Linguistics, Chinese Academy of Social Sciences [China]-Revision of Contemporary Chinese Dictionary, Beijing: Commerce and Trade Press, April 1997.
2. Peter·Drucker [the United States of America], Managing the Non-Profit Organization Beijing: Mechanical Industry Press, September 2007.
3. Peter Drucker [the United States of America]. The Practice of Management Beijing: Mechanical Industry Press, January 2006.

Study of Erroneous Diagnoses of Kawasaki Disease

Meimei Zhang

The Fifthly Affiliated Hospital of Zhengzhou University, Zhengzhou, Henan 450001, China

Received May 10, 2008

Abstract

Kawasaki's disease (KD) is an acute febrile illness of infants and children in which redness of the mucous membrane; skin and tongue are associated with swelling and desquamation of the hands and feet. Forty-four samples of the erroneous diagnosis of Kawasaki disease were studied. The coronary artery pathological change was found very few in regular diagnosis. On the other hand, the most often erroneous diagnoses of Kawasaki disease being as hypersensitivity vasculitis, upper respiratory tract infection, cervical lymphadenopathy, acute nephritis and scarlatina are learned and demonstrated in this report. [Life Science Journal. 2009; 6(3): 89 – 92] (ISSN: 1097 – 8135)

Keywords: Kawasaki's disease (KD); febrile illness; mucous membrane; diagnosis; hypersensitivity vasculitis; cervical lymphadenopathy; acute nephritis; scarlatina

1. Introduction

Some signs include swollen lymph nodes of the neck, redness and swelling of the eyes, sores in the mouth (stomatitis) and swollen lips (chelitis). After a week or two the skin of the hands and feet begin to peel starting around the nails. Upwards of 20% of patients develop coronary artery complications, however most patients have uneventful recoveries without any long term problems. The peak age of incidence is 1 year of age with a mean of 2.6 years and it is uncommon over 8 years of age. The cause of Kawasaki's disease (KD) is not known and is generally seen during the winter and spring of the year. There are 3 phases of the disease. Phase I: Abrupt onset of fever, lasting around 12 days or so, followed by most of the principal symptoms of the disease condition. This phase develops a red rash usually first seen on the palms and soles that then spreads to involve the torso within a couple days. The most common appearance is a hive-like rash; however it may also resemble measles (morbilliform rash), erythema multiforme or a scarletina like rash. It is more impressive on the hands and feet than the torso and the hands and feet generally develop some swelling as well. Phase II: This is a subacute phase that can last around 30 days during which fever, arthritis and arthralgia, thrombocytosis, desquamation, and carditis generally resolve. This is the phase with the highest risk of sudden death. The desquamation occurs in this phase with significant peeling of the hands and feet starting at the tips of the digits. In addition most of the dangerous cardiac abnormalities occur such as dysrhythmias, heart failure and left ventricular dysfunction. Phase III: This is the convalescent period and generally starts 8-10 weeks after the beginning of the illness; it basically starts when all symptoms resolve and lasts until all tests have returned to normal. Icelandic Moss (Cetraria islandica) has been used to treat inflammation and dryness of the pharyngeal mucosa in the naturopathy for many years. It contains substances with protective and antiinflammatory effects for the oral mucosa [1]. It was reported that the patient with advanced gastric cancer with Virchow's lymph node metastasis who successfully received curative resection following neoadjuvant chemotherapy with a single oral anticancer drug [2].

The diagnosis of KD depends on several criteria. First there must be an elevated temperature of greater than 102.50 F for at least 5 days; then 4 out of 5 of the following:

Bilateral conjunctival injection (redness of eyes).

At least one swollen lymph node in the anterior cervical lymph nodes (front of neck).

A widespread scarlet fever like erythroderma (redness of

the skin), with areas of sharply marginated rash, deeply erythematous maculopapular rash and iris lesions.

At least one of the following: erythema of the palms and soles, edema of the hands and feet, generalized desquamation around the tips of the fingers and toes.

At least one of the following changes found in and around the mouth: injected/fissured lips, injected pharynx (back of the mouth) and "strawberry" tongue (a bright red appearance of the tongue).

The majority of people with KD recover without long term complications. However about 20% of patients develop some form of vascular involvement such as: coronary artery aneurysms, myocarditis, heart attack (myocardial infarction), peripheral vascular occlusion, small bowel obstruction or stroke. Historically about 1% of patients die from complications of KD.

Early diagnosis is critical so as to try and prevent cardiovascular complications. It is generally accepted that failed infrainguinal bypass with prosthetic material significantly compromises arterial run off, which may limit future revascularization. It is well known that the negative consequences of early vein graft thrombosis are limited, but the effect of failed peripheral angioplasty on the distal vasculature is poorly studied [3]. It was reported that A coronary stent may be lost in the peripheral or visceral arterial system with an incidence ranging from 0.9 to 8.4%, however, a limb or organ ischemia after stent migration is very uncommon [4]. Patients should be hospitalized during the phase I period to monitor for complications. The primary treatment is aspirin 100 mg/kg/day until the fever has passed, after which the dose is reduced to 5-10 mg/kg/day until all lab tests return to normal. High dose intravenous gamma globulin (IVIG) has been used to reduce the risk of coronary aneurysms and myocardial infarction. KD is also named as mucocutaneous lymph node syndrome found by Dr. Kawasaki in 1967 at Japan. The special pathognomics of KD include coronary vasculitisand coronary vasculitis. The male to female ratio of morbidity of KD is about 1.5 and 80% of the patients being under five years old. The mortality is 0.3% to 0.5%. Rate of recrudesce is about 3%.

2. Data acquisition and analysis

Forty-four samples were collected where 30 are males and 14 females. The ages of the patients were between 3 months to seven years old. The male to female ratio is 2.1. Thirty two samples are for the ages between 1 year to 3 years old, 72.7％ of the total forty four samples. In Table I, it depicts the clinical manifestation of the 44 samples.

Table 1: List of KD-clinical manifestation

KD-clinical manifestation（n＝44）	
Description	Percentage
Fever, 7-15days averagely 9.4days	44（100%）
Edema, hands and feet	39（88.6%）
Edema, hands and feet in seven days	41（93.2%）
Bulbus oculi tunica in seven days	44（100%）
chapped skin in seven days	44（100%）
scaly rash	34（77.3%）
Anus decrustation	17（38.6%）
Neck lymph gland swelling	40（90.9%）
Proteinuria	13（29.5%）
Leukocytosis	33（75%）
Thrombocythemia	34（77.3%）

3. Erroneous Diagnoses of Kawasaki Disease

Erroneous diagnoses of Kawasaki Disease may happen due to the clinical manifestations look the same with other diseases. The possibilities of the erroneousness include upper respiratory tract infection, cervical lymphadenopathy, acute nephritis, scarlatina and medical rash etc. Table II lists several erroneous diagnoses of Kawasaki Disease in our study.

Table 2: Erroneous Diagnoses of Kawasaki Disease

Erroneous Diagnoses	Specimen (percentage)
upper respiratory tract infection	21 (47.7%)
cervical lymphadenopathy	3 (6.8%)
acute nephritis	1 (2.3%)
medical rash	2 (4.5%)
scarlatina	1 (2.3%)
pulmonitis	1 (2.3%)

All the patients listed were cured by administration with oral aspirin, cortex and IVID.

4. Discussion

Heart failure (HF) decompensation continues to account for approximately 1 million hospitalizations per year in the United States. Pulmonary congestion is the hallmark sign of worsening HF [5].

The origin of disease of KD is still not clear. After the massive epidemiology research, a preferred thought is that KD is an immunity disease caused by one kind or many kinds of pathogenic microorganism that enters into human immune system. Although KD has the self-recovery tendency, its coronary artery expansion and the coronal aneurism formation rate reaches as high as 25% to 40% [7]. Kawasaki disease is an acute self-limited vasculitis of childhood that is characterized by fever, bilateral nonexudative conjunctivitis, erythema of the lips and oral mucosa, changes in the extremities, rash, and cervical lymphadenopathy. Coronary artery aneurysms or ectasia develop in approximately 15% to 25% of untreated children and may lead to ischemic heart disease or sudden death [6]. Because of being deficient in the specificity diagnosis standard, early diagnosis receives certain limitation. The rate of erroneous diagnosis appears very high. Recommendations for the initial evaluation, treatment in the acute phase, and long-term management of patients with Kawasaki disease are intended to assist physicians in understanding the range of acceptable approaches for caring for patients with Kawasaki disease. The ultimate decisions for case management must be made by physicians in light of the particular conditions presented by individual patients [7].

Group case of illness gets reliable diagnose in three days being only 16.25%. Misdiagnoses diseases reach to six different kinds of erroneous diagnosis. The upper respiratory tract infection is a common and frequently-occurring disease to be in erroneous diagnosis of KD. The early symptoms including high fever, cornea hyperemia red, cervical lymphadenopathy must be distinct from KD [8,9]. Specifically, diagnoses of KD may show similarity of the upper respiratory tract infection skin rash, cornea hyperemia only happens in single side and echocardiogram inspection lacks of the confirmation of coronary artery harm etc. Scarlet fever may be another erroneous diagnosis for similar clinical early symptoms. The major symptoms including the skin rash, rubra must be distinct from KD. Basically, scarlatina should have the contact history. The skin rash of scarlatina may have its characteristic value. Etiology inspection can exhibit a group of second grade hemolytic streptococcus as the dissimilarity.

The childhood reheumatoid arthritis can be seen in 2-4 years old babies and infants. The symptom begins

with high fever, accompanies by polymorphic skin rash, lymph node tumescent and heart damage. None hand and foot rigid dropsy with typical coronary artery damage can be found in our cases study. However, mainly because the acquisition of information being in short of analysis of the early echocardiogram, the diagnosis may not be able to find the temporary coronary artery expands. Most of the cases, patients recovered in 30 days

Our study revealed especially that KD needs a long-term observation. KD has the peak contract to damage the coronary artery in course of 15 days. Patients leave the hospital may still keep most of the trouble of having coronary artery expansion and the aneurism danger. Early diagnosis, treatment, close observation of the patients enhance the KD curing rate as well as reducing the possibilities to damage the coronary artery.

References

1 Kempe, C., Gruning, H., Stasche, N. and Hormann, K. (1997) [Icelandic moss lozenges in the prevention or treatment of oral mucosa irritation and dried out throat mucosa]. Laryngorhinootologie **76**, 186-188

2 Iwazawa, T., Kinuta, M., Yano, H., Matsui, S., Tamagaki, S., Yasue, A., Okada, K., Kanoh, T., Tono, T., Nakano, Y., Okamoto, S. and Monden, T. (2002) An oral anticancer drug, TS-1, enabled a patient with advanced gastric cancer with Virchow's metastasis to receive curative resection. Gastric Cancer **5**, 96-101

3 Joels, C. S., York, J. W., Kalbaugh, C. A., Cull, D. L., Langan, E. M., 3rd and Taylor, S. M. (2008) Surgical implications of early failed endovascular intervention of the superficial femoral artery. J Vasc Surg **47**, 562-565

4 Siani, A., Siani, L. M., Mounayergi, F. and Baldassarre, E. (2008) Lower limb ischemia after migration of a coronary artery stent into the femoral artery. Interact Cardiovasc Thorac Surg **7**, 447-448

5 Daleiden-Burns, A. and Stiles, P. (2007) Proactive monitoring: implications of implantable devices for future heart failure management. Crit Care Nurs Q **30**, 321-328

6 Newburger, J. W., Takahashi, M., Gerber, M. A., Gewitz, M. H., Tani, L. Y., Burns, J. C., Shulman, S. T., Bolger, A. F., Ferrieri, P., Baltimore, R. S., Wilson, W. R., Baddour, L. M., Levison, M. E., Pallasch, T. J., Falace, D. A. and Taubert, K. A. (2004) Diagnosis, treatment, and long-term management of Kawasaki disease: a statement for health professionals from the Committee on Rheumatic Fever, Endocarditis and Kawasaki Disease, Council on Cardiovascular Disease in the Young, American Heart Association. Circulation **110**, 2747-2771

7. Wang HW. Questions of the cornary damages by Kawasaki disease. Journal of Chinese Pediatrics（21）10：730－731, 2006

8. http://www.nlm.nih.gov/medlineplus/ency/article/000989.htm

9. http://www.americanheart.org/presenter.jhtml?identifier=4634

Nature of genetic variants in the *BRCA1* and *BRCA2* genes from breast cancer families in Taiwan

Yuan-Ping Lin [1], Yi-Ling Chen[1], Hong-Tai Chang [2] and Steven Shoei-Lung Li [1*]

[1] *Institute of Biomedical Sciences, National Sun Yat-Sen University, Kaohsiung, Taiwan, ROC;* [2] *Department of Surgery, Kaohsiung Veterans General Hospital, Kaohsiung, Taiwan, ROC;* [3] *Graduate Institute of Medicine, Kaohsiung Medical University, Kaohsiung, Taiwan, ROC*

Received February 2, 2008

Abstract

A total of six families with two cases of breast cancer from southern Taiwan were identified, and the nature of genetic mutations was analyzed. One novel missense substitution of Gln1886Pro (A5885C), as well as one novel silent nucleotide change of A4806G at Thr1526, of the *BRCA2* gene was found in a breast cancer family. Four missense substitutions of Pro871Leu (C2731T), Glu1038Gly (A3232G), Lys1183Arg (A3667G) and Ser1613Gly (A4956G), and two silent nucleotide changes of T2430C at Leu 771 and T4427C at Ser1436 of the *BRCA1* gene, as well as one silent nucleotide change of T4035C at Val1296 of the *BRCA2* gene, were identified in five other breast cancer families. All of the *BRCA1* and *BRCA2* variations identified thus far in Taiwan are compared with those reported from China. [Life Science Journal. 2009; 6(3): 93 – 97] (ISSN: 1097 – 8135).

Keywords: *BRCA1*, *BRCA2*, variants, breast cancer, Taiwan

1. Introduction

Breast cancer is the most common malignancy among women. The *BRCA1* (MIM#113705) [Miki et al., 1994] and *BRCA2* (MIM#600185) [Wooster et al., 1995] genes are associated with inherited susceptibility to breast cancer, and the mutations in these two genes accounted for about 5-10% of all breast cancer cases [Szabo and King, 1997]. It is about twice as many have either a first-degree or a second-degree relative with breast cancer [Johnson et al., 1995]. The risk conferred by a family history of breast cancer has been assessed in both case-control and cohort studies, using volunteer and population-based samples, with generally consistent results [Pharoah et al., 1997]. Both males and females can inherit and transmit an autosomal dominant cancer predisposition. A male who inherits a cancer predisposition and shows no evidence of it can still pass the altered gene on to his sons and daughters.

BRCA1 and *BRCA2* are involved in a myriad of functions within cells including homologous DNA repair, genomic stability, transcriptional regulation and cell cycle control [Gudmundsdottir and Ashworth, 2006]. Nearly 2,000 distinct mutations and sequence variations in *BRCA1* and *BRCA2* have already been described. Approximately one in 400 to 800 individuals in the general population may carry a pathogenic mutation in *BRCA1* and *BRCA2* [Ford et al., 1995; Whittemore et al., 2004]. Our laboratory had previously reported the nature of mutations in the *BRCA1* and *BRCA2* genes from 18 breast cancer families in Taiwan [Li et al., 1999], and here we describe the nature of genetic variations in these two genes among six new breast cancer families in Taiwan.

2. Materials and methods

Samples

A total of six new families with two breast cancer cases from southern Taiwan were identified. The younger patients from each family were analyzed for the mutations at all exons and exon-intron junctions of the *BRCA1* and *BRCA2* genes, and the identified variations were confirmed from second patient and/or other members of each family.

DNA extraction/polymerase chain reaction

Genomics DNAs were isolated from peripheral blood lymphocytes by phenol/chloroform extraction method, and the DNA fragments were amplified using the previously published 48 and 58 PCR primer pairs for the *BRCA1* and *BRCA2* genes, respectively [Li et al., 1999].

*Corresponding Author: Steven Shoei-Lung Li
e-mail: lissl@kmu.edu.tw

Subcloning/DNA sequencing

The normal and variant alleles from the some heterozygotes were separately isolated by subcloning into the pUC19 vector (Fermentas, MD, USA). All fragments were sequenced on both strands. The sequencing reactions were performed with a dye-labeled terminators kit (Perkin-Elmer) using the cycle sequencing method. Both separation of DNA fragments and sequence analysis were performed in an ABI Prism 377 DNA sequencer.

3. Result

The clinical information of patients and the nature of genetic variations at the *BRCA1* and *BRCA2* genes from six new breast cancer families in Taiwan are summarized in Table 1 and Table 2.

Table 1. The clinical information of patients from six new breast cancer families in Taiwan

Family	Sample ID *	Age at diagnosis	Disease $	Stage	Histological type
A	AI 1	63	BC	Stage 1	Invasive ductal carcinoma
	AII 2	40	BC	Stage 1	Invasive ductal carcinoma
B	BII 1	53	BC	Stage 0	Intraductal carcinoma
	BII 2	43	BC	Stage 3a	Invasive ductal carcinoma
C	CII 1 #	—	BC	—	—
D	DI 2 #	—	BC	—	—
	DII 2	45	BC	Stage 1	Invasive ductal carcinoma
E	EIII 4	47	BC	Stage 2a	Invasive ductal carcinoma
F	FI 2 &	—	BC	—	—
	FII 1	50	BC	Stage 2a	Invasive ductal carcinoma

* Family: A—F; Generation: I—II; Age from oldest to youngest: 1—4. $ BC: breast cancer. # The patients were taken from external hospital, no information. & The patient was dead, no information.

Table 2. The nature of genetic variations at the BRCA1 and BRCA2 genes from 6 new breast cancer families in Taiwan

Sample ID*	Gene	Exon	Sequence variants	Amino acid change	The mutation site of family members
AII 2	BRCA2	11	A4806G	Thr1526	—
AII 2	BRCA2	11	A5885C	Gln1886Pro	—
BII 2	BRCA2	11	T4035C	Val1269	—
CII 1	BRCA1	13	T4427C	Ser1436	—
CII 1	BRCA1	16	A4956G	Ser1613Gly	Daughter CIII 1 is normal
DII 2	BRCA1	13	T4427C	Ser1436	—
DII 2	BRCA1	16	A4956G	Ser1613Gly	—
EIII 4	BRCA1	11	T2430C	Leu771	—
EIII 4	BRCA1	11	A3232G	Glu1038Gly	Sister EIII 5, EIII 7 have heterozygote mutation
EIII 4	BRCA1	13	T4427C	Ser1436	—
EIII 4	BRCA1	16	A4956G	Ser1613Gly	Sister EIII 1, EIII 2, EIII 3, EIII 5, EIII 6, EIII 7 have heterozygote mutation
#FII 1	BRCA1	11	C2731T	Pro871Leu	Son FIII2 has homozygote mutation; sister FII 5, 2 nieces FIII4, FIII10, and nephew FIII11 have heterozygote mutation
#FII 1	BRCA1	11	A3232G	Glu1038Gly	The same as above
#FII 1	BRCA1	11	A3667G	Lys1183Arg	The same as above

* Family: A—F; Generation: I—II; Age from oldest to youngest: 1—4. # These three BRCA1 mutations are on the same chromosome.

In the A family, the daughter had breast cancer diagnosed at age 40 years, and her mother had breast cancer diagnosed at age 63. Both patients had stage 1 invasive ductal carcinoma. One novel missense substitution of Gln1886Pro (A5885C), as well as one novel silent nucleotide change of A4806G at Thr1526, of the *BRCA2* gene was found to be heterozygous. In the B family, the younger sister had stage 3a invasive ductal carcinoma diagnosed at age 43, and her elder sister had stage 0 intraductal carcinoma diagnosed at age 53. Only one previously reported silent nucleotide change of T4035C at Val1269 of the *BRCA2* gene was detected. In the C family, the younger sister had breast cancer diagnosed at 51, and her elder sister also had breast cancer, but their pathological data were not available. In the D family, the daughter had stage 1 invasive ductal carcinoma diagnosed at age 45, and her mother also had breast cancer. In both C and D families, the previously reported missense substitution of Ser1613Gly (A4956G) and silent nucleotide change of T4427C at Ser1436 of the *BRCA1* gene were found. However, the variant alleles in the C family are heterozygous, while those in the D family are either homozygous or hemizygous (loss of normal allele). In the E family, the patient had stage 2a invasive ductal carcinoma diagnosed at age 47, and her cousin also had breast cancer. Two previously reported missense substitutions of Glu1038Gly (A3232G) and Ser1613Gly (A4956G), as well as two silent nucleotide changes of T2430C at Leu771 and T4427C at Ser1436, of the *BRCA1* gene were found to be heterozygous. Both normal and variant alleles were separately isolated by subcloning and sequenced to confirm these missense substitutions. In the F family, the daughter had stage 2a invasive ductal carcinoma diagnosed at age 50, and her mother died of breast cancer. Three previously reported missense substitutions of Pro871Leu (C2731T), Glu1038Gly (A3232G) and Lys1183Arg (A3667G) of the *BRCA1* gene were found to be heterozygous, and different alleles were subcloned using the 5' and 3' primers to amplify these three variants (Figure 1). It is of interest that all three normal amino acids (Pro-Glu-Lys) are on one haplotype, whereas all three variant amino acids (Leu-Gly-Arg) are on another haplotype. A younger sister and two nieces were found to be heterozygous for these three missense substitutions, but thus far they are free of breast cancer.

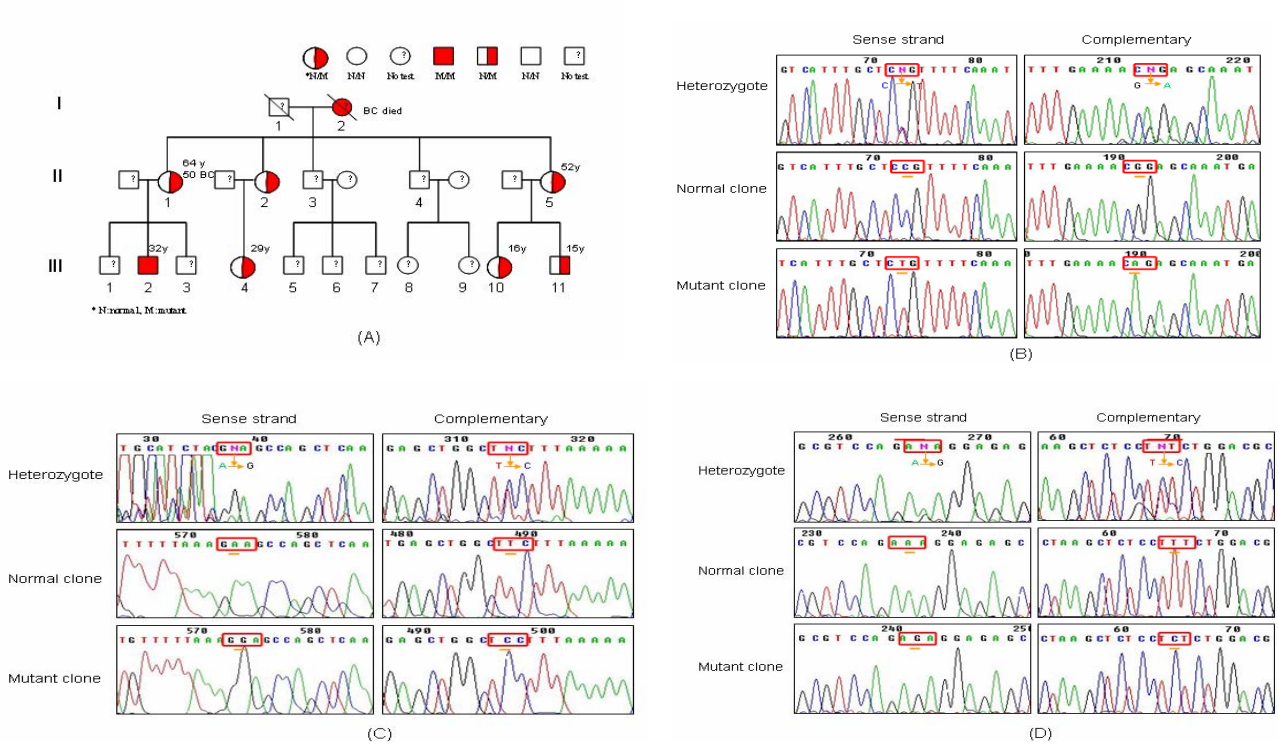

Figure 1. DNA sequence of exon 11 of the sense and complementary strand from a familial patient (designated as FII1) reveals three heterozygous mutation on the same allele. (A) The family F pedigree FII1 is a breast invasive ductal carcinoma patient and the detection of the (B) Pro871Leu (2731C→T), (C) Glu1038Gly (3232A→G) and (D) Lys1183Arg (3667A→G) missense mutation from exon 11 of BRCA1.

4. **Discussion**

Although the molecular nature of mutations in these two genes has been extensively analyzed among Caucasians, only some *BRCA1* and *BRCA2* mutations were reported among Asian populations (Table3), http://research.nhgri.nih.gov/bic/). In this investigation, the novel missense substitution of Gln1886Pro (A5885C) and silent nucleotide change of A4806G at Thr1526 of the *BRCA2* gene were found in one of these six Taiwanese breast cancer families. The four missense substitutions of Pro871Leu, Glu1038Gly, Lys1183Arg and Ser1613Gly of *BRCA1* gene which were detected in this investigation, as well as the substitutions of Pro346Ser of *BRCA1* gene and Asn289His, His372Asn, Asn991Asp and Ile3412Val of *BRCA2* gene, were previously reported among 18 Taiwanese breast cancer families [Li et al., 1999]. The pathological effect of these amino acid substitutions at *BRCA1* and *BRCA2* genes remain to be determined as either disease-associated mutations or benign polymorphisms (Table 4). Some of missense mutations at exon splicing enhancer sequences were shown to cause exon skipping, resulting in breast cancer [Fakenthal et al., 2002; Campos et al., 2003]. Among the 24 breast cancer families analyzed thus far in Taiwan, the same splicing mutation of *BRCA1* gene observed in two unrelated families and three different deletions of *BRCA2* gene are clearly associated with breast cancer [Li et al., 1999]. It may be noted that these breast cancer associated mutations deleted in Taiwan are different from those reported from Hong Kong [Khoo et al., 2000] and Tainjin (northern China) [Zhi et al., 2002].

Table 3. The *BRCA1* and *BRCA2* mutations were reported among Caucasians and Asian populations

Gene	Exon	Sequence variants	Amino acid change	Previously reported	[a] Alleles found in Taiwanese	[b] Alleles reported in Asia	[c] Alleles reported in the world
BRCA1	11	T2430C	Leu771	Yes	2	5	25
BRCA1	11	C2731T	Pro871Leu	Yes	2	5	26
BRCA1	11	A3232G	Glu1038Gly	Yes	2	7	36
BRCA1	11	A3667G	Lys1183Arg	Yes	2	5	32
BRCA1	13	T4427C	Ser1436	Yes	2	7	33
BRCA1	16	A4956G	Ser1613Gly	Yes	2	9	33
BRCA2	11	T4035C	Val1269	Yes	2	2	5
BRCA2	11	A4806G	Thr1526	No	1	1	1
BRCA2	11	A5885C	Gln1886Pro	No	1	1	1

[a] The mutations in Taiwanese from this study and Li, et al., (1999) [b] The mutations in Asia (including Taiwanese)
[a, b, c] Breast cancer information core (Bic) http://research.nhgri.nih.gov/bic/

Table 4. The BRCA1 and BRCA2 amino acid mutation effect

Gene	Exon	Sequence variants	Amino acid change	PI change	Mutation effect
BRCA1	11	T2430C	L771	5.98	Silent mutation
BRCA1	11	C2731T	P871L	6.48? 5.98	Small nonpolar residue ? Hydrophobic residue
BRCA1	11	A3232G	E1038G	3.22? 5.97	Acidic side chains ? Small nonpolar residue
BRCA1	11	A3667G	K1183R	9.74? 10.76	Basic side chains ? Basic side chains
BRCA1	13	T4427C	S1436	5.68	Silent mutation
BRCA1	16	A4956G	S1613G	5.68? 5.97	Small polar residue ? Small nonpolar residue
BRCA2	11	T4035C	V1269	5.97	Silent mutation
BRCA2	11	A4806G	T1526	5.87	Silent mutation
BRCA2	11	A5885C	Q1886P	5.65? 6.48	Uncharged polar side chains ? Small nonpolar residue

Acknowledgements

This investigation was supported by a grant from Kaohsiung Veterans General Hospital.

References

1. Campos B, Díez O, Domènech M, Baena M, Balmaña J, Sanz J, Ramírez A, Alonso C, Baiget M. RNA analysis of eight *BRCA1* and *BRCA2* unclassified variants identified in breast/ovarian cancer families from Spain. Hum Mutat 2003; 22: 337.
2. Fackenthal JD, Cartegni L, Krainer AR, Olopade OI. *BRCA2* T2722R is a deleterious allele that causes exon skipping. Am J Hum Genet 2002; 71: 625-31.
3. Ford D, Easton DF, Peto J. Estimates of the gene frequency of BRCA1 and its contribution to breast and ovarian cancer incidence. Am J Hum Genet 1995; 57: 1457-62.
4. Gudmundsdottir K, Ashworth A. The roles of BRCA1 and BRCA2 and associated proteins in the maintenance of genomic stability. 2006; 25: 5864-74
5. Johnson N, Lancaster T, Fuller A, Hodgson SV. The prevalence of a family history of cancer in general practice. Fam Pract 1995; 12: 287-9.
6. Khoo US, Ngan HY, Cheung AN, Chan KY, Lu J, Chan VW, Lau S, Andrulis IL, Ozcelik H. Mutation analysis of *BRCA1* and *BRCA2* genes in Chinese ovarian cancer identifies 6 novel germline mutations. Hum Mutat 2000; 16: 88-9.
7. Li SS, Tseng HM, Yang TP, Liu CH, Teng SJ, Huang HW, Chen LM, Kao HW, Chen JH, Tseng JN, Chen A, Hou MF, Huang TJ, Chang HT, Mok KT, Tsai JH. Molecular characterization of germline mutations in the *BRCA1* and *BRCA2* genes from breast cancer families in Taiwan. Hum Genet 1999; 104: 201-4.
8. Miki Y, Swensen J, Shattuck-Eidens D, Futreal PA, Harshman K, Tavtigian S, Liu Q, Cochran C, Bennett LM, Ding W, Bell R, Rosenthal J, Hussey C, TranT, McClure M, Frye C, Hattier T, Phelps R, Haugen-Strano A, Katcher H, Yakumo K, Gholami Z, Shaffer D, Stone S, Bayer S, Wray C, Bogden R, Dayananth P, Ward J, Tonin P, Narod S, Bristow PK, Norris FH, Helvering L, Morrison P, Rosteck P, Lai M, Barrett JC, Lewis C, Neuhausen S, Cannon-Albright L, Goldgar D, Wiseman R, Kamb A, Skolnick MK. A strong candidate for the breast and ovarian cancer susceptibility gene *BRCA1*. Science 1994; 266: 66-71.
9. Pharoah PD, Day NE, Duffy S, Easton DF, Ponder BA. Family history and the risk of breast cancer: a systematic review and meta-analysis. Int J Cancer 1997; 71: 800-9.
10. Szabo CI, King MC. Population genetics of *BRCA1* and *BRCA2*. Am J Hum Genet 1997; 60: 1013-20.
11. Whittemore AS, Gong G, John EM, McGuire V, Li FP, Ostrow KL, Dicioccio R, Felberg A, West DW. Prevalence of BRCA1 mutation carriers among U.S. non-Hispanic Whites. Cancer Epidemiol Biomarkers Prev 2004; 13: 2078-83.
12. Wooster R, Bignell G, Lancaster J, Swift S, Seal S, Mangion J, Collins N, Gregory S, Gumbs C, Micklem G. Identification of the breast cancer susceptibility gene *BRCA2*. Nature 1995; 378: 789-92.
13. Zhi X, Szabo C, Chopin S, Suter N, Wang QS, Ostrander EA, Sinilnikova OM, Lenoir GM, Goldgar D, Shi YR. *BRCA1* and *BRCA2* sequence variants in Chinese breast cancer families. Hum mutat 2002; 20: 474.

Index of Authors